ACS Catalysis

pubs.acs.org/acscatalysis
Perspective

Operando Modeling of Zeolite-Catalyzed Reactions Using First-Principles Molecular Dynamics Simulations

Veronique Van Speybroeck,* Massimo Bocus, Pieter Cnudde, and Louis Vanduyfhuys

Cite This: ACS Catal. 2023, 13, 11455−11493
Read Online

ABSTRACT: Within this Perspective, we critically reflect on the role of first-principles molecular dynamics (MD) simulations in unraveling the catalytic function within zeolites under operating conditions. First-principles MD simulations refer to methods where the dynamics of the nuclei is followed in time by integrating the Newtonian equations of motion on a potential energy surface that is determined by solving the quantum-mechanical many-body problem for the electrons. Catalytic solids used in industrial applications show an intriguing high degree of complexity, with phenomena taking place at a broad range of length and time scales. Additionally, the state and function of a catalyst critically depend on the operating conditions, such as temperature, moisture, presence of water, etc. Herein we show by means of a series of exemplary cases how first-principles MD simulations are instrumental to unravel the catalyst complexity at the molecular scale. Examples show how the nature of reactive species at higher catalytic temperatures may drastically change compared to species at lower temperatures and how the nature of active sites may dynamically change upon exposure to water. To simulate rare events, first-principles MD simulations need to be used in combination with enhanced sampling techniques to efficiently sample low-probability regions of phase space. Using these techniques, it is shown how competitive pathways at operating conditions can be discovered and how broad transition state regions can be explored. Interestingly, such simulations can also be used to study hindered diffusion under operating conditions. The cases shown clearly illustrate how first-principles MD simulations reveal insights into the catalytic function at operating conditions, which could not be discovered using static or local approaches where only a few points are considered on the potential energy surface (PES). Despite these advantages, some major hurdles still exist to fully integrate first-principles MD methods in a standard computational catalytic workflow or to use the output of MD simulations as input for multiple length/time scale methods that aim to bridge to the reactor scale. First of all, methods are needed that allow us to evaluate the interatomic forces with quantum-mechanical accuracy, albeit at a much lower computational cost compared to currently used density functional theory (DFT) methods. The use of DFT limits the currently attainable length/time scales to hundreds of picoseconds and a few nanometers, which are much smaller than realistic catalyst particle dimensions and time scales encountered in the catalysis process. One solution could be to construct machine learning potentials (MLPs), where a numerical potential is derived from underlying quantum-mechanical data, which could be used in subsequent MD simulations. As such, much longer length and time scales could be reached; however, quite some research is still necessary to construct MLPs for the complex systems encountered in industrially used catalysts. Second, most currently used enhanced sampling techniques in catalysis make use of collective variables (CVs), which are mostly determined based on chemical intuition. To explore complex reactive networks with MD simulations, methods are needed that allow the automatic discovery of CVs or methods that do not rely on a priori definition of CVs. Recently, various data-driven methods have been proposed, which could be explored for complex catalytic systems. Lastly, first-principles MD methods are currently mostly used to investigate local reactive events. We hope that with the rise of data-driven methods and more efficient methods to describe the PES, first-principles MD methods will in the future also be able to describe longer length/time scale processes in catalysis. This might lead to a consistent dynamic description of all steps—diffusion, adsorption, and reaction—as they

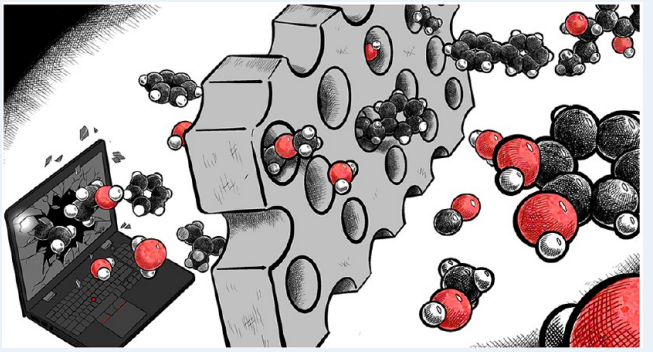

continued...

Received: April 30, 2023
Revised: July 27, 2023
Published: August 15, 2023

https://doi.org/10.1021/acscatal.3c01945
ACS Catal. 2023, 13, 11455−11493

take place at the catalyst particle level.

KEYWORDS: *molecular dynamics, kinetics, diffusion, operating conditions, enhanced sampling, density functional theory, zeolites, catalysis*

1. INTRODUCTION ON THE COMPLEXITY OF CATALYSIS AT OPERATING CONDITIONS

Catalytic reactions taking place in nanoporous materials have an intriguing complex nature which is difficult to grasp from both experimental and theoretical points of view. Substantial progress has been made in the past decade in understanding the catalytic function thanks to major advances in operando characterization, detailed kinetic studies, and molecular simulation methods. However, still today it remains a formidable challenge to grasp the complexity of realistic catalytic solids under industrially relevant conditions. In this paper, we give a critical perspective on the role of first-principles molecular dynamics (MD) methods in understanding the catalytic function at operating conditions.

Before moving on, it is important to properly define the terminology of first-principles MD methods. First-principles MD methods are methods where the dynamics of the nuclei is followed in time by integrating the Newtonian equations of motion with a potential energy that is found from first principles, i.e., by solving the quantum-mechanical many-body problem for the electrons. First-principles MD simulations are also sometimes referred to as ab initio molecular dynamics (AIMD) or Born−Oppenheimer MD. The latter terminology refers to the fact that the electronic degrees of freedom are treated separately from the nuclear degrees of freedom, given their large difference in mass. Within first-principles MD, it is assumed that the nuclei may be treated as classical particles moving on an underlying potential energy surface (PES) that is determined by solving the electronic structure problem. In such an approach, it is assumed that nuclear quantum effects are not important. This assumption may not always be valid, certainly when light particles such as protons are involved and at lower temperatures.[1] Extensions of Born−Oppenheimer MD methods have become available. For example, the path integral molecular dynamics (PIMD) approach relies on Feynman's path integral formulation of quantum mechanics and allows to account for nuclear quantum effects.[1−3] However, these methodologies remain still computationally quite expensive and are certainly not used on a routine basis. While it is tempting to assume that nuclear quantum effects might not be of major importance in the field of zeolite catalysis, given the relatively higher temperatures involved, it was recently shown that the kinetics of proton hoppings may still be seriously impacted by the inclusion of nuclear quantum effects at temperatures of ca. 473 K. Given the fact that zeolites will also be used in future technologies under milder conditions, it might be interesting to also consider these effects.[4]

Referring back to the initial question, namely, how first-principles MD methods may help to understand the catalytic function at operating conditions, we further elaborate on the various levels of complexities occurring within catalysis taking place in nanoporous materials. This Perspective focuses primarily on zeolite catalysis; however, many concepts discussed are much more broadly applicable to catalysis taking place in other materials such as metal−organic frameworks and covalent organic frameworks, which all belong to the class of nanoporous materials.

Catalytic solids used in industrial applications show a high degree of complexity at both the level of the catalytic particle and beyond. The latter refers to complexities of how the catalyst particles are dispersed within binders or other supports and the way they are embedded within industrial reactors.[5] As nicely pointed out by Buurmans and Weckhuysen,[6] individual catalyst particles show heterogeneities in both space and time. Realistic crystals have a certain morphology and finite size, varying from the order of nanometers to the micrometer scale, influencing transport properties and the catalytic function.[7] Additionally, active sites are heterogeneously distributed, defects are inherently present and often introduced on purpose to optimize the activity and lifetime.[8,9] All previous factors contribute to spatial heterogeneities that are inherently present in realistic materials. Additionally, realistic materials are highly dynamic and are characterized by a broad range of intrinsic time scales. From a holistic point of view, the structure of the catalyst may completely change during operation, which is sometimes referred as the intrinsic lifecycle of a catalyst particle.[10,11] These observations lead to the concept of spatiotemporal evolution of a material, where the dynamics of the material is entangled with the material's spatial properties.[6,12,13] For important zeolite catalyzed reactions, major advances have been made to visualize the spatiotemporal evolution of molecules and active sites during chemical conversions.[13,14]

When interested in the catalytic function of nanoporous materials, it is important to realize that the state and the function of the catalyst depend critically on the external conditions in which the material performs the work. Operating conditions may refer to the true working temperature, applied external pressure, presence of moisture, external fields, etc. Around 2000, the field of operando characterization was launched within catalysis, referring to one or more spectroscopy or microscopy techniques used to interrogate the catalytic behavior under realistic conditions with real-time on-line analysis of products.[15−21] The field of operando spectroscopy has evolved greatly since its launch, and systematic more advanced spectroscopic methods have been developed that allow us to follow the dynamic evolution of heterogeneous catalytic solids in situ—within the reactor during exposure to reactants—with systematically better spatial and temporal resolution. Ideally, experimentalists can make a molecular movie with high temporal and spatial resolution, but this target remains very ambitious.[6,22,23]

Nowadays, the term "operando" is also used in the field of modeling, where one aims to model the function of the material under realistic conditions of temperature, pressure, moisture, and external fields.[24−27] Reaching this goal is certainly not possible by a single method. Instead a range of models based on MD methods, microkinetic models, kinetic Monte Carlo methods, and machine learning algorithms are currently explored.[27−29] Within this Perspective, we specifically highlight how first-principles molecular dynamics techniques may contribute toward understanding the catalytic function in zeolites at operating conditions. Moreover, at various places, we elaborate on how first-principles MD methods can be integrated into an overall computational catalysis workflow.

The term "operando characterization" should not be confused with "in situ characterization".[21] From an experimental point of view, the term "in situ characterization" refers to the character-

https://doi.org/10.1021/acscatal.3c01945
ACS Catal. 2023, 13, 11455−11493

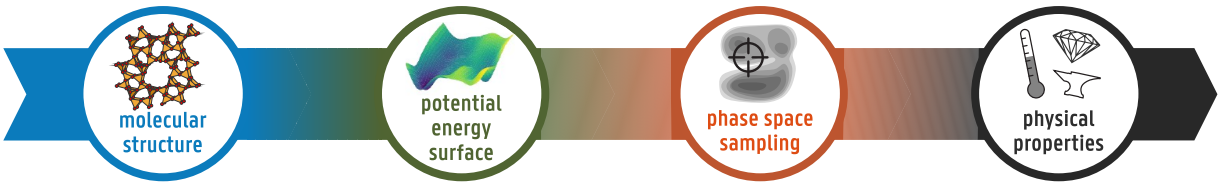

Figure 1. Sequence of a modeling exercise where the basic quantity is the multidimensional potential energy surface (PES) for a well-chosen molecular structure. This PES needs to be sampled in the interesting regions, after which the target properties at operating conditions can be derived. From ref 30. CC BY 4.0.

ization of a material in its working environment, where in situ means on site, in position. Within catalysis this refers to the real-time investigation of a catalyst within the reactor, typically by spectroscopy or microscopy techniques, during exposure to reactants or other external stimuli. The term "in situ modeling" has not been used so frequently, but when trying to make the analogy with the experimental conditions, in situ modeling would refer to models that aim to give a realistic representation of the catalyst as it is found in the reactor. To pursue modeling of a realistic catalyst, one needs models that account for spatial heterogeneities at the individual catalyst level and beyond.

Ideally one could model realistic catalysts under operating conditions. However, current modeling techniques have not reached this ambitious target, which is mainly related to the experimentally relevant time and length scales. These are substantially larger than the theoretically accessible spatiotemporal windows. The problem of operando and in situ modeling within catalysis is thus intimately connected to multiscale modeling techniques. The next section gives a brief overview on relevant and accessible length and time scales both from experiment and theory within the field of catalysis.

2. CURRENT STATUS ON THEORETICAL ACCESSIBLE LENGTH AND TIME SCALES WITHIN THE FIELD OF NANOPOROUS MATERIALS

To set the scene on the accessible length and time scales from a modeling perspective, it is essential to reflect on the general steps undertaken when performing a molecular modeling exercise, where one starts from the atomistic or molecular level and tries to make the connection with properties that are experimentally measurable. Theoretically accessible length and time scales are inherently linked to the method used to describe the potential energy surface. The PES plays a central role in a general modeling strategy, which consists of following steps (Figure 1): (i) setting up a reliable structural model to represent the material in a realistic way, (ii) construction of the PES via an adequate level of theory, (iii) sampling the interesting regions of the PES, and (iv) extracting and interpreting the interesting properties under the right conditions which at best can be compared to experiment.[30] The PES is a high-dimensional function in terms of the internal coordinates, and the level of theory used to describe it (vide infra) effectively determines the accessible length and time scales within first-principles molecular simulations.

The first step, namely, the construction of a reliable structural model to represent the catalyst, is of utmost importance. As mentioned in the Introduction, realistic catalysts have a finite size and are represented by spatial heterogeneities at various scales. Recent literature clearly provides evidence that size matters and that inclusion of proper spatial disorder at various length scales may have a major impact on catalytic performance. In this sense, a representative model should in principle account for these spatial heterogeneities. Most of the current structural models used in zeolite catalysis focus on an accurate description of the local environment of the active site and the confinement of adsorbed species. To appropriately represent the porous zeolite environment, various approaches have been followed, which can mainly be categorized as cluster models or periodic models.[31,32] Within cluster models, the zeolite is represented by a fragment that is cut out of the lattice. While earlier cluster models were very limited in size, currently with the increase of computational power, clusters having hundreds of T atoms are routinely used. Such larger clusters are also able to capture the long-range interactions of the microporous environment.[33,34] Periodic models account for one or more unit cells of the zeolite, give a very natural description of various zeolite topologies, and have even been used to represent external surfaces. In the latter case, slab models are constructed by cutting the bulk along given crystallographic planes and saturating them with terminating groups.[35−37] It needs to be stressed that construction of such spatially extended models representing, for example, the external surface is a challenge on its own even with the broad variety of current methodologies.[30,38,39] The construction of atomistic structural models which are representative of realistic zeolites having defects and spatial heterogeneities at various length scales can be regarded as a research topic on its own. For the latter, a close interaction with experimentalists is necessary to obtain input on the structure by various spectroscopic and imaging techniques with different spatiotemporal resolution.[30] Recent reviews have elaborated more on the challenge of building structural models that have sizes comparable to experimentally used crystals.[9,30]

The second step concerns the determination of the PES, which is a central quantity in the modeling sequence. The PES is a high-dimensional function describing how the energy varies in terms of the various nuclear coordinates. In principle, the PES needs to be constructed by solving the electronic Schrödinger equation for fixed nuclear coordinates. The latter assumes the Born−Oppenheimer approximation, where the dynamics of the electronic degrees of freedom can be separated from the nuclear motion, which is in most cases a valid assumption given the large mass difference between nuclei and electrons. To obtain the complete PES, one in principle needs to calculate the energies and forces along all nuclear degrees of freedom, which is a computationally very expensive task for realistic materials used in catalysis, given the many degrees of freedom at play.

A catalytic process is inherently characterized by a broad variety of length and time scales, as illustrated in Figure 2. Before any catalytic reaction can take place, reactants need to enter the pores and diffuse to the active sites either at the exterior or interior of the crystal, where they adsorb and reactive events take place. When the chemical reaction has taken place, the products can finally desorb and be released from the catalyst. Diffusion is typically a process taking place over longer distances and longer

https://doi.org/10.1021/acscatal.3c01945
ACS Catal. 2023, 13, 11455−11493

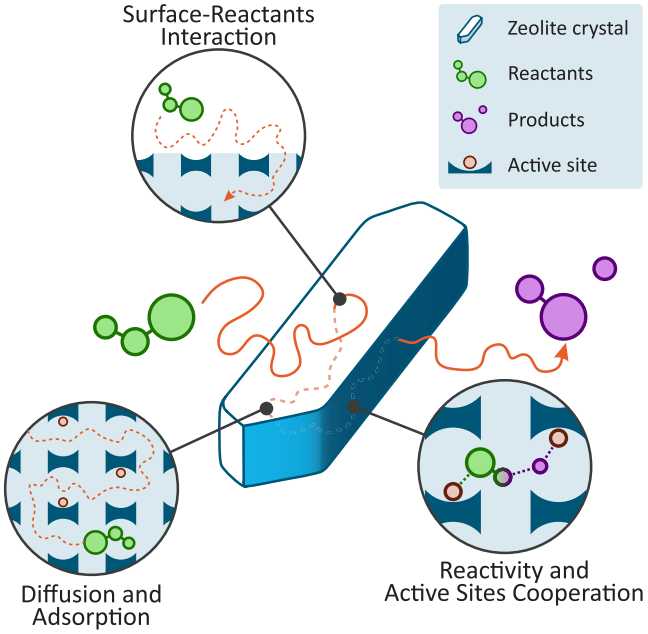

Figure 2. A zeolite-catalyzed reaction comprises multiple steps. The reactants first interact with the catalyst surface and then can diffuse inside the crystal. Adsorption on the active site can result in a reactive event, and the so-formed products can then be released from the catalyst.

time scales and is currently not straightforwardly accessible via quantum-mechanical (QM) methods. However, as we will illustrate in section 4.4, recent studies have appeared where quantum-mechanics-based methods in combination with enhanced-sampling MD methods have been used to calculate diffusional barriers for molecules to hop from one cage to the other in zeolites through small pore windows.[40,41] Reaction dynamics, on the other hand, takes place in a rather localized environment around the active site and is an activated process. Reactive events need to be modeled at the quantum-mechanical level, as chemical bonds are formed/broken and the electronic structure completely rearranges during a chemical reaction. Currently, density functional theory (DFT) is the method of choice to describe the PES at the quantum-mechanical level, thanks to its attractive trade-off between accuracy and speed. The accuracy of DFT methods critically depends on the exchange−correlation functional[42−46] and the description of long-range dispersion interactions.[47−51] Exchange−correlation funtionals are commonly classified into various categories following an analogy with Jacob's ladder proposed by Perdew.[52] The lowest step corresponds to the Hartree world, which is exchange−correlation-free, and the higher steps aim to reach the heaven of chemical accuracy. In between, we find generalized gradient approximation (GGA) functionals, meta-GGA, hybrid-GGA, double hybrids, etc. When climbing the ladder, the methods also become computationally more expensive. More extensive reference works can be found elsewhere.[53] Within the field of zeolite catalysis, GGA functionals are still very frequently used; for example, the Perdew−Burke−Ernzerhof (PBE) functional is particularly popular.[54,55] These functionals are typically amended with some models to describe the long-range dispersion interactions. One of the most commonly used methods to describe the dispersion interactions is by adding a posteriori a pairwise correction to the DFT energy, the so-called D-correction schemes proposed by Grimme.[47,51,56−58] The particular choice of the energy functional and description of the long-range interactions is certainly not trivial and may have an important impact on the stability of intermediates in the pores of zeolites.[42−46] As DFT with the current generation of functionals often does not reach the stringent criteria of chemical accuracy, complicated composite schemes, wavefunction-based methods, and embedding schemes have been devised to target chemical accuracy in various application areas.[46] With the extension of computational power, fully periodic post-HF single-point calculations have also become possible, but given their high computational cost, they are sparingly used as high-level reference data.[59] Obviously, performing brute-force MD simulations with these advanced composite schemes or post-GGA methods in zeolite catalysis is beyond current computational capabilities, and therefore, most of the applications using first-principles MD use GGA DFT levels of theory. Very recently, innovative schemes have been proposed to perform first-principles MD simulations with more accurate energies compared to standard GGAs relying also on machine learning concepts, as will be explained later in this Perspective. In any case, the combination of MD with an appropriate electronic structure method that yields sufficiently accurate energies and forces is a major point of attention when using first-principles MD within zeolite catalysis.

Currently attainable length scales when modeling the system at the quantum-mechanical level using DFT are situated on the order of a few nanometers, which are still considerably smaller than experimental crystal sizes, which vary from several nanometers to micrometers.

Big zeolite crystals may extend to several micrometers but are more often used on the laboratory scale to understand the phenomena taking place in the inner parts of the zeolite, whereas in industrial applications much smaller crystals are used to shorten the diffusion paths of the reactants and products. Various efforts have been undertaken to reduce the crystallite sizes by making nanosheets, nanoslabs, etc., and sizes ranging from a few to hundreds of nanometers have been reached.[9] Apart from the morphology and dimensions of individual catalysts particles, they also need to be dispersed in supports to be brought to industrial implementation.[60] Interestingly, various efforts have been undertaken recently to also synthesize hierarchical materials having both micro- and mesopores. For example, Li et al. reported preparation of ZSM-5 monoliths which were then also tested for methanol to olefin (MTO) conversion.[61] Clearly, current molecular modeling focuses on much smaller scales, and even the heterogeneities at the individual particles are not yet fully accounted for.

To also obtain information on the time evolution of the system, the PES, which is a multidimensional surface, needs to be sampled in the regions of interest. In principle, one can use both Monte Carlo and MD methods to sample the PES; however, when interested in extracting the time evolution of the system, it is best to resort to MD techniques.[62] The main drawbacks of first-principles MD methods are the currently attainable time scales, which are limited to a few hundred picoseconds for typical zeolitic systems. Reactive events within catalysis are activated and thus catalogued as rare events, where the probability to sample these events during regular MD simulations is extremely low. Consequently, much longer time scales would be necessary to sample them with sufficient probability. To circumvent this problem, MD techniques can be used in combination with enhanced sampling techniques which allow the less probable regions to be sampled in a more efficient

https://doi.org/10.1021/acscatal.3c01945
ACS Catal. 2023, 13, 11455−11493

way.[63−67] Despite various successful contributions using enhanced-sampling simulations in the field of zeolite catalysis, it remains a formidable challenge to grasp the dynamics of a catalytic system, which is inherently characterized by a broad variety of disparate time scales.[68] The accessible length and time scales can, in principle, be extended by using cheaper methods to calculate the PES, such as classical force field-based methods. With classical force fields, the interactions between the atoms are approximated by simple analytical functions, neglecting the quantum description of the electrons. The parameters taken up in the analytical functions may be obtained by fitting to experimental data or to smaller-sized systems on which accurate quantum-mechanical calculations can be performed.[69,70] With the use of classical force fields, the accessible length and time scales increase to tens of nanometers and hundreds of nanoseconds; furthermore, one can perform the analysis of the energy contributions at the level of the individual classes of interactions. The development of force fields for nanoporous materials and their interactions with guest species is a research field of its own. We refer the interested reader to some seminal reviews on the topic.[71−73] In general terms, construction of force fields yields a trade-off between desired accuracy (i.e., how accurate are the properties of interest computed), computational efficiency, and transferability (i.e., the prediction of properties outside of the conditions or systems for which it was parametrized). Classical force fields have been indispensable in the whole scale of molecular simulation methods; however, by design, they are not able to describe reactive events, except when specific reactive force fields are constructed (vide infra). In this sense, they are less suited to use in molecular dynamics simulations where also reactive events can occur or where specific host−guest interactions take place. Specifically for zeolites, a wide variety of classical force fields have been proposed, which have been successfully used to describe a variety of structural properties, transport properties, etc.[74] Despite their broad usage within the field of zeolites, it needs to be stressed that when specific host−guest interactions are occurring, force fields may not describe these specific interactions appropriately, as was recently shown for the diffusion of alkenes through small-pore zeolites with Brønsted acidic sites. More information on this particular case is given in section 4.4.[41] For the description of adsorption, force fields have been extensively used for example in grand canonical Monte Carlo simulations (vide infra).[75,76] Construction of transferable force fields is far from trivial.[70] Notable examples exist where transferable force fields for adsorption were constructed, such as the TraPPE-zeo model, which relies on a parametrization to match experimental adsorption isotherms of *n*-heptane, propane, carbon dioxide, and ethanol.[77] This model was found to achieve transferability for the description of adsorption and diffusion of a broader range of guest species and a wide range of thermodynamic conditions.[77] In principle, force fields can be developed to reach higher accuracy than DFT-based energy evaluation at the GGA-D3 level by extensive development and fitting for the specific system at hand to either higher-level ab initio data or precise experimental measurements. Although such force fields are specifically parametrized to reach high accuracy for a set of systems or conditions, they are often not transferable to other systems.[73] Lastly, there are some notable examples of reactive force fields which allow simulation of reactive events within the field of catalysis, but still the overall outcome depends on the parametrization of the force field.[78−81] Interesting new directions are currently being explored to derive machine learning potentials (MLPs), where starting from underlying quantum-mechanical data sets a numerical potential is derived to describe the PES using a nonlinear regression method.[82−91] This approach is very promising, but the applications in the field of zeolite catalysis, which is characterized by an enormous complexity at various levels, is nearly nonexistent.[4,92−94] We elaborate in Outlook and Future Directions on new possibilities within the field of modeling zeolite catalysis when having access to cheaper methods to evaluate the PES.

Previous observations allow us to conclude that there still exists a huge gap between theoretically attainable length scales and experimental observations. Fundamentally new directions will have to be explored to further close the length/time scale gap between theory and experiment (see section 5).

3. FIRST-PRINCIPLES MOLECULAR DYNAMICS SIMULATIONS TO SIMULATE CHEMICAL REACTIONS AT OPERATING CONDITIONS: SOME KEY CONCEPTS AND CHALLENGES

As nicely pointed out by Grajciar et al. in their review on operando computational modeling in heterogeneous catalysis, no single method is able to bridge the gap from modeling at idealized conditions to realistic operating conditions.[27] Idealized conditions are also referred to as ultrahigh vacuum conditions, where the system is considered at low reactant concentrations and at 0 K. To reach realistic operating conditions for complex zeolite-catalyzed reactions, a combination of methods is necessary, such as biased molecular dynamics, microkinetic models of reaction networks, kinetic Monte Carlo methods to reconcile events characterized by disparate time scales, machine learning approaches, etc. Herein we particularly highlight the role of molecular dynamics techniques in our endeavor to model the catalyst at work. The interested reader is referred to some textbooks and reviews on molecular dynamics methods.[62,68,95−97] In section 5, we reflect on the role of first-principles MD methods within the whole ecosystem of modeling methods for zeolite-catalyzed reactions at various length and time scales.

Within molecular dynamics simulations, the time evolution of the system is described by numerical integration of the Newtonian equations of motion, where the nuclei are treated as classical particles moving on the PES:

$$M_I \frac{\mathrm{d}^2 \mathbf{R}_I}{\mathrm{d}t^2} = \mathbf{F}_I(\mathbf{R}_1, ..., \mathbf{R}_N) = -\nabla_I U(\mathbf{R}_1, ..., \mathbf{R}_N) \quad (1)$$

where $\mathbf{R}_I$ is the position of the nucleus I with mass M_I, $\mathbf{F}_I$ is the force acting on nucleus I, and $U(\mathbf{R}_1, ..., \mathbf{R}_N)$ is the multidimensional PES determined by solving the electronic structure problem at various positions of the nuclei. Previous equations of motion are written in their most simple form within the microcanonical or *NVE* ensemble, where the total energy is a conserved quantity. To make the link toward operating conditions, it is necessary to work in other thermodynamic ensembles where the temperature or pressure is controlled, a target that is achieved by using appropriate thermostats and/or barostats. One of the main advantages of MD simulations is their ability to describe the real-time evolution of the system, in contrast to so-called static approaches where only a limited number of points are considered on the PES. However, to obtain physically meaningful time averages, excessive sampling is necessary, which makes MD techniques much more expensive

https://doi.org/10.1021/acscatal.3c01945
ACS Catal. 2023, 13, 11455−11493

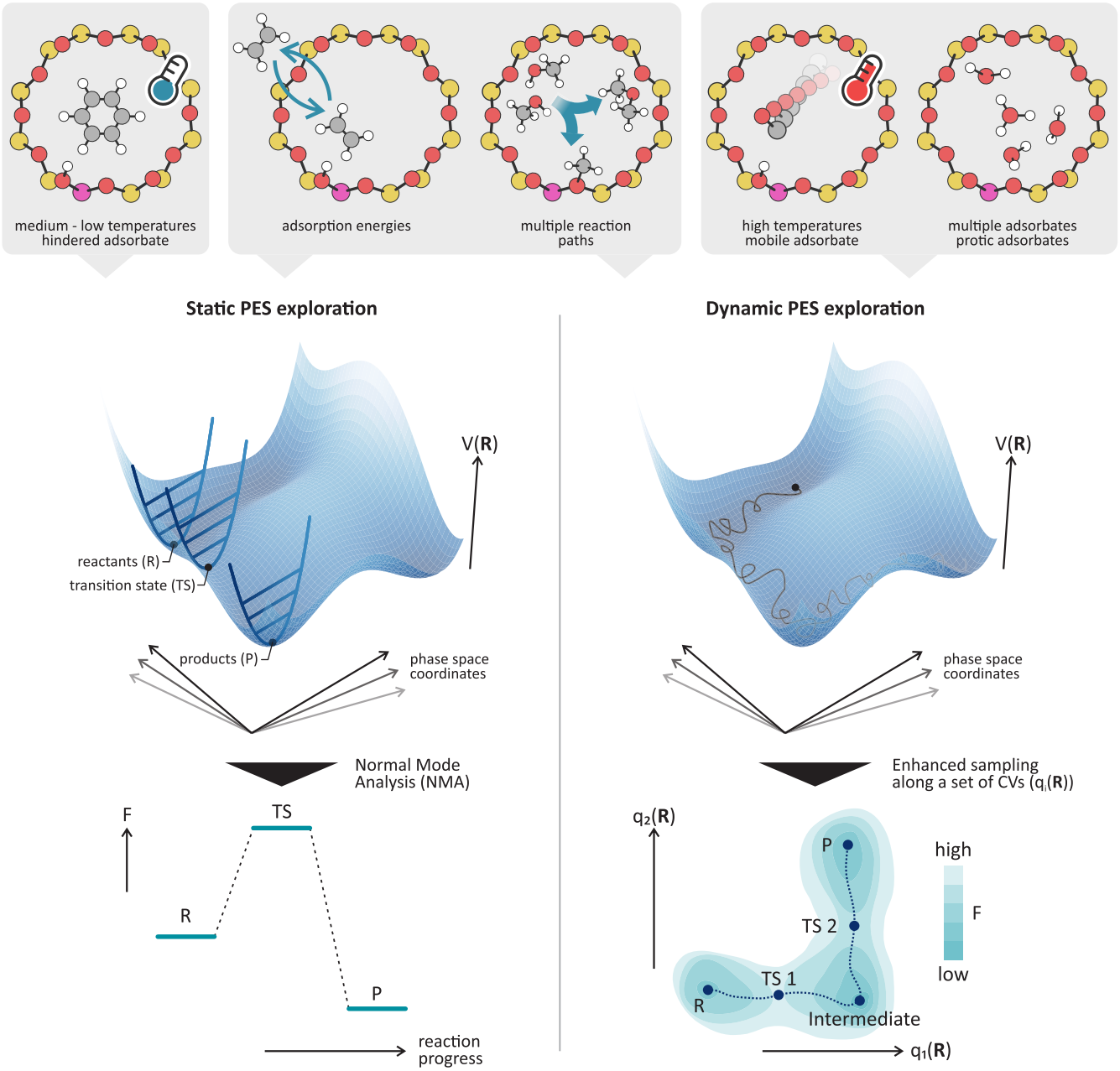

Figure 3. Schematic comparison between a static calculation, where free energies of the intermediates are retrieved through a normal-mode analysis, and a dynamic simulation, where they can be retrieved using an enhanced sampling technique along a set of collective variables. The top panel shows a noncomprehensive and nonstrict collection of cases where one method could be better suited than the other to explore the system PES (which is here shown as a two-dimensional surface for the sake of visualization).

compared to static approaches, as for each configuration of nuclei an electronic structure calculation is necessary.

The difference between static and dynamic approaches is further illustrated for the simulation of a chemical reaction (Figure 3). When simulating a chemical reaction within a static approach, only a limited number of points are calculated on the PES, corresponding to the adsorbed state, the transition state, and products. Afterward, thermodynamic properties (reaction enthalpies, entropies, etc.) can be obtained by applying the tools of statistical mechanics, where via the molecular partition function, which allows linking of the microscopic properties to macroscopic properties, thermal corrections may be obtained. To obtain kinetic information, one mostly relies on transition state theory or some straightforward extension.[98−100] In the following subsections we elaborate on some key concepts of first-principles MD simulations with the aim to simulate reactions and obtain free energy profiles and kinetic information. Furthermore, some practical considerations are given, and a critical reflection is given on how first-principles static and dynamic methods can be used to compare with experimental kinetic data.

3.1. Enhanced Sampling Methods. To simulate chemical reactions using MD simulations, one needs to combine the MD protocol with enhanced sampling methods to enable efficient sampling of low-probability regions of configuration space corresponding to the activated regions. A plethora of enhanced sampling methods has been proposed in the literature, such as umbrella sampling, thermodynamic integration, metadynamics,

https://doi.org/10.1021/acscatal.3c01945
ACS Catal. 2023, 13, 11455−11493

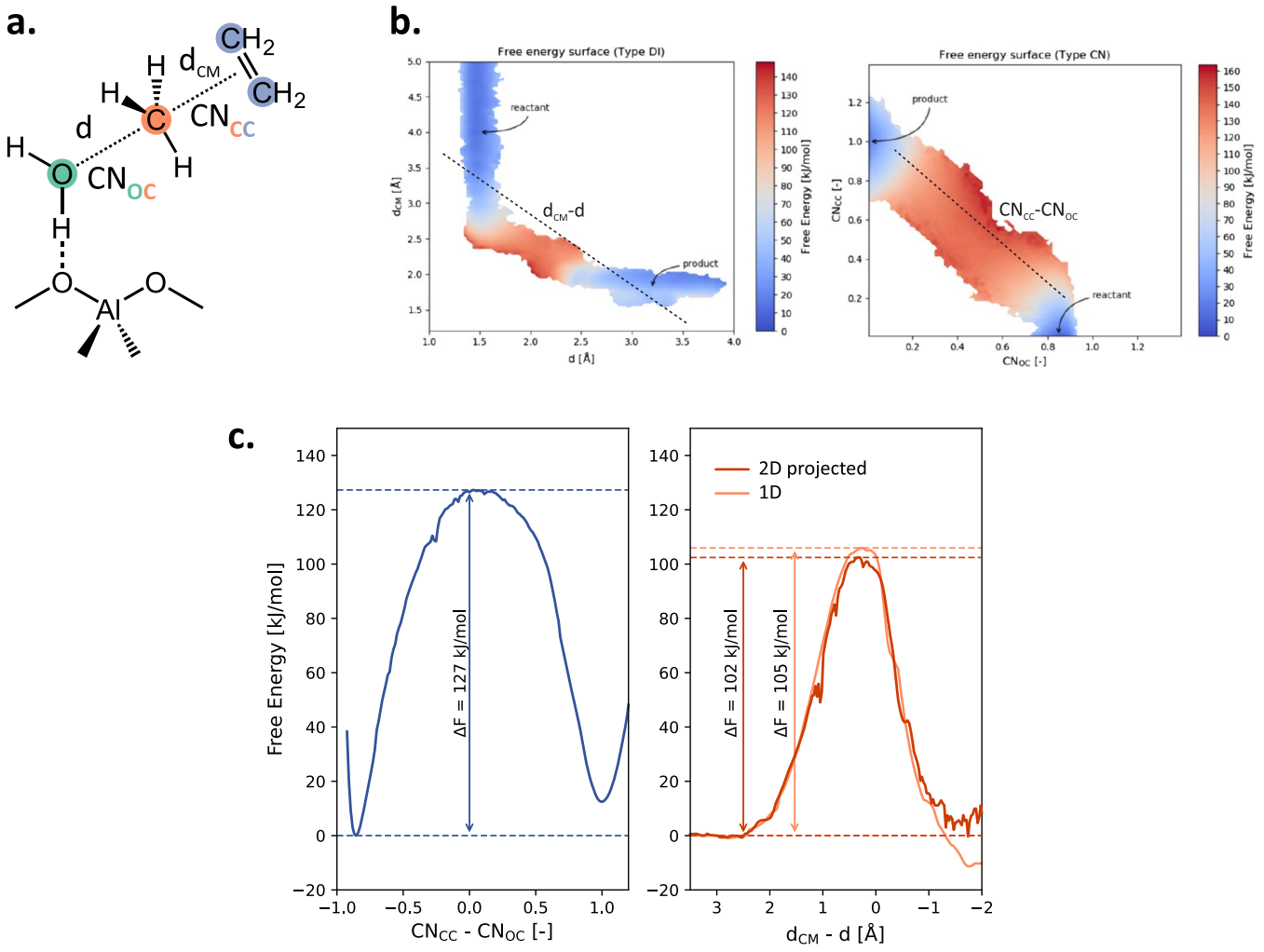

Figure 4. (a) Schematic depiction of the distances (d) and coordination numbers (CNs) used to describe the methylation of ethene in H-ZSM-5. (b) Two-dimensional free energy surfaces (FESs) of the ethene methylation reaction using the DI and CN collective variables. (c) Projections of the profiles in (b) along the difference of distances or coordination numbers. In the right-hand profile, the projected FES is also compared to the one obtained directly from a 1D umbrella sampling simulation. Adapted with permission from ref 120. Copyright 2020 Elsevier.

variationally enhanced sampling, etc.[63−66,101] Most of the enhanced sampling methods currently used in catalysis rely on the definition of some selected predefined degrees of freedom, the so-called collective variables (CVs), along which one enhances sampling instead of sampling freely along all degrees of freedom. The enhanced sampling methods based on definition of CVs can in general terms be defined as gradient-based ones such as thermodynamic integration, the blue-moon ensemble method, and non-Boltzmann sampling methods like umbrella sampling, metadynamics, etc. Apart from these CV-based methods, another series of methods relies on the generation of many replicas of the system at different conditions, such as parallel tempering or free energy perturbation methods. However, as many configurations are necessary to obtain reliable statistics, these methods are less frequently used in the field of catalysis. Very good reviews on the broad variety of enhanced sampling methods and their application in catalysis have appeared recently, and we refer the interested reader to these works and references therein.[68]

Another category of methods, namely, methods based on transition path sampling (TPS), aim to sample the transition path without prior knowledge of transition states and without using CVs. Within these methods an ensemble of unbiased dynamical trajectories between the reactants and products is created by systematically generating new trial paths through modification of a previous path in a Monte Carlo fashion.[102−105] Interestingly, the statistics of the transition path ensembles can be directly used to compute reaction rates.[104,106] However, to obtain rates, it is best to resort to variants like transition interface sampling (TIS) or more efficient variants like replica-exchange TIS (RETIS), which defines a series of interfaces that distinguish between reactant and product states, from which a rate constant can be deduced based on the crossing probabilities.[105,107−109] So far, TPS or TIS (RETIS) methods have not been used frequently in the field of nanoporous materials, as when used in combination with DFT the method is at the limit of what is computationally feasible today. One would need thousands of trajectories to obtain reliable quantitative data.[110−114,116] However, if one would have access to cheaper methods to determine to determine the PES with quantum accuracy compared to DFT, TPS-related methods show great potential within the field of catalysis.[115] For some selected cases, TPS has been used in the field of computational catalysis to receive further mechanistic insights in the reaction, however without computation of reaction rates.[110−114,116] TPS methods have been used to understand qualitative features of complex

https://doi.org/10.1021/acscatal.3c01945
ACS Catal. 2023, 13, 11455−11493

catalyzed reactions but are often combined with dedicated enhanced sampling methods, relying on CVs to deduce accurate quantitative data on reaction kinetics. For more extensive reviews on various sampling methods, we refer readers to dedicated reviews on the topic.[63−66]

3.2. Collective Variables and Free Energy Profiles. As most of the applications of enhanced-sampling MD methods within the field of computational catalysis rely on the definition of CVs to steer the dynamics, some further methodological insights are given concerning their pros and cons. First, a proper selection of CVs for complex chemical reactions taking place in nanoporous materials remains a true challenge. "Good" CVs must fulfill some basic requirements: they can only depend on the instantaneous point in phase space where the system is found, and they should be able to distinguish between all (meta)stable states and transition states of interest along the reaction paths. More extensive information on the proper definition of a CV can be found in the work of Peters.[117] In addition to this, the number of CVs used in a simulation cannot—in general—be greater than 2 to keep the computational cost feasible. There exist methodologies to find the best reaction path in a higher-dimensional CV space, such as path metadynamics or the string method,[118,119] but these are outside the scope of this Perspective. Typical CVs can be any function of the microscopic coordinates of the system, such as distances, angles, coordination numbers, etc. For a given system, it might be possible to define various sets of CVs, each perfectly suited to describe the reaction of interest. Depending on the choice, the resulting free energy profiles will be uniquely shaped, although in principle, they should lead to the same derived properties (assuming proper convergence of the results). To better illustrate this concept, some recent results by Bailleul et al. are highlighted on the methylation of ethene with methanol in the H-ZSM-5 zeolite.[120] This reaction, being among the best benchmarked in zeolite catalysis, is one of the few for which experimental kinetic data are available.[121,122]

To describe the methylation reaction, two sets of collective variables were tested, as schematically shown in Figure 4a. The former (type DI) is given by the distance between the methanol carbon and methanol oxygen (d) and the distance between the methanol carbon and the center of mass of the two ethene carbons (d_{CM}). The latter (type CN) uses coordination numbers, which are defined as

$$\mathrm{CN}_{AB} = \sum_{i\in A}\sum_{j\in B}\frac{1-\left(\frac{d_{ij}}{d_0}\right)^n}{1-\left(\frac{d_{ij}}{d_0}\right)^m} \tag{2}$$

where A and B are two groups of atoms, d_{ij} the distance between atoms i and j, and typically $n = 6$ and $m = 12$. d_0 is a parameter that, if chosen to be roughly equal to the d_{ij} distance at the transition state, makes CN_{AB} approximately equal to the number of bonds between the atoms in the two groups. In this case study, the first coordination number is between the methanol carbon and the methanol oxygen, while the second is between the methanol carbon and the two ethene carbons. Therefore, both sets of CVs encode the same chemical reactivity, simply in different functional forms. For such a simple reaction, one's chemical intuition is usually sufficient to identify the relevant reactive bonds and angles that need to be included in the CV choice. For more complex reactive processes that may involve many steps and/or many atoms, on the other hand, deducing a sensible CV can become almost impossible and likely lead to an inappropriate sampling of the reaction path. Later, the possibility of going toward (semi)automated procedures to generate the reaction CVs will be discussed in more detail.

Figure 4b shows the two-dimensional free energy surfaces (FESs) obtained for ethene methylation from umbrella sampling (US) simulations with the two sets of CVs. As can be seen, they both allow us to distinguish between the reactant and product valleys. A one-dimensional FES can then be constructed in terms of a governing reaction coordinate which, as shown in Figure 4b, can in this case simply be defined as the difference between the two original distances or CNs. The projection of a two-dimensional FES $F(q_1, q_2)$ on a new collective variable $q(q_1, q_2)$ that is a function of the two original ones can be expressed as follows:

$$F(q) = -k_B T \ln\left[\int_{-\infty}^{+\infty}\int_{-\infty}^{+\infty} e^{-\beta F(q_1,q_2)}\delta(q - q(q_1, q_2))\, dq_1\, dq_2\right] \tag{3}$$

The resulting projected one-dimensional FESs are shown in Figure 4c, where it can be clearly seen how a different CV choice leads to a significantly different FES. The free energy profiles in terms of different CVs have not only different shapes but also substantially different free energy barriers, meaning that deriving free energy barriers by just taking the difference between the maximum and minimum of the free energy surface is not a good practice. Before outlining how to derive in a more robust way kinetic information, some more details are given on how to transform free energy profiles obtained with different CVs. If the CV space is sufficiently sampled, one can easily convert one free energy profile to another by applying following transformation formula:[120]

$$F(q_2) = -k_B T \ln\left[\int_{-\infty}^{+\infty} p_{2|1}(q_2|q_1) e^{-\beta F(q_1)}\, dq_1\right] \tag{4}$$

where $p_{2|1}(q_2|q_1)$ is the conditional probability of CV q_2 in terms of CV q_1 and encodes the correlation between the two collective variables (i.e., we know how likely q_2 is for a certain value of q_1). $p_{2|1}(q_2|q_1)$ can be estimated from a molecular simulation by constructing histograms of the occurrence of q_2 for the second CV in the subset of the simulation data for which the first CV takes the value q_1. More details are given in the Supporting Information of ref 120.

In the original paper by Bailleul,[120] first sampling in terms of two CVs was performed. However, for this particular reaction one could have performed US simulations directly in one dimension, obtaining the same results with a reduced computational cost (Figure 4c, right). For this reaction, this is possible since the one-dimensional reaction coordinate $q = d_{CM} - d$ is also a suitable reaction coordinate to drive the reaction. However, reducing the FES dimensionality is not always easy or recommended. Indeed, the more degrees of freedom are included in a single CV, the higher is the risk of poorly exploring important regions of the reaction path. When having performed sampling initially in one dimension, it is also possible to perform the inverse operation, where a one-dimensional FES is converted to a new FES function of one or more new collective variables. This procedure is particularly interesting to detect whether the chosen CV is capable of sampling the part of the phase space in which one is interested. When going from one to two CVs, the formula takes the following form:

$$F(q_1, q_2) = -k_B T \ln\left[\int_{-\infty}^{+\infty} e^{-\beta F(q)} p(q_1, q_2|q)\, dq\right] \tag{5}$$

https://doi.org/10.1021/acscatal.3c01945
ACS Catal. 2023, 13, 11455−11493

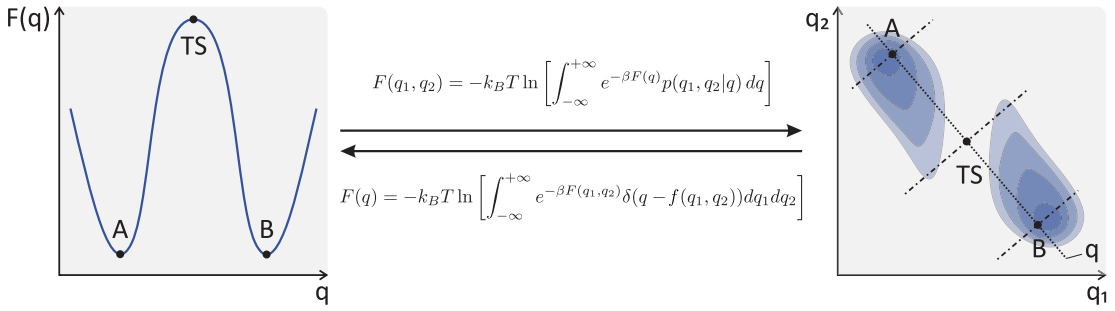

Figure 5. A one-dimensional FES can be converted into a two-dimensional one and vice versa thanks to some statistical analysis. In this example the two-dimensional FES exhibits a very clear discontinuity which is not detectable in the one-dimensional profile. Indeed, if the one-dimensional q is chosen to be the dotted line in the right figure, the transition state region appears to be continuously sampled despite in reality being made by the merging of two nonoverlapping regions in the two-dimensional CV space.

whose key ingredient is the conditional probability $p(q_1, q_2|q)$, which encodes the system's likelihood of being in the (q_1, q_2) state on the condition that the original CV has a value q. In other words, the free energy of a (q_1, q_2) state is computed from the probability of the (q_1, q_2) state, which in turn is expressed as a sum over q states of the probability of the q state (the Boltzmann factor $e^{-\beta F(q)}$) weighted with the conditional probability $p(q_1, q_2|q)$ of visiting the (q_1, q_2) state on the condition of the system having an original CV value of q. The convenience of this deprojection procedure is illustrated schematically in Figure 5, where a continuous and smooth one-dimensional FES unravels clear discontinuities when deprojected in two dimensions, indicating that the reaction path cannot be adequately sampled with the chosen CV.

3.3. Kinetic Information from Enhanced Sampling MD Simulations. We now turn our attention to how to obtain in a more robust way kinetic information from the obtained free energy profiles. Clearly the min−max difference in free energy obtained from an FES is not a suitable quantity to derive reaction kinetics, as it strongly depends on the CV choice. Therefore, one would rather compute the rate constant of the reaction under study, which being a macroscopic measurable quantity is independent of the CV choice, provided that the CV itself is well-suited to describe the process under study (see the previous paragraph). This can be done by resorting to the Bennett−Chandler (BC) approach to reaction rate theory, where the kinetic constant of an elementary reaction step can be expressed as follows:[62]

$$k^{\mathrm{BC}}_{\mathrm{R}\to\mathrm{P}}(t) = \frac{\langle \dot{q}\delta(q(0) - q^*)\theta(q(t) - q^*)\rangle}{\theta(q^* - q)} \tag{6}$$

where q^* is the CV value at the transition state. When investigating the content of the previous equation, it is convenient to rewrite it in the following fashion:

$$k^{\mathrm{BC}}_{\mathrm{R}\to\mathrm{P}}(t) = \langle \dot{q}(0)\theta(q(t) - q^*)\rangle_{q(0)=q^*} \frac{e^{-\beta F(q^*)}}{\int_{-\infty}^{q^*} e^{-\beta F(q)}\, dq} \tag{7}$$

A graphical depiction of the various terms is shown in Figure 6.

The kinetic rate constant contains two main ingredients: the ratio of the transition state probability to the reactants state probability (which represents thermodynamic information that can be extracted from the raw FES) and the prefactor measuring the "rate" at which the collective variable changes in time at the transition state, which represents kinetic information that cannot be extracted from the raw FES and hence requires

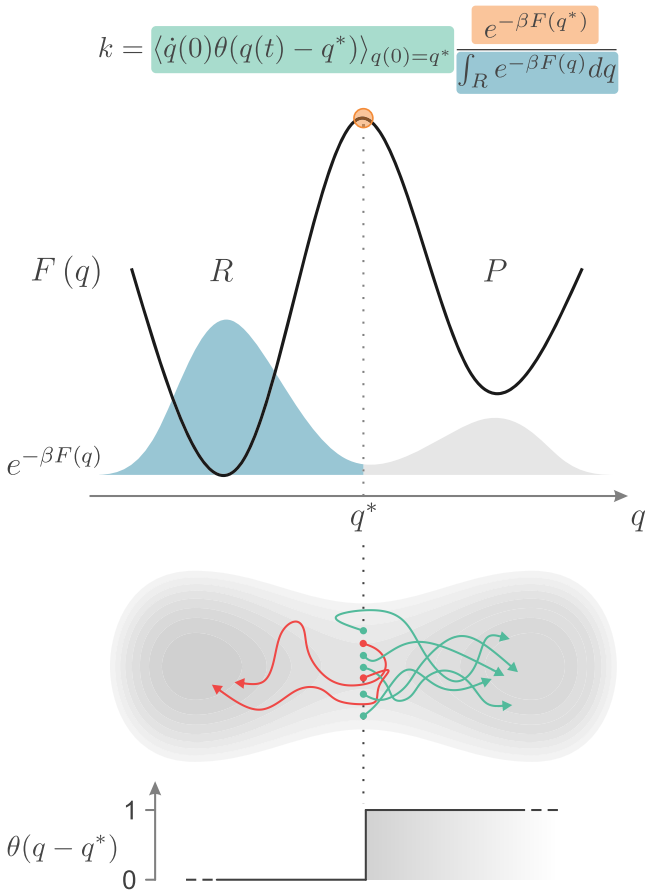

Figure 6. In the Bennett−Chandler approach to reaction rate theory, the kinetic constant of a reaction is the product of two terms: a kinetic term (in green), representing the rate at which the system crosses the transition state assuming it ends up in the products state, and a thermodynamic term, which is the ratio of the transition state probability (orange) to the reactant state probability (blue).

additional assumptions or simulations. The complete prefactor $\langle \dot{q}(0)\theta(q(t) - q^*)\rangle_{q(0)=q^*}$ represents this average rate on the condition that after a certain amount of time t the system has not recrossed the TS back toward the reactant state (which is encoded by the Heaviside function $\theta(q(t) - q^*)$). Explicitly obtaining this prefactor is computationally challenging, as—if using the reactive flux formalism, for instance—hundreds of MD trajectories must be initiated atop the transition state and their time evolution must be monitored in order to assess whether they end up in the reactant or product basin. When DFT is used

https://doi.org/10.1021/acscatal.3c01945
ACS Catal. 2023, 13, 11455−11493

to evaluate the forces, it is computationally not feasible to perform such direct kinetic evaluations. However, we recently performed a proof-of-concept study where the forces were evaluated using an MLP, which made it possible to obtain the kinetic rate constant directly using the BC approach.[4]

In most of the cases, one resorts to the transition state theory (TST) approximation, whereby setting the chances of barrier recrossing to zero, the following expression can be obtained:

$$k_{R\to P}^{TST} = \lim_{t\to 0^+} k_{R\to P}^{BC}(t) = \sqrt{\frac{1}{2\pi\beta}}\,\langle|\nabla_x q|\rangle_{q=q^*}\frac{e^{-\beta F(q^*)}}{\int_{-\infty}^{q^*} e^{-\beta F(q)}\,dq} \tag{8}$$

By performing an analytical integration over momenta, the prefactor is here rewritten as an ensemble average of the q gradient with respect to the mass-weighted coordinates of the system when the system is located at the transition state. For the methylation of ethene in H-ZSM-5, it was shown that the rate constants obtained using the formula above from the umbrella sampling simulations were independent of the CV choice, whereas the underlying free energy profiles in terms of the different CVs were different in shape as illustrated above.

As working directly with kinetic constants can be quite cumbersome and as in standard literature, one often refers to free energy barriers to construct overall free energy diagrams and identify the rate-determining steps and intermediates that are most stable. Therefore, the concept of a phenomenological free energy barrier was introduced by Bučko et al.[123] This quantity is defined as follows, which is obtained by plugging the kinetic constant into Eyring's classical TST equation:

$$\begin{aligned}\Delta F_{phen} &= -\frac{1}{\beta}\ln(k_{R\to P}^{TST}\beta h)\\ &= F(q^*) - \frac{1}{\beta}\ln\left(\sqrt{\frac{\beta}{2\pi}}\,\frac{h\langle|\nabla_x q|\rangle_{q=q^*}}{\int_{-\infty}^{q^*} e^{-\beta F(q)}\,dq}\right)\end{aligned} \tag{9}$$

Analogous approaches to derive accurate kinetic constants from enhanced-sampling simulations have also been successfully applied to metadynamics and blue-moon sampling.[124−126] More detailed information on some enhanced sampling methods within the field of catalysis can be found in a recent review by Rousseau and co-workers.[68] In any case, the awareness that FEPs obtained from enhanced-sampling simulations are not a "free energy analogue" of a minimum-energy path and that extra care needs to be taken to retrieve reaction free energies is rapidly growing in the literature.[123,127,128] Finally, after having completed all previous steps, one can also check the reliability of the results and the sampling by performing a committor analysis or a follow up MD simulation where the FES is inverted and used as a bias. More details on the previous methodological aspects can be found in the paper by Bailleul et al.[120]

3.4. Practical Considerations and Challenges for Complex Reactions in Catalysis. From previous subsections, it became clear that using enhanced-sampling MD simulations for the simulation of complex chemical conversions in nanoporous materials cannot be regarded as a "black-box" method. Even when disposing of the required computational time, a lot of insight is necessary in the methods to correctly interpret and analyze the obtained results. In view of this, it is important to have access to automatic analysis tools to process the simulations. In this respect we refer to our recently launched ThermoLIB code,[129] which is a python/cython library to construct and manipulate FESs as a function of a priori chosen collective variables from output of molecular simulations. The package allows transformation and/or (de)projection of the FES a posteriori to different collective variables as well as extraction of thermodynamic and kinetic properties from it. Furthermore, it is important to have thorough error analysis tools available in terms of data reliability to make sure that the simulations are sufficiently converged and yield statistically relevant results. In this respect, the ThermoLIB code also fully supports error estimation on the obtained thermodynamic and kinetic properties, using the Fisher matrix for maximum likelihood estimators of free energy profiles or more conventional statistical tools such as block averaging.

In terms of computational cost, the use of enhanced sampling methods may become quite expensive. For example, the umbrella sampling approach used in the previous ethene methylation example required about 2000 ps of simulation time. Luckily, the main advantage of US is that the individual umbrellas can be run in parallel. In that case, the reaction path was partitioned into 40 umbrellas, each consisting of 50 ps of simulation. Other enhanced sampling methods such as metadynamics or variationally enhanced sampling are computationally more efficient to generate one-dimensional FESs, but these techniques are not parallelizable (unless a variation such as multiple-walker metadynamics is used). For some reactions, it might not be clear a priori whether the chosen CVs are suited to describe the reactive process. In that case, it might be interesting to perform some exploratory metadynamics runs after which more refined US simulations can be performed. The overall accessible simulation time is of course determined by the method used to simulate the PES. So far, GGA DFT remains the standard methodology to evaluate energies and forces in the field of computational catalysis, as was explained in section 2. Using DFT limits the accessible time scales, as even after simulation for hundreds of picoseconds, the sampling of slow molecular motions may remain incomplete. Luckily, interesting new directions are being explored from a methodological point of view, namely, the development of machine learning potentials. Despite a still scarce application within the field of zeolite catalysis, MLPs show a great deal of potential and may lead to significant breakthroughs in the methodological limitations that are nowadays affecting the length and time scales accessible in computational catalysis. Some more information on the potential of MLPs together with the challenges for the field of zeolite catalysis will be given in section 5.

As previously stated, the selection of proper CVs remains a nontrivial task. If an important degree of freedom is missed, it would lead to misinterpretation of the free energy profile. Recently, new methods have been proposed to systematically investigate whether CVs are missing and which CVs would have to be added.[130,131] However, we are not aware of the application of such methods within the field of zeolite catalysis.

For the methylation reaction illustrated above, definition of CVs was rather straightforward; however, for other reactions, for example, β-scission of reactive alkenes, definition of collective variables may become cumbersome. Recently, various data-driven methods have been proposed to discover proper CVs in a more automated way.[131−134] The field is rapidly evolving, and we direct the interested reader to recent specialized reviews on the topic.[131−133,135] In general terms, automated CV discovery techniques started with linear dimensionality reduction

https://doi.org/10.1021/acscatal.3c01945
ACS Catal. 2023, 13, 11455−11493

techniques such as principal component analysis and multi-dimensional scaling.[131] However, for complex molecular systems as envisaged here, nonlinear dimensionality reduction techniques are beneficial, as they allow mapping of more complex patterns of atomic coordinates to CVs. In this field, deep learning techniques based on artificial neural networks for discovery of high-variance nonlinear CVs have been proposed.[134,136,137] Additionally, various techniques have been proposed to discover the slow CVs, which aim to find linear or nonlinear functions of the configurational coordinates that mimic the slowest-evolving molecular motions of the system. In this last category, many methods exist; however, their applicability within the field of catalysis or nanostructured complex materials remains very limited. For the description of phase transitions in metal−organic frameworks, time-lagged independent component analysis (TICA), a well-established statistical modeling technique incorporated into Markov state modeling that aims to reduce the dimensionality of the problem while minimizing the loss of kinetic information, has successfully been applied.[138] However, the applications of such data-driven methods within the field of catalysis are nearly nonexistent, apart from some recent notable exceptions.[139] Clearly, the field could benefit greatly from the development and implementation of such automated CV discovery methods for the description of catalytic phenomena.

Lastly related to the definition of CVs, we also mention that it is sometimes necessary to introduce additional potential walls to prevent the system from visiting unwanted parts of configurational space. This can be useful, for instance, to limit the diffusion motion of an adsorbate into the catalyst pores or to block a secondary (unwanted) reactive path that could be triggered by biasing along the chosen CVs. The wall selection and placement is generally done in a trial-and-error manner. While it is clear that limiting the available phase space of a mobile reactive molecule will certainly impact its free energy, we are not aware of systematic studies in which the effect of walls on computed properties has been extensively investigated.

From this section, it has become clear that molecular dynamics techniques, in particular enhanced-sampling MD techniques, for the simulation of chemical reactions within the field of catalysis can give substantial new insights. However, various challenges are ahead to integrate them in a standard computational catalysis workflow, and at this point they may not be regarded as mainstream black-box methods. Some of the challenges and hurdles have already been touched upon briefly in this section, but we elaborate more extensively at the end on the challenges ahead of MD techniques in the field of catalysis and how to integrate them into an overall computational workflow for studying catalysis at multiple length/time scales.

3.5. Static versus MD-Based Methods and Comparison with Experimental Kinetic Data. Despite the computational burden and the methodological hurdles that must be overcome with enhanced-sampling MD simulations, they have proven their use for simulating complex chemical conversions under operating conditions, as will be illustrated by some examples in the next sections. One could rightfully ask the question whether there is still a place and position for static methods in the field of computational catalysis. As will become clear from the examples given in the next section, static and dynamic techniques may give complementary insights. In any case, static methods are essential to find those reactions for which more in-depth investigations using MD methods are preferable or even necessary. Furthermore, as within a static or local approach only a few points on the PES need to be determined, it is possible to use computationally much more expensive and accurate electronic structure methods than DFT methods to obtain more accurate electronic energies, as was explained in section 2.

In previous subsections, we mainly focused on how to determine kinetic information from the enhanced sampling simulations; however, comparing theoretical rate constants with experimental values requires not only intrinsic barriers but also information on the adsorbed states. Some more information on adsorption will be given in the next section through the use of some case studies. It will become clear that MD methods when used in combination with DFT-based evaluation of forces are less suited to determine adsorption enthalpies, as extensive MD simulations are necessary. From first-principles MD simulations of reactions one obtains intrinsic reaction rates, i.e., referred to the state where all species are adsorbed on the catalyst.[98,140,141] To compare to experimental data, one needs the apparent rate constants, which include the adsorption energy, unless the reaction is zeroth-order in the reactant concentrations. In the latter case, the surface active sites are completely covered with the reactant having a reaction order of zero, so that no dependence of the kinetics is observed over the whole measurement range.[141] There are only a few examples available in the literature where kinetics from static and dynamic approaches are compared on one hand and where theoretical kinetic rate constants are compared with experimental kinetic data. This lack of comparative studies can be related to the fact that it is very difficult to measure the kinetic information on single reactions in zeolites. In most cases, many reactions take place simultaneously, prohibiting a one-to-one comparison between experimental and theoretically obtained kinetic information. One of the best benchmarked reactions in zeolite catalysis is the earlier-discussed methylation reaction of alkenes in Brønsted acidic zeolites.[121,122] This reaction has been the topic of various theoretical studies using a plethora of techniques ranging from static methods to MD methods.[120,140,142,143] It is not the intention to give a complete overview of the literature here, but for the sake of completeness, we elaborate on how to compare theoretical with experimental kinetic data and the role of first-principles MD simulations in this endeavor for the methylation of alkenes. As determining adsorption enthalpies directly from first-principles MD simulations is particularly difficult, a possible strategy to compare theoretical and experimentally measured kinetic data is a hybrid approach where the adsorption of ethene is determined from static periodic calculations and the intrinsic rate constant is determined from first-principles MD simulations.[120] The concept and relation between the apparent and intrinsic rate constants are illustrated in Figure 7. The static simulations allow estimation of the equilibrium constant, whereas the dynamic simulations yield the intrinsic rate constant. The finally obtained value for the apparent rate constant is very sensitive to the specific methodology used to calculate the adsorption free energy. The discussion given here clearly shows that it remains a challenge to compare kinetic information from MD simulations with experimental kinetic information. In the endeavor to establish methods for obtaining chemical kinetics of zeolite-catalyzed reactions, a range of methods based on static simulations has been developed by Sauer and co-workers to calculate with chemical accuracy the rate constant for the methylation reaction.[143] A strategy was adopted where very accurate electronic energies were obtained by systematically refining DFT energies with inclusion of dispersion interactions

https://doi.org/10.1021/acscatal.3c01945
ACS Catal. 2023, 13, 11455−11493

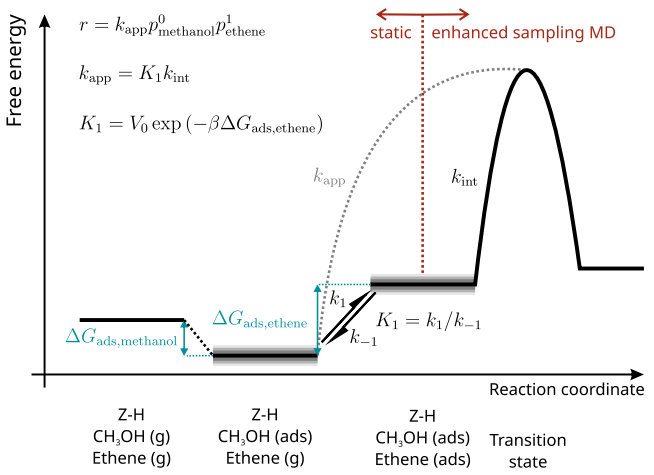

Figure 7. Schematic depiction of the method used by Bailleul et al. to obtain apparent and intrinsic rate constants for the ethene methylation reaction. Adsorption free energies were computed with various static schemes (as highlighted by the gray uncertainty shading), while the reactive step was modeled with enhanced-sampling molecular dynamics. Adapted with permission from ref 120. Copyright 2020 Elsevier.

by expensive wavefunction-based methods. The thermal and entropic contributions were obtained beyond a standard harmonic oscillator approximation by including anharmonic corrections for each vibrational mode.[144,145] For this particular reaction, this strategy was shown to yield results that agree with experiment with chemical accuracy; however, this methodology cannot be regarded as a standard approach. First of all, the methodology is computationally very expensive due to the expensive wavefunction-based methods. Second, for some reactions, proper definition of well-defined reactant and transition states is less trivial, as we will show in the case studies below. This is particularly the case for reactions taking place at higher temperature or in complex reaction environments, i.e., in the presence of water or other guest species. Furthermore, as we will also illustrate in section 4.3, it is not always possible to identify one particular transition state, and broad transition regions might occur. In this case, an MD sampling approach is certainly preferred. Alternatively, one might adopt strategies to account for more transition states in a static approach, but the finally obtained transition state free energies and particularly the entropy might be quite sensitive to the selection of transition states.[146−148]

Previous considerations lead us to conclude that a direct comparison of theoretical and experimental kinetic data with chemical accuracy remains very challenging both with static and MD-based methods. Ideally, methods will become available where one can determine with very good accuracy the electronic energies of the system (i.e., sample the PES with chemical

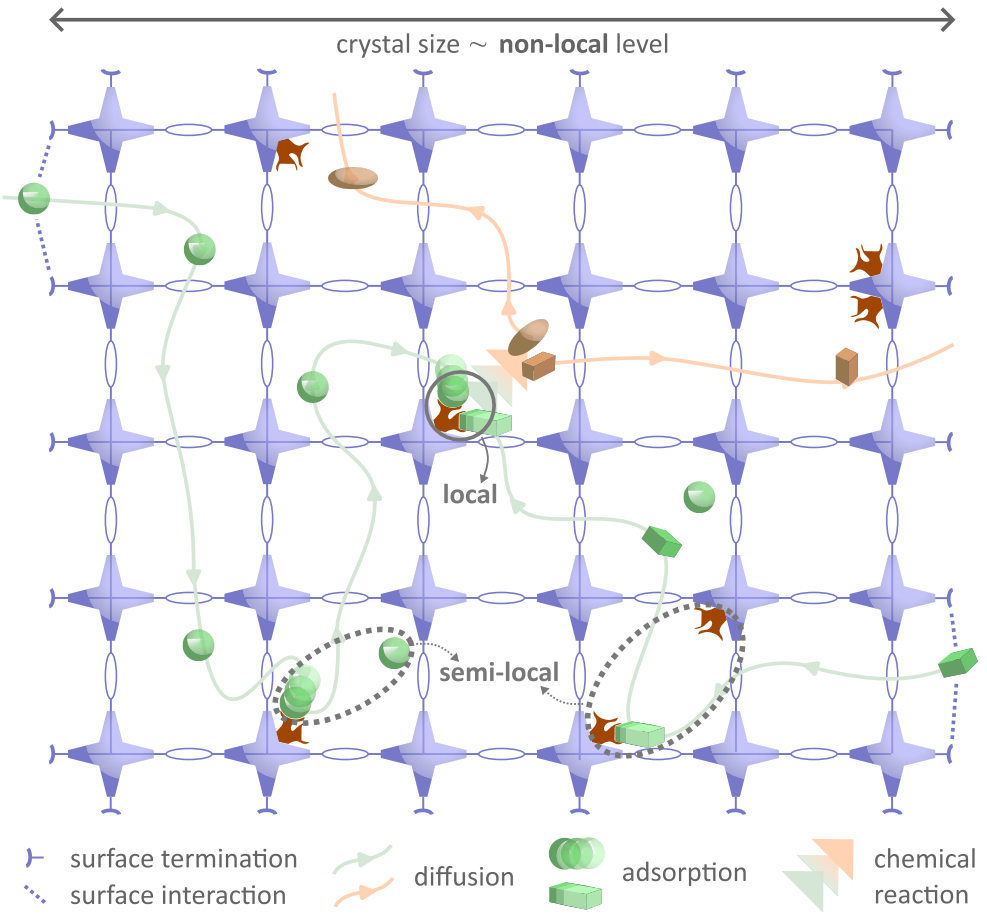

Figure 8. Schematic illustration of the local, semilocal, and nonlocal levels. The local or short-range level comprises the active site and reactive species in direct contact with the active site and has roughly dimensions of 0.1 to 1 nm. The semilocal level encompasses other guest molecules solvated in the pores of the material and possibly other active sites in the neighborhood of the active site. The nonlocal or long-range level extends further to the crystal size level and has dimensions ranging from ca. 2 nm to the crystal size dimensions.

https://doi.org/10.1021/acscatal.3c01945
ACS Catal. 2023, 13, 11455−11493

accuracy) at a reasonable computational cost and use such high-accuracy methods in combination with enhanced sampling protocols as currently used in MD. Such a strategy would allow one to obtain with high accuracy enthalpic and entropic contributions of the chemical reactions of interest.

4. SELECTED CASE STUDIES ILLUSTRATING THE PROS AND CONS OF FIRST-PRINCIPLES MOLECULAR DYNAMICS SIMULATIONS WITHIN ZEOLITE CATALYSIS

In this section, some case studies are discussed to highlight how different aspects of the catalytic process can be discovered by MD simulations. As mentioned in the Introduction, the complexity of a catalytic process is situated at various levels which may be categorized in terms of locality with respect to the active site. A schematic representation is shown in Figure 8. The local reactive level or short-range level includes the active site and reactive species in direct contact with the active site and has dimensions of roughly 0.1 to 1 nm. In the case active sites cooperate, they both need to be present at the local level. The second level—hereafter referred to as the semilocal or midrange level—encompasses other guest molecules solvated in the pores of the material and possibly other active sites in the neighborhood. To further define the semilocal level, we can make the analogy with solvated ions, where this semilocal level would correspond to the second solvation shell. It is clear that the conditions and the number and nature of the molecules present in the semilocal level have an important effect on the reactivity. During the course of a catalytic process, molecules that were originally in the semilocal level can dynamically enter the local level. The spatial extent of the semilocal level has dimensions extending to approximately 2 nm maximum, which would also correspond to the definition of micropores according to the IUPAC convention of porous materials.[149] A third level consists of the nonlocal or long-range level, having dimensions in the range from 2 nm to the crystal size. The latter may vary from 50 nm to the micrometer level. This nonlocal level is typically very important for transport of reactants, products, and other species present in the reaction feed. Transport itself is a very complex phenomenon and encompasses not only intracrystalline diffusivity but also interactions of reactants with external surfaces of the catalyst particle. Diffusivity may be hindered or free, and transporting molecules may interact with specific active sites. In this sense the distinction between the three levels is made to structure the discussion, but it is important to realize that during the lifetime of a catalytic process, there may be dynamic interchanges between the local, semilocal, and nonlocal levels. Lastly, the distinction made here takes the active site as the reference point; in reality, active sites are distributed over the catalytic sample, and ensemble averages of reactivities from different active sites will finally lead to the observed experimental reactivity.

The case studies taken up in this section give insight into various aspects of the catalytic phenomenon and will particularly highlight how MD simulations can give insights into the various levels introduced above. Hereafter the four case studies are briefly introduced. The first case study illustrates how MD simulations can reveal the nature of reactive intermediates at operating conditions, where it is discussed how MD simulations are essential to discover the nature of adsorbed alkenes on Brønsted acidic sites. It will be shown that static simulations are not sufficient to uncover how adsorbed alkenes behave at extreme reaction conditions, i.e., temperatures higher than 500 °C, which are typically found in catalytic cracking. The second case study deals with the dynamic change of the active site itself under reactive conditions. The third case study deals with the importance of competitive reaction routes and shows how MD is quintessential to revealing the importance of multiple reaction pathways under operating conditions. These first three case studies are all situated at the local and semilocal level. The fourth case study discusses some results on the diffusion of reactive intermediates at operating conditions and shows how MD can give insights into intracrystalline diffusion. Diffusion obviously takes place at the nonlocal level, but we will show how first-principles MD simulations can also give insight into diffusion at operating conditions when the diffusion is hindered.

4.1. Reactive Intermediates at Operating Conditions and Adsorption Enthalpies.

To illustrate how first-principles MD methods may be extremely useful to obtain insight into the nature of reactive intermediates at operating conditions, the case of alkene adsorption on Brønsted acid sites (BASs) is discussed in this subsection. This case study is inspired by alkene cracking over zeolites but is of broader importance for any chemical transformation within a Brønsted acidic zeolite where a double bond needs to be activated. Zeolite-catalyzed alkene cracking typically occurs at very high temperatures, i.e., higher than 500 °C. At these high temperatures, tracking the reactive intermediates with in situ and operando techniques is very difficult. Furthermore, some intermediates are very reactive and may quickly transform into other species.[150−152] Also, in other important chemistries like the zeolite-catalyzed C_1 catalysis where methanol, carbon dioxide, and dimethyl ether are converted to platform chemicals, the importance of dynamic sampling was revealed to determine the reactive intermediates at operating conditions.[153−156] Standard static approaches—also sometimes called local approaches—may completely fail in describing the correct nature of the reactive intermediates at operating conditions.[42,148,157,158] The reason for this shortcoming lies in the fact that static methods search for local minima on the 0 K PES and afterward thermal corrections are added to obtain thermodynamic quantities such as adsorption enthalpies, entropies, etc. However, at the alkene cracking conditions, starting from minima obtained from the 0 K PES is not a good assumption, as some of them may not prevail at the higher reaction temperatures. Within this respect, it is important to acknowledge the difference between the PES and the free energy surface (FES). The FES is obtained by accounting for contributions originating from the partition function evaluated in the appropriate thermodynamic ensemble. The most common ensembles used in theory are constant temperature, constant volume (NVT) or constant temperature, constant pressure (NPT) ensembles. However, a lot of other ensembles are possible depending on the thermodynamic control variables.[62,159] The terminology "free energy" is often colloquially used, whereas in fact it may refer to the Helmholtz free energy $F(N, V, T)$ when N, V, and T are constant or the Gibbs free enthalpy $G(N, P, T)$ when N, P, and T are constant. When interested in finding reactive intermediates at operating conditions, we should explore the FES to find (meta)stable states or interesting paths between various intermediates. The PES is an essential ingredient of the FES, but the FES may drastically differ from the underlying PES, certainly when the stability of intermediates is evaluated at higher temperatures. A schematic figure showing an abstract representation of a high-dimensional PES and derived low-dimensional FES profiles in

https://doi.org/10.1021/acscatal.3c01945
ACS Catal. 2023, 13, 11455−11493

terms of certain important reaction coordinates is shown in Figure 9. Figure 9b from top to bottom shows the lowest-energy

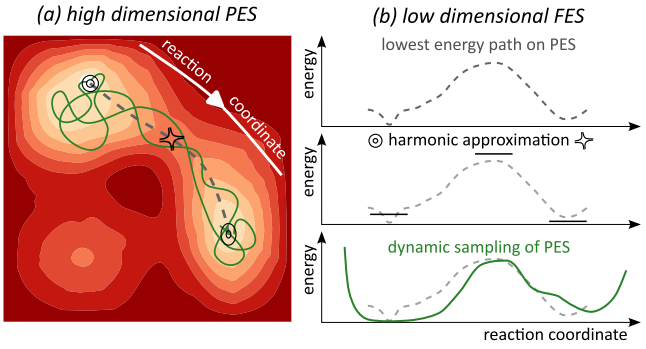

Figure 9. Abstract representation of a high-dimensional PES and derived low-dimensional free energy profiles in terms of important reaction coordinates.

path on the PES, the free energy differences between two minima connected by a maximum in the harmonic oscillator approximation (thereby neglecting dynamic sampling on the PES), and the free energy profile obtained when sampling dynamically at the right operating conditions. It is clearly seen that the green curve has a significantly different profile than the dotted curve on the PES, indicating the difference between the lowest energy path on the PES and the free energy curves.

Hereafter, we specifically illustrate these concepts for the adsorption of alkenes in Brønsted acidic zeolites. When an alkene adsorbs within the zeolite, four possible adsorbed states can be identified, which are schematically depicted in Figure 10a for 2-pentene. When the alkene interacts via weak dispersion interactions with the zeolite walls, a physisorbed van der Waals complex (indicated as freely adsorbed 2-pentene in the figure) is formed; when the double bond interacts with the acid proton, a physisorbed π complex is formed; in the case where the double bond gets protonated by the zeolite, a carbenium ion is formed; and last, a framework-bound alkoxide can be formed when a covalent C−O bond is formed between the alkyl chain and the lattice.

The relative probability of finding the various intermediates depends on a variety of factors, such as the zeolite confinement, the carbon number of the alkene, its degree of branching, and the operating conditions. More specifically, the temperature may drastically change the fate of the various intermediates. Molecular simulations have the potential to shed light on the nature of the reactive intermediates at the molecular scale; however, the outcome of the theoretical predictions may be strongly dependent on the method used to describe the PES and the representation of the zeolite model. Within this Perspective, we want to highlight the potential added insights obtained from MD simulations. Therefore, we will only briefly comment on the impact of the electronic structure method and zeolite model on the stability of the various adsorbed species. More extensive reviews on these aspects can be found in the literature.[32,46,160,161] In short, from these dedicated studies, the following conclusions were found. First, earlier zeolite models consisting of a small number of T atoms, which only accounted for a very limited part of the zeolite environment, predicted alkoxides as the most stable intermediates.[162−164] Upon shifting to a more realistic representation of the zeolite host (periodic models or extended cluster models), the relative stability is drastically changed, and alkoxides do not always remain the most stable species, even at low temperatures. Of course the degree of branching is very important in this sense, as tertiary alkoxides experience more steric repulsion with the framework and are therefore less stabilized compared to primary or secondary alkoxides. Carbenium ions follow the opposite stability order, with the tertiary being more stable than the secondary and primary. Second, the adopted electronic level of theory plays a decisive role in the relative stability of various intermediates. In particular, dispersion interactions or other nonbonding interactions with the zeolite walls may profoundly impact the energetics. Within the current literature, most theoretical calculations use DFT methods with some particular exchange−correlation functionals amended with a method to describe the dispersion interactions. In this respect, the DFT-D methodology proposed by Grimme, where the standard DFT energy is corrected with a parametrized damped dispersion term, has become very popular.[51] The success of this methodology is rooted in the computational ease of the DFT-D method, although it was recently shown that the DFT-D method also has its limitations, especially for the description of relative stabilities of dispersion-dominated species.[44,46,59,161,165,166] For example, the PBE-D level of theory has become the standard method within a broad range of solid-state studies, but it overestimates the stability of carbenium ions compared to physisorbed π complexes.[165,167] Various reports have recently appeared within the field of zeolite catalysis and adsorption, where expensive wavefunction methods or hybrid methods have been proposed to obtain more accurate adsorption energies (vide infra). These specific methods are computationally very demanding and were almost exclusively used in a static simulation protocol.[43,142,166−171] Given their computational expense, the use of such methods to perform MD runs spanning long simulation times is not feasible. Recently, new approaches were suggested to obtain in a computationally more feasible way accurate free energies for adsorbed complexes, combining sampling by means of MD and refinements at higher levels of theory.[161,165,172,173] On the other hand, low-scaling periodic implementations of advanced methods such as MP2, double hybrids, and the random phase approximation (RPA) are becoming available in mainstream computational chemistry software.[174−177] Given the concomitant increase in data efficiency of the most recent machine learning potential architectures, it seems likely that soon it will be possible to perform cheap MLP simulations on a chemically accurate PES learned from a limited set of high-level single-point calculations.

To illustrate the impact of temperature on the nature of the prevailing intermediates at operating conditions, some results on MD simulations of linear and branched pentenes within H-ZSM-5 at three temperatures, namely, 50, 300, and 500 °C, performed with the revPBE-D3 methodology, are shown in Figure 10b,c. Each of the simulations started from a carbenium ion configuration, which was followed during an MD run of 100 ps.[42,148,158] The nature of the adsorbed species was identified based on a distance criterion between the carbon backbone of the alkene and the zeolite lattice. The linear pentyl carbenium ion was found to be unstable and immediately deprotonated into a physisorbed pentene π complex at 50 and 300 °C. However, at 500 °C, some (de)protonations of *n*-pentene occurred during the MD run, resulting in a short lifetime for the linear carbocation. As a result, linear carbenium ions were concluded to be metastable at cracking temperatures. Furthermore, linear secondary alkoxides were stable intermediates at the lowest temperature but had the tendency to quickly transform into

https://doi.org/10.1021/acscatal.3c01945
ACS Catal. 2023, 13, 11455−11493

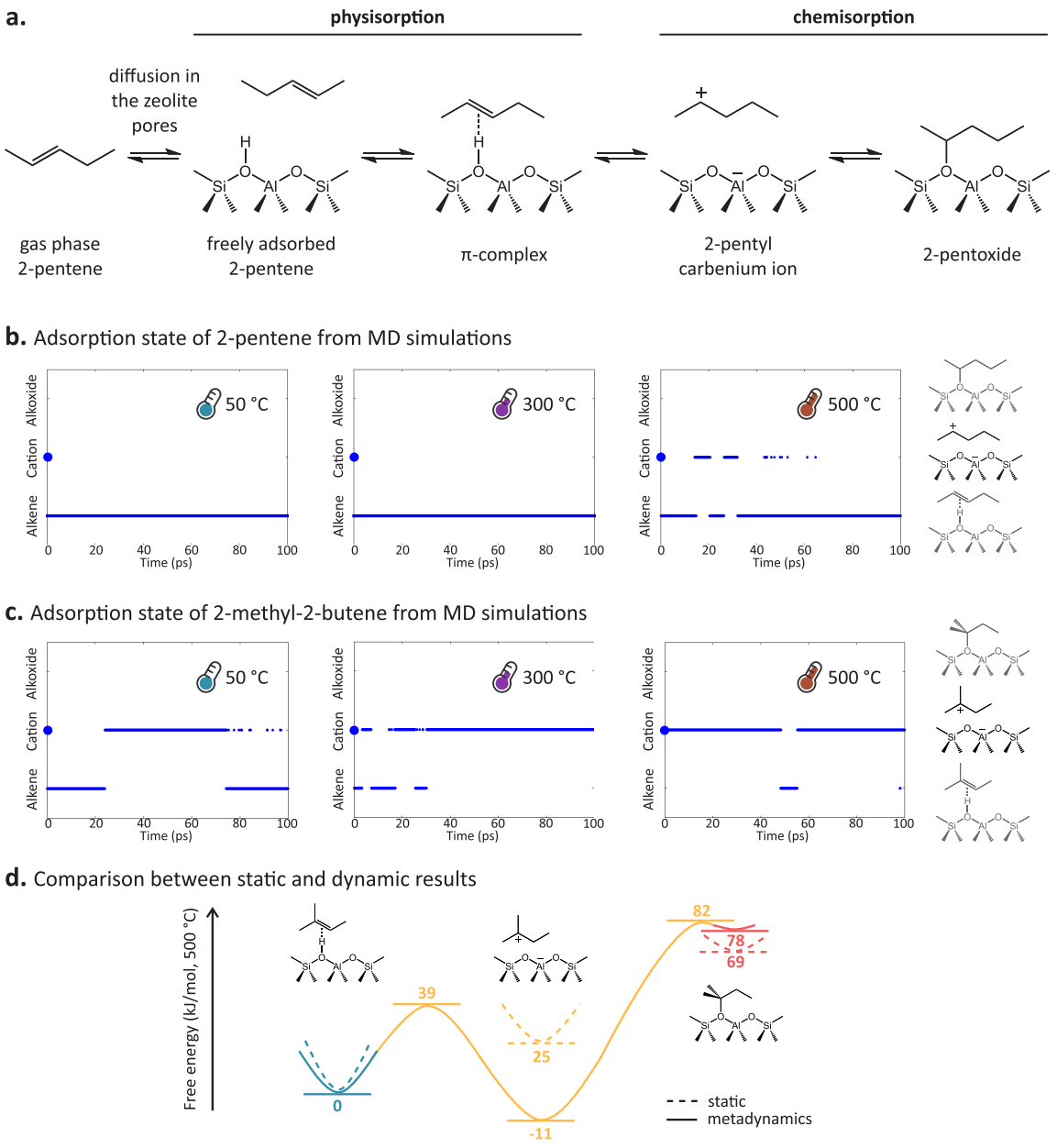

Figure 10. (a) When an alkene is adsorbed in a zeolite, its interaction with the Brønsted acidic site can lead to the formation of a physisorbed π complex or a chemisorbed carbenium ion. The latter can then bind to the framework to form a surface alkoxide species. (b) Time evolution of the various intermediates of 2-pentene during a regular MD simulation starting from the 2-pentyl cation within H-ZSM-5 at three different temperatures. (c) Time evolution of the various intermediates of 2-methyl-2-butene during a regular MD simulation starting from the 2-methyl-2-butyl cation at three different temperatures. The states indicated with an alkene are a combination of the π complex and the van der Waals complex. (d) Free energy differences between the 2-methyl-2-butene within H-ZSM-5 intermediates obtained from static calculations and metadynamics simulations at 500 °C.

physisorbed species at higher temperatures. At 500 °C, frequent transitions were also observed between the two physisorbed states (vdW complex and π complex). The π complex is energetically more stabilized due to the π−H interaction between the Brønsted proton and the double bond; however, the vdW complex may move more freely inside the zeolite pores and thus gain entropic stabilization at higher temperature. In principle, it would be very interesting to disentangle the enthalpic and entropic contributions from these simulations; however, very long simulation times would be necessary. Some more information about these aspects is given later in this section. For a recent perspective on various methods to account for dynamics and anharmonicity in the calculation of entropies within the field of heterogeneous catalysis, we refer to the paper of Rousseau and co-workers.[157]

For branched alkenes, the stability of carbenium ions is expected to increase because of the possibility of forming tertiary carbocations. In contrast to 2-pentene, when simulating the branched 2-methyl-2-butyl carbenium ion during an MD simulation (Figure 10c), the carbocation state is visited throughout the majority of the simulation time and is characterized by very long lifetimes, even at lower temperature. Furthermore, the tertiary 2-methyl-2-butoxide immediately transformed into a carbenium ion or physisorbed alkene at all temperatures. As the temperature increases, the lifetime of the carbenium ion also increases, and thus, it may be concluded that

https://doi.org/10.1021/acscatal.3c01945
ACS Catal. 2023, 13, 11455−11493

at operating conditions branched carbenium ions would be stable and important reactive intermediates.

Previous results show that regular MD simulations allow one to give insight into the probability of finding reactive intermediates at operating conditions and also illustrate the impact of temperature on the nature of the intermediates. In general, higher temperatures promote species with more configurational freedom, such as carbenium ions and physisorbed alkenes, whereas at lower temperatures, enthalpically stabilized species, such as alkoxides, may be promoted. Care needs to be taken in estimating the nature of the prevailing intermediate solely on one parameter (i.e., here the temperature), as other parameters such as branching, chain length, and topology also affect the stability of the various species.[113,178−181] In any case, MD simulations are particularly useful to properly account for the mobility of the ensemble of possible adsorbate configurations at higher temperatures.

In the next step, it is very interesting to also quantitatively determine the relative free energies of the various intermediates and barriers separating them. The MD simulations shown so far do not allow to extract this precise information. First of all, the sampling time, albeit being hundreds of picoseconds, is too short to deduce accurate free energy differences. Second, some of the intermediates are separated by an activation barrier. During regular MD simulations, some transitions were observed between the various adsorbed species; however, the number of transitions is insufficient to also deduce free energies or activation barriers from such simulations. To also determine free energy profiles, one has to resort to enhanced-sampling simulations as explained in section 3. For the case of the branched C_5 species 2-methyl-2-butene, such a free energy profile was determined at 500 °C using two one-dimensional metadynamics simulations. In the first simulation, a collective variable was introduced to describe the proton transfer from the zeolite framework to the alkene double bond, forming a tertiary carbenium ion, whereas in the second simulation, the collective variable described the formation of the covalent C−O bond between the carbenium ion and the zeolite lattice. Note that, alternatively, one could also perform a single two-dimensional metadynamics simulation, biasing two CVs, where the resulting 2D free energy surface can be reduced to a 1D free energy profile by searching the minimum free energy path connecting the different local minima.[182] The resulting free energy profile is shown in Figure 10d, together with the free energies obtained from static calculations at the same level of theory, where thermal corrections were added through the harmonic oscillator approximation. It is immediately clear that at high temperature the 2-methyl-2-butyl carbenium ion becomes substantially more stabilized relative to the physisorbed alkene compared to the static calculation predictions. Upon inspection of the MD trajectories, it becomes clear that within the MD run, the carbenium ion is rather mobile at 500 °C and thus becomes entropically favored. Also notice that due to the high entropic penalty of forming a covalent bond with the framework at this high temperature, the alkoxide formation is characterized by a high barrier, and the 2-methyl-2-butoxide is highly unstable.

The previous case study clearly shows the added value of MD simulations to reveal the nature of reactive intermediates under operating conditions and furthermore shows how free energies obtained from static calculations may severely differ from the dynamics-based predictions. The importance of first-principles dynamic sampling for determination of important intermediates was shown in various other papers, where also experimental evidence was given for the prevalence of crucial intermediates.[183,184] Despite the advantages of MD simulations, some critical remarks and potential future directions are worth mentioning here.

First of all, previous simulations—both regular MD and enhanced-sampling MD—are inherently limited by the attainable simulation time. For the regular MD simulations, a total simulation time of 100 ps was achieved; hence, using a time step of 0.5 fs, at least 200 000 individual electronic energy calculations at the DFT level have to be performed. The small time step of 0.5 fs is necessary to obtain adequately converged simulations and sample also the highest frequency modes with sufficient accuracy. Each energy calculation was performed on a fully periodic model of H-ZSM-5 with about 300 atoms in the unit cell. Previous works have shown that also the zeolite topology plays an important role in the stabilization of the various adsorbed alkene intermediates, and thus, it would be very interesting to obtain in a more systematic way information on how various parameters—temperature, topology, branching, etc.—influence the stability of these intermediates.[113,148,178−181,185186] With the brute-force MD approach sketched above, where all energy and force calculations have to be done at the DFT level or even more accurately by electronic structure methods, it is therefore far from possible to perform such systematic investigations. The limitations associated with expensive ab initio simulations might be overcome in the future by using more efficient machine learning potentials that are parametrized on underlying accurate first-principles data (vide infra).

A second point concerns the choice of collective variables. Previous free energy profiles were obtained by performing two separate 1D metadynamics simulations requiring between 40 and 70 ps of simulation time each. Ideally it would be possible for this particular case study to employ a more complex collective variable that enables all intermediates to be included in a single free energy profile, as we have recently done to study the formation of surface ethoxide species in the ethylation of benzene with ethene.[187] We showed that while it is indeed feasible to use a linear combination of coordination numbers to perform one-dimensional umbrella sampling simulations, this approach can also result in poor sampling of potentially important regions of the phase space. On the other hand, with the statistical tools presented in the previous section, this issue can be straightforwardly identified and addressed with, for instance, the addition of extra two-dimensional umbrellas along the reaction path.

Lastly, it would be very interesting to disentangle the separate enthalpic and entropic contributions from the free energy profile obtained with enhanced sampling of MD simulations. When interested in adsorption data that can be used in microkinetic models or reaction networks, it would be necessary to obtain adsorption enthalpies with chemical accuracy, i.e., having an accuracy of 4 kJ/mol compared to exact benchmark values.[188] In contrast to static calculations, where by construction one immediately receives the various contributions to the free energy barriers, the separate enthalpic and entropic contributions do not straightforwardly follow from MD simulations. On the other hand, static calculations do not account properly for the configurational mobility, thus resulting in inaccurate predictions of the entropies.[165] To obtain the separate entropic and enthalpic contributions from an MD simulation, one could in principle use a brute-force approach where the entropies are estimated by subtracting the internal energy from the free energy

https://doi.org/10.1021/acscatal.3c01945
ACS Catal. 2023, 13, 11455−11493

obtained from the enhanced-sampling MD simulation. Bučko et al. performed this procedure for monomolecular cracking of propane in chabazite, where the free energies were obtained from thermodynamic integration.[112] The major problem with this direct approach is that excessive sampling is necessary to obtain accurate internal energies from MD simulations. In principle, to determine the entropic contribution to differences in free energy between various molecular states from MD simulations, there are various options to proceed. First of all, one could perform very long regular MD simulations where the reactive species dynamically switches between states labeled with A, B, and C. In this case A, B, and C would correspond to the alkene, the carbocation, and the alkoxide, respectively. Sufficiently long MD runs would be necessary to sample the transitions between all various states with high enough frequency; only then would the relative probability (and hence stability) be reliably represented. From such simulations, one could determine the probability p of each state and compute the corresponding free energy from $F = -k_B T \ln p$. This information then also allows the entropy to be extracted through various possible procedures: (a) for each state one could determine the average enthalpy H and compute the entropy S using the standard thermodynamic formula $(H - F)/T$, or (b) the free energies F could be computed at different temperatures $T_1 = T - \Delta T$ and $T_2 = T + \Delta T$ and the numerical differentiation approximation to the expression $S = -\left(\frac{\partial F}{\partial T}\right)_{V,N}$, leading to $S(T) \approx -\frac{F(T+\Delta T) - F(T-\Delta T)}{2\Delta T}$, could then be used to compute the entropy. From a purely conceptual point of view, this procedure could be followed; however, there are some hurdles which may prevent us from doing so: first, it is not always trivial to unambiguously identify the states A, B, and C, and second, the most critical point is the length of the simulations and the resulting sampling of the transitions between the various states with sufficiently high frequency. The straightforward determination of all these thermodynamic properties from MD simulations is quite sensitive to statistical noise (e.g., numerical differentiation magnifies statistical noise), and prohibitively long simulations would have to be performed, which are certainly beyond what is feasible today with DFT simulations.

To determine adsorption enthalpies, various calculation schemes have been proposed to obtain these quantities with near chemical accuracy, i.e., with an accuracy of 4 kJ/mol compared to exact benchmark values.[188] Many of them are based on static calculations, but recently new schemes have been proposed based on machine learning concepts, MD simulations, and a thermodynamic perturbation approach to obtain adsorption enthalpies with near chemical accuracy at a feasible computational cost.[45] The method relies on the Δ-ML method, where first an inexpensive MD run is done at a computationally feasible level of theory, and afterward a limited number of data points are selected along the trajectory, which are calculated with a very accurate level of theory such as RPA. On the selected configurations, an ML model is trained to estimate afterward the difference between the lower- and higher-level configurations for all samples. Finally, a thermodynamic perturbation approach is used to reweight the energy differences from the lower level of theory and obtain the correct statistical distribution at the higher level of theory. The interested reader is referred to the original paper of Rocca and co-workers.[45] For the sake of clarity we mention the key formulas derived in the cited paper to obtain the adsorption enthalpy along these lines:

$$\Delta_{ads}H(T) = \langle V'_{zeolite+adsorbate}\rangle_{H'} - [\langle V'_{zeolite}\rangle_{H'} + \langle V'_{adsorbate}\rangle_{H'}] - k_B T \quad (10)$$

where $\langle V'_X\rangle_{H'}$ is the ensemble average of the potential energy of species X evaluated at the higher level of theory to which the Hamiltonian H' is associated. Using thermodynamic perturbation theory, one can prove that the expensive $\langle V'_X\rangle_{H'}$ can be calculated using following formula:

$$\langle V'_X\rangle_{H'} \approx \frac{\sum_{i=1}^{N_{tot}} V'_i \exp\left(-\frac{V'_i - V_i}{k_B T}\right)}{\sum_{i=1}^{N_{tot}} \exp\left(-\frac{V'_i - V_i}{k_B T}\right)} = \frac{\sum_{i=1}^{N_{tot}} V'_i \exp\left(-\frac{\Delta V_i}{k_B T}\right)}{\sum_{i=1}^{N_{tot}} \exp\left(-\frac{\Delta V_i}{k_B T}\right)} \quad (11)$$

where the summation runs over all N_{tot} configurations generated in the production run and where V is associated with the less expensive QM approximation and V' is associated with the higher level of theory. As the ΔV_i can now be calculated in a computationally very cheap way by means of the ML model, this method gives a reliable way of calculating adsorption enthalpies in a computationally affordable way.

In their work Bučko et al. applied the scheme to calculate adsorption enthalpies of CH_4 and CO_2 on all silica and protonated chabazite frameworks and found values which are very close to experimental data. Some side notes are interesting. The method will only provide accurate results in the case that the low- and high-level Hamiltonians sample similar parts of configuration space. In cases where the overlap between the phase space sampled at the lower and higher levels of theory is very small, the perturbative approach would give lower accuracy. The method can only be successfully used if the training set includes all necessary states to capture the adsorption behavior. For example, in the case of alkene adsorption, further testing would be necessary on how to specifically choose the training set in order to obtain an accurate adsorption landscape encompassing the physisorbed π complex, the carbocation, and the alkoxy species. The work of Bučko and Rocca was later extended to also obtain accurate activation energies for chemical reactions.[173] As this field is evolving very fast, also other groups have recently proposed advanced hybrid calculation schemes, where MD simulations are to some extent part of the scheme to sample beyond the local minima one usually explores with static simulations.[161,189]

Summarizing this section, MD is very beneficial to obtain qualitative insights into the nature of the adsorbed species at operating conditions; however, due to the expensive ab initio-based methods used for evaluating the forces, it is less trivial to obtain accurate thermodynamic quantities such as enthalpies or entropies. Future directions should investigate methods where the expensive force evaluations at the quantum-mechanical level can be circumvented in order to allow for more extensive sampling of phase space. In the previous sentence, we intentionally wrote at the quantum-mechanical level, as DFT methods by themselves may not be accurate enough for the purpose of obtaining quantitative adsorption energies and enthalpies.

4.2. Dynamic Evolution of Catalytic Active Sites within Zeolite Catalysis. Active sites may dynamically change when exposed to operating conditions, such as varying temperatures, the presence of guest molecules, pressure, etc. Traditionally, zeolites were thought to be rather static materials with well-defined pores and windows and a very stable framework

https://doi.org/10.1021/acscatal.3c01945
ACS Catal. 2023, 13, 11455−11493

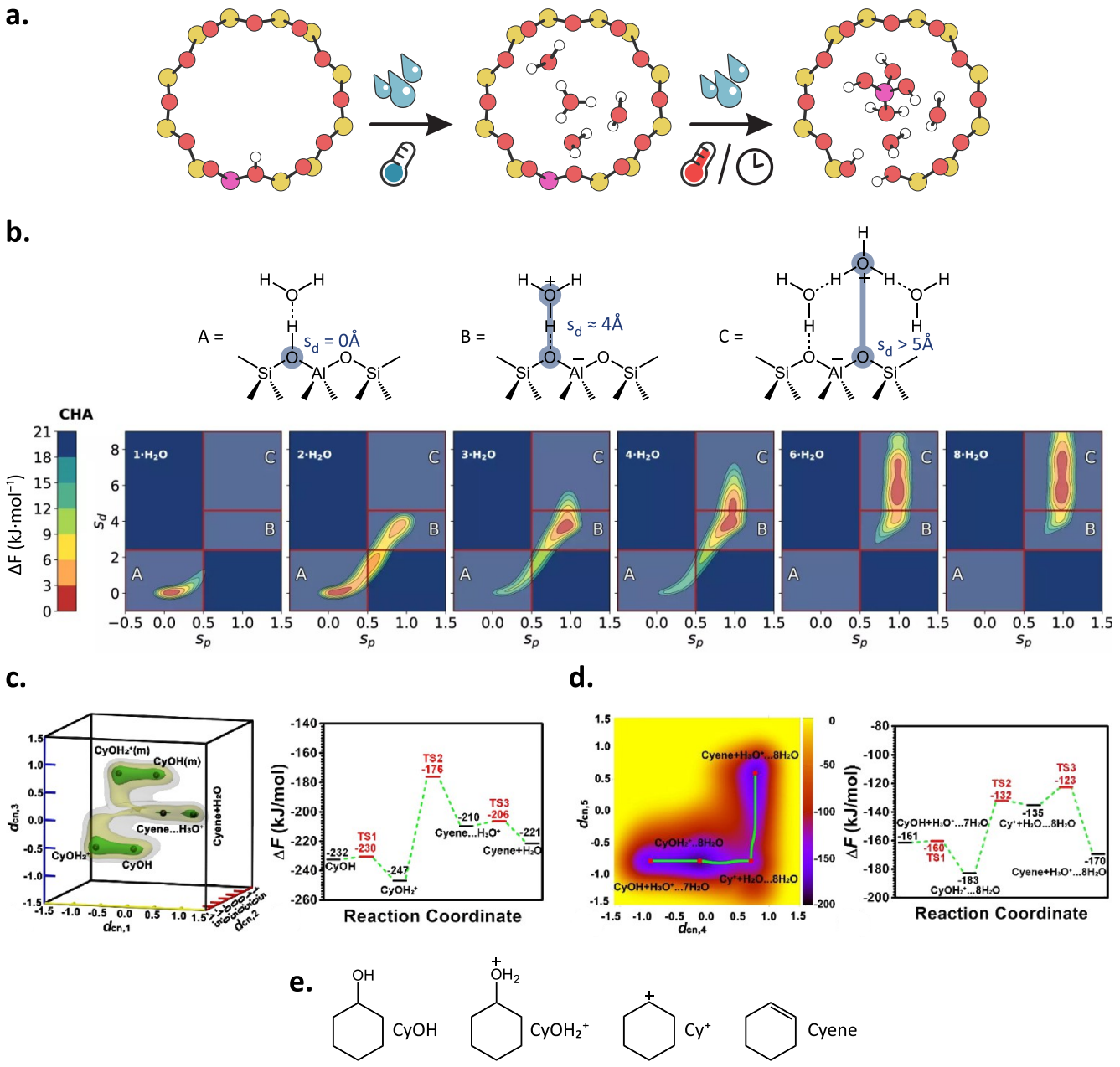

Figure 11. (a) Schematic depiction of the water-induced evolution of a pristine BAS to a solvated hydronium ion and, with longer times and/or higher temperatures, to EFAL-type species. (b) Two-dimensional free energy profiles (300 K) illustrating the BAS solvation in H-CHA for different water loadings using the collective variables recently proposed by Grifoni et al.[210] Three regions can be identified in the FES. The first one (A) corresponds to the BAS located on the framework, which fundamentally disappears with three water molecules/unit cell (u.c.). The second (B) corresponds to a hydronium ion in the proximity of the framework Al and remains significant in the range of two to four water molecules/u.c. Finally, the third region (C) is a fully solvated and mobile hydronium ion, which becomes prevalent with six water molecules/u.c. (c) Three-dimensional FES for the conversion of cyclohexanol to cyclohexene in anhydrous H-Beta together with the minimum free energy path one-dimensional profile. (d) Two-dimensional FES for the conversion of cyclohexanol to cyclohexene in H-Beta with 8 additional water molecules in the unit cell, together with the minimum free energy path one-dimensional profile. e. Intermediates nomenclature used in c and d. Adapted with permission from ref 210. Copyright 2021, Springer Nature and ref 217. Copyright 2021, American Chemical Society.

consisting of relatively strong Si−O and Al−O bonds (Figure 2). However, recent awareness has grown that the catalytically active sites can reorganize dynamically with varying process conditions.[190−195] A typical example is represented by metal-loaded zeolites, where it has been shown that metal cations coordinated to the zeolite active site can become mobilized after interaction with the reactants or the reaction intermediates.[193] For instance, in the selective catalytic reduction (SCR) of NO_x with copper-loaded H-SSZ-13 zeolite, enhanced sampling techniques have been used with success to unravel the mobility of the reacting catalytic diaminocopper(I) complex at low temperature (473 K).[190] More recently, we used umbrella sampling simulations to further investigate the diffusion process and discovered that in the presence of an excess of reacting NH_3 and NO molecules, the formation of bulkier complexes hinders the passage of copper in the 8-ring window of the H-SSZ-13 zeolite.[196] In this case, given the high mobility of the species

https://doi.org/10.1021/acscatal.3c01945
ACS Catal. 2023, 13, 11455−11493

involved, the reaction would not be suited to be studied with static methodologies.

While the mobility of metal ions gives rise to a great deal of fascinating chemistry, in the remainder of this section we will focus on the dynamic active site evolution triggered by the adsorption of water in Brønsted acidic zeolites. This topic has gained a lot of attention recently, as the new feedstocks that are expected to gradually substitute fossil resources—biomasses in particular—often carry a large water content, and their conversion typically requires milder conditions than the traditional petrochemical processes.[197] The interaction of water with Brønsted acidic zeolites is particularly fascinating because of the multiscale nature of the active site modifications that can occur in the framework. When water adsorbs in the zeolite pores, it readily solvates the BAS, forming mobile hydronium ions with remarkable changes in the catalytic properties of the material (Figure 11a). Within the framework of the methanol conversion taking place on zeolites, similar solvation of BAS was observed with other protic molecules, like methanol, where at higher methanol loadings protonated clusters were observed which may also be the onset for further reactions.[98,191] On longer time scales, water can also directly attack the framework bonds, provoking even more extended modification to the zeolite properties and forming new active sites such as extraframework aluminum species (EFALs) (Figure 11a).

In the following paragraphs, a selection of case studies where enhanced sampling has provided fundamental insights on the role of water in dynamically changing the nature of the zeolite BAS over various time scales are reported. We do not attempt to cover zeolite−water interactions in detail, as excellent reviews are already present in the literature, but rather focus on the use of enhanced sampling methods to understand the phenomenon.[198−201]

BAS solvation upon water adsorption is, interestingly, strongly dependent on the number of water molecules that interact with the BAS itself. Seminal work using MD simulations provided early evidence that there exists a critical threshold in the number of protic molecules that are required to solvate and mobilize the BAS.[147,202−208] Expectedly, this number decreases with increasing acidity of the BAS (for instance, going from a Si-doped AlPO framework to an Al-doped Si one) and increasing basicity of the adsorbate (for instance, changing water to methanol). To make these observations more quantitative, Liu et al. used multiple-walker well-tempered metadynamics to investigate the free energy landscape of proton transfer reactions in H-ZSM-5 at 330 K.[209] They found that the proton resides on the framework when one water molecule is adsorbed. With two water molecules, the proton shuttles between the framework and the water cluster with a barrier of only 0.4 kcal·mol^{-1}. Finally, with three water molecules, complete solvation as hydronium ion, $[H_3O(H_2O)_n]^+$, is observed. Similar results were obtained by Grifoni et al., who used metadynamics to systematically investigate the effect of multiple water loadings over a broad range of zeolite frameworks.[210] Figure 11b shows the two-dimensional free energy surfaces obtained with H-CHA (the trend is qualitatively similar in all investigated frameworks). As is visible, starting from two water molecules per unit cell, the free energy minimum in the distance between the protonated site and the oxygens surrounding the Al defect shifts toward larger and larger values. It is obvious that BAS solvation leads to quite a few remarkable changes in its reactivity. Despite becoming somewhat similar to a hydronium ion in bulk liquid water, the confinement effects of the zeolite micropores do create a more active hydronium ion toward acid-catalyzed reaction. We refer the interested reader to the pioneering work of Lercher and co-workers on the topic.[211−213]

To showcase how enhanced sampling is essential to provide mechanistic details about reactions conducted in the presence of water, we focus on alcohol dehydration, although other reactions where water is important, such as the methanol to olefins (MTO) process, have also been subjects of investigation.[214,215] Thanks to the high content of oxygenated compounds in biomasses, alcohol dehydration has become an important case study in the literature. Recently, Mei and co-workers investigated the mechanism of cyclohexanol dehydration in H-ZSM-5 using multiple-walker well-tempered metadynamics.[216,217] They tested the reaction mechanism both in the presence of zero to eight water molecules in the unit cell and found that when water is present, the mechanism switches from E_2 to E_1, with the formation of an intermediate cyclohexyl cation (Figure 11c−e). The authors attribute this change in mechanism to the low Lewis acidity of the water cluster as well as the potential partial solvation of the cyclohexyl cation by the water. In this case, the detailed atomistic information obtained from enhanced-sampling simulations can help to support and shed light on previous experimental observations.[218] A second example concerns ethanol dehydration to diethyl ether in the H-Beta zeolite with five water molecules.[219] Using metadynamics to investigate the reaction, it was shown that the S_N2 transition state resides at the periphery of the protonated $[H_3O(H_2O)_4]^+$ water cluster, with a minor disruption in the hydrogen-bonding network and an experimentally observed −1 order in water pressure. At higher water loadings, on the other hand, more severe water inhibition is observed, which is attributed to the formation of more extended water networks and consequently a more significant disruption of the hydrogen-bonding network by the reaction transition state.

Up until now, the focus has been restricted to solvation of the BAS by water while keeping the overall framework structure intact. However, it is now understood that water can have a much deeper impact on the zeolite active sites. The first clear evidence that the H-CHA framework presents labile bonds even at room temperature in the presence of liquid water came from the pioneering study of Heard and co-workers, who showed through a combination of blue-moon sampling and NMR measurements that not only Al−O bonds but also Si−O bonds are very labile, with an expected free energy barrier of only 63 kJ·mol^{-1}.[220] A combined experimental−theoretical study showed that a similar lability is present in the aluminophosphate version of the material as well.[221] The general idea that water enhances framework lability is of course not so new (albeit at harsher conditions), as steaming has been for a long time a known technique to modulate the catalyst's acidity by creating extraframework and framework-associated aluminum species through dealumination.[222] Using umbrella sampling simulations, we showed that the stepwise hydrolysis of the four Al−O bonds when going from a pristine BAS to a silanol nest + $Al(OH)_3OH_2$ is significantly reduced in the presence of additional water molecules.[223] This is the case because the additional water can act as a proton-transferring agent via Grotthuss-type mechanisms, enormously facilitating the H-transfer reactions that are requested to hydrolyze the framework's bonds. While similar conclusions are attainable with static methodologies as well, capturing the hydronium ion mobility and the dynamic restructuring of hydrogen-bonding

https://doi.org/10.1021/acscatal.3c01945
ACS Catal. 2023, 13, 11455−11493

networks with very high water loadings is a task that only dynamic methods can hope to achieve.[224] More recently, Liu et al. showed through metadynamics simulations of H-Beta loaded with four water molecules that breakage of the Al−O bonds involved in five-membered rings is easier than breakage of the bonds involved in larger 12-membered rings (17−21 vs 50−69 kJ·mol^{-1}).[225]

This overview on the importance of enhanced sampling techniques in modeling water−zeolite interactions leads us to the two—in our opinion—main challenges that still need to be addressed in order to attain results that would enable a better comparison with experiment.

The first challenge concerns the estimation of water loading under realistic experimental conditions. This is made challenging by the fact that, as discussed before, the BAS's degree of solvation is dependent on the water loading, and traditional force fields are not suited to model such a reactive event. Even regular GGA functionals like the "standard" PBE-D3, which have been shown to provide adsorption energies for water in H-CHA in reasonable agreement with higher levels of theory, are way too expensive to perform a complete grand canonical Monte Carlo (GCMC) simulation.[59] So far, most of the work in zeolite catalysis has used one of the following approaches to estimate the amount of water. In many cases, either a (partially) arbitrary amount of water is included with the purpose of scanning various water loadings or to reproduce the few available experimental data.[210,217] Another approach is to include a number of water molecules to reproduce the water density at the conditions of interest.[220] Lastly, one can indeed perform GCMC simulations to determine the water loading; however, given the computational expense, it is standard to perform these with force fields, as a large number of energy calculations—up to a million—must be performed to produce the adsorption isotherm. The number of necessary energy evaluations may depend on the guest species and nanoporous framework, but isotherms for nanoporous materials with large pore volumes that include both regions of strongly attractive and orientation-dependent interactions and regions of low interaction energy are typically more difficult to converge.[75] Simulation of water adsorption in porous materials, including metal−organic frameworks and zeolites, is a notoriously difficult case where convergence might be extremely slow, and in view of this, also various acceleration schemes have been proposed to mitigate this issue.[226] In any case, performing such a large number of first-principles calculations is clearly beyond the feasibility of what can be done with DFT calculations on a routine basis. One alternative that has been performed is to perform GCMC simulations with a parametrized version of ReaxFF, which allows for bond breaking and forming.[80,223] It needs to be mentioned that reactive force field parametrization is notoriously challenging. There is certainly room to develop methods to determine with quantum-mechanical accuracy the adsorption isotherms. Some suggestions have been made in the literature to determine Henry coefficients based on importance sampling, where first sampling is performed at the force field level and afterward for a selected set of states refinements are performed at the quantum-mechanical level.[227] In a similar philosophy, recently a hybrid GCMC approach was proposed by Bai et al. to compute the water loading in zeolites, in which MC moves are not proposed at random but instead presampling with molecular mechanics force fields is used to generate trial configurations, which are then accepted or rejected on a DFT potential energy surface.[228] The presampling with inexpensive force fields in combination with a parallelization algorithm allows the simulation efficiency to be improved.[228] Alternatively, Bukowski and co-workers proposed computing an extensive free energy as the Helmholtz free energy of the zeolite−water system minus the chemical potential of an external water reservoir times the number of adsorbed water molecules, as a function of the water loading.[219,229] This energy is minimized for optimal water density under the chosen conditions. The reader interested in the fundamentals of the methodology is referred to specific references.[230−233] While it provides interesting information about the thermodynamics of the system, this approach also requires a full MD simulation at every water loading of interest and thus is quite far from routinely applicable.

The second grand challenge consists of the inclusion of realistic framework defects in the calculation. Indeed, it is now accepted that framework-associated and extraframework aluminum species will be present in significant amounts when water is present in the framework.[222] To the best of our knowledge, it is still not clear how to determine their structure, as not only can single Al sites present various degrees of coordination but their migration in the framework could also preferentially lead to the formation of multinuclear species or to interactions between EFALs and pristine BASs.[234,235] While experimentally a lot of effort is being made to understand the dynamic evolution of Al sites in zeolites, especially through NMR spectroscopy, its computational investigation is only in its infancy.[236,237]

4.3. Competitive Pathways at Operating Conditions and Broad Transition State Regions. Many catalytic reactions in zeolite chemistry cannot simply be described by one transition state from which chemical kinetics comparable to experiments can be derived. At realistic operating conditions, the scene is far more complex: various reactions can take place simultaneously or in a competitive way, various guest molecules in the pores may influence the reactive behavior, and the free energy surface at operating conditions may differ substantially from the 0 K energy surface from which the transition states were initially derived. To illustrate this further, it is interesting to give some examples. For the cracking of a tertiary 2,4-dimethyl-2-hexyl carbenium ion via β-scission, yielding isobutene and 2-butyl cation, a multitude of transition states were found, which gave rise to substantially different free energy barriers when evaluating the latter within a static approach relying on the commonly used harmonic oscillator approximation.[148] Cracking typically takes place at very high temperatures (>500 °C), and minima found on the 0 K PES are not necessarily stable intermediates at higher temperatures, as was explained in section 4.1. Clearly the zeolite environment plays a crucial role in the stabilization of the various discrete transition states, but also entropic effects at the elevated temperatures may substantially contribute to the stabilization of intermediates and transition states. Similar conclusions were found by Bučko et al. on propane cracking in chabazite and Chizallet et al. on isomerization and cracking of C_7 alkenes in chabazite.[112,114,238] The complex chemistry taking place at elevated cracking temperatures cannot simply be distilled from discrete points derived from the 0 K PES, for which free energies are deduced by adding thermal corrections using the harmonic oscillator approximation. Even computational schemes where anharmonic corrections are used around the optimized minima or transition states may be insufficient to extract the correct chemistry of the true catalytic process.

Another example where standard methods based on a single transition state proved to be insufficient is for reactions where a

https://doi.org/10.1021/acscatal.3c01945
ACS Catal. 2023, 13, 11455−11493

lot of configurational freedom is possible. Typical examples may be found in large-pore zeolites, where adsorbed molecules can rotate and translate in an almost free manner. For benzene methylation taking place in AFI materials having straight 12-ring channels, many isoenergetic minima were found from static calculations.[147,239] This is a typical reaction where not one single transition state determines the overall reaction kinetics and one needs to account for larger portions of phase space. In this case, the multitude of various states was taken into account by using enhanced-sampling MD simulations from which free energy barriers were estimated. Figure 12 shows some representative

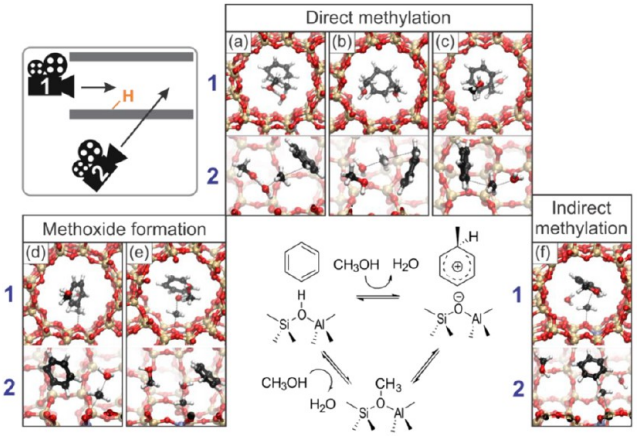

Figure 12. Snapshots of the (a−c) direct and (d−f) stepwise methylation of benzene by two methanol molecules in H-SSZ-24 at 350 °C, seen in the direction of the 1D channel (camera viewpoint 1) and in a cross section of the channel (camera viewpoint 2). The snapshots taken from the MD simulations clearly show that a wide variety of transition paths are possible for the various steps in the methylation reaction in the large-pore zeolite and that one or more methanol molecules can be involved. Reproduced with permission from ref 147. Copyright 2015 Wiley-VCH.

snapshots of the transitions, indicating the existence of a wide variety of transition paths for a given chemical reaction. In this particular case, various transition states differ not only in their particular orientation in the zeolite pores but also the number of guest molecules participating in activated complexes. In principle, as these snapshots result from MD simulations, one cannot strictly speak about the existence of one transition state but must consider more of a region in phase space characteristic for activated complexes. From such simulations, one can in principle derive free energy barriers and kinetic information with the procedures described in section 3. In more general cases when complex transition state regions are present, it might be impossible to fully capture them with a single collective variable. In a multidimensional CV space, a curved transition state region would be impossible to project on simple linear combinations of the underlying CVs. Therefore, the equations outlined in section 3 would have to be extended to higher-dimensional spaces. To the best of our knowledge, however, such an extension is far from trivial and has therefore not been reported in the literature yet.

Methylation reactions in zeolites showcase examples where the reaction mechanism can take place via a concerted or stepwise mechanism, as shown in Figure 12. There is a wealth of information available on which mechanism dominates at particular operating conditions.[240] Indeed, it has been found that depending on the temperature, loading of guest molecules, or zeolite topology, one or the other mechanism prevails.[215,241−250] Brogaard et al. suggested that the entropy difference for the two pathways is an important factor, which led to the conclusion that the stepwise mechanism would be preferred at higher temperatures, as the lower entropy loss due to intermediate water release in the stepwise mechanism might become more pronounced.[249] Such enthalpy−entropy trade-offs were shown to be crucial to discriminate between the associative and dissociative methanol dehydration routes in zeolites by Jones and Iglesia.[244] Given these considerations, it would be highly desirable to disentangle entropic and enthalpic effects from MD simulations, as was discussed in the previous section. The MD approach gives many qualitative insights into prevailing pathways at operating conditions, but given the computational expense, also other approaches, namely, DFT-based microkinetic models, have been suggested to determine the predominant pathways at operating conditions.[251] These approaches are very valuable; however, it needs to be stressed that the input in such models still relies on adsorption enthalpies and reaction rates determined from static DFT calculations. In the future, it might be desirable to go beyond such assumptions in models that go from the molecular to the industrial scale.

To study competitive pathways with molecular dynamics simulations, it would be desirable to define a complete set of collective variables capable of sampling all competitive paths and intermediates in a single *N*-dimensional free energy surface which is able to capture the relevant competitive pathways. This is the case because the use of different simulations (and CVs) for different reaction pathways does not necessarily ensure that the phase space sampled in simulations corresponding to the same state (reactants, for instance) perfectly overlaps. This creates potential problems when different states must be aligned and compared. For the particular case of benzene methylation in AFI, we introduced three CVs, as schematically indicated in Figure 12. Of course, increasing the number of CVs exponentially increases the required computational time. Furthermore, even if long enough simulation times would be achievable, it remains a true challenge to perform an adequate error analysis and ensure that the simulation is statistically well-converged. In this case, it might be more interesting to introduce more complicated CVs, which allow us to reduce the dimensionality of the CV space. Recently, we tackled a similar problem in a more reliable way for the zeolite-catalyzed aromatic electrophilic substitution reaction (S_EAr) in the synthesis of ethylbenzene from benzene and ethene.[187] Two reaction paths are possible. In the first, ethene directly attacks the aromatic ring with concerted activation from the zeolite BAS. In the second, ethene is first chemisorbed as a surface ethoxide species (SES), which then attacks the benzene ring in the S_EAr step. Interestingly, it was debated whether the S_EAr step proceeds or not with the formation of a metastable arenium ion, commonly known as the Wheland intermediate. By using two linear combinations of coordination numbers to account for the breaking and formation of all the reacting bonds (Figure 13a), we were able to sample the S_EAr reaction using multiple-walker well-tempered metadynamics. The advantage of this approach is that the Wheland complex can spontaneously appear in the two-dimensional FES as minimum or not, depending on its stability (Figure 13b). Interestingly, we found that when both ethene and the SES are used as ethylating agents, the Wheland complex appears as shallow minimum in the two-dimensional FES (Figure 13c), in line with spectroscopic experimental observations.[252]

https://doi.org/10.1021/acscatal.3c01945
ACS Catal. 2023, 13, 11455−11493

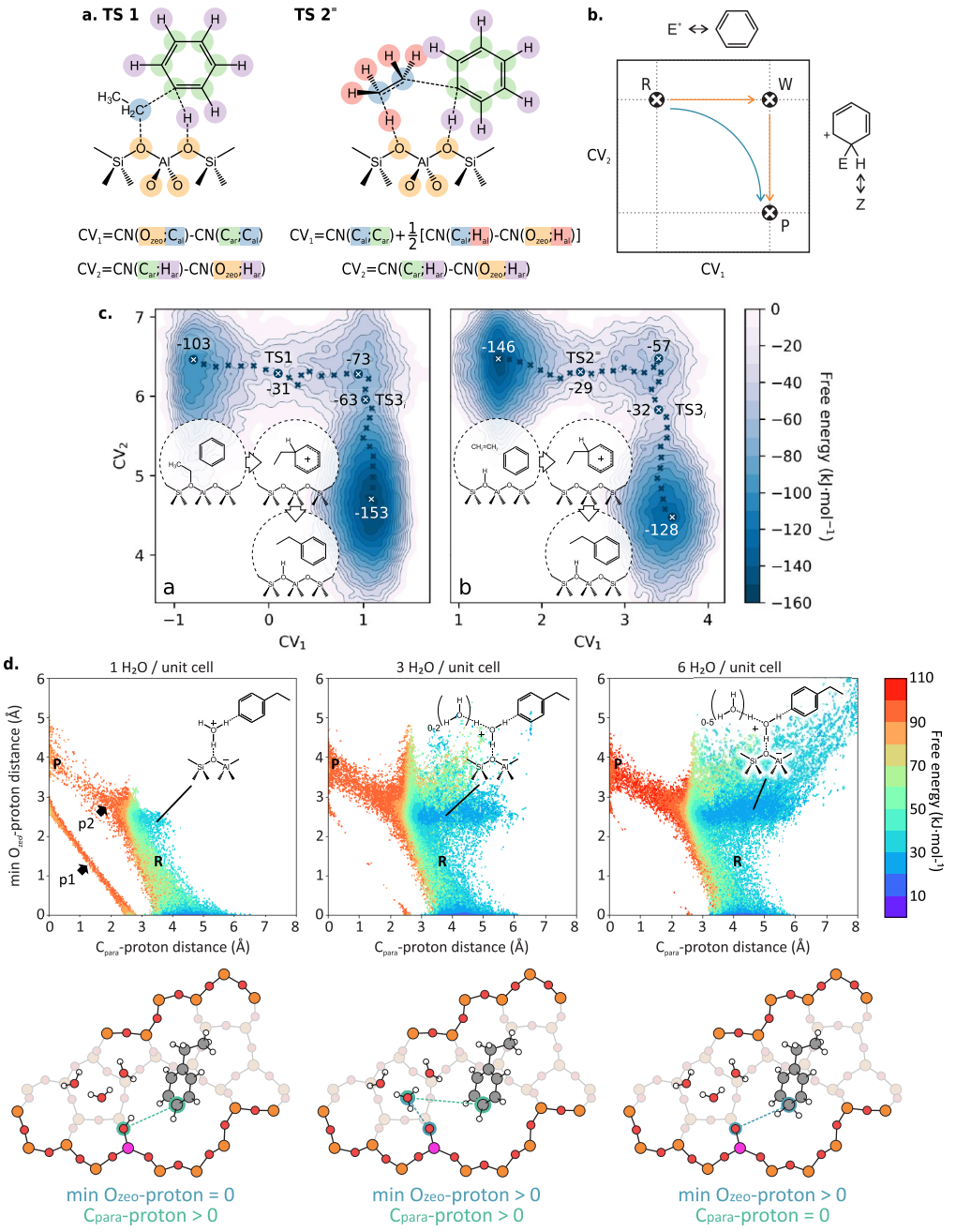

Figure 13. (a) Summary of the linear combination of coordination numbers used to describe the S_EAr reaction of benzene with ethene and a surface ethoxide species. (b) Schematic depiction of the preferred reaction path in the two-dimensional CV space for a concerted S_EAr (blue arrow) or a stepwise S_EAr going through a Wheland intermediate. (c) Free energy surfaces for the S_EAr reaction of benzene with ethene and a surface ethoxide species in H-ZSM-5, highlighting how in both cases the spontaneous formation of a Wheland complex is observed. (d) Free energy surfaces for the water-mediated para protonation of ethylbenzene in H-ZSM-5, where it can be seen how the BAS becomes more and more solvated with an increasing water loading in the zeolite unit cell. From ref 187.

Another aspect of the reaction that was explored with enhanced sampling techniques is the role of water in assisting the protonation of the Wheland complex. As highlighted in section 4.2, the high mobility and strong interaction with the BAS of water is ideally suited to be investigated with enhanced sampling techniques. The para protonation of ethylbenzene was investigated in the presence of one, three, and six water molecules in the zeolite unit cell using a simple one-dimensional CV. Afterward, the statistical tools of ThermoLIB (see section 3) were used to expand the original FEP in a two-dimensional FES in order to investigate the location of the extra proton in the system (Figure 13d). This allowed us to find two distinct protonation paths, one related to the direct transfer of the BAS from the zeolite to the ethylbenzene (p1 in Figure 13d) and another going through the formation of a hydronium ion (p2). Increasing the amount of water leads to the disappearance of p1, as states in which the water does not interact with the BAS become less and less likely. At the same time, the solvation of the BAS as the hydronium ion (which corresponds to the states in the center of the FESs in Figure 13d) becomes predominant. By determining the reaction kinetics with the tools discussed in section 3, we found that the opening of p2 with the addition of

https://doi.org/10.1021/acscatal.3c01945
ACS Catal. 2023, 13, 11455−11493

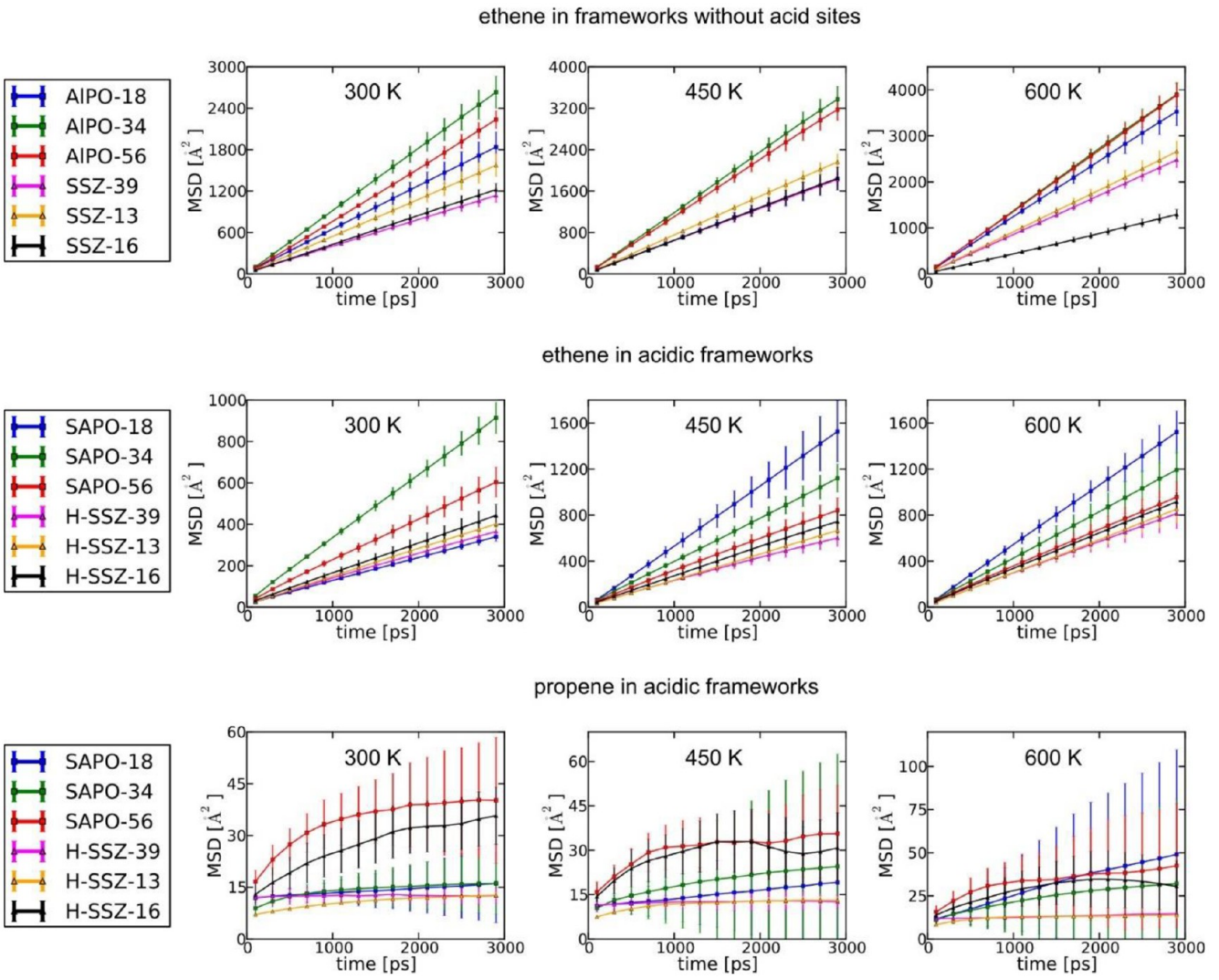

Figure 14. MSDs (in units of Å^2, with error bars) of ethene and propene at different temperatures computed within a series of various aluminophosphate zeotype materials having spacious cages and 8-ring windows, with and without acid sites. The simulations were performed with a force field as defined in ref 256. Reproduced from ref 256. Copyright 2015 American Chemical Society.

one water molecule speeds up the protonation reaction by about one order of magnitude, while at higher coverages the BAS solvation overstabilizes it, lowering the rate to similar values as in the anhydrous case.

Concluding this section, it is clear that first-principles MD simulations are of huge added value to learn more about the possibility of reacting via competitive pathways. Certainly many qualitative aspects may be learned, as was shown for the methylation reaction of benzene or for the zeolite-catalyzed benzene ethylation through the electrophilic aromatic substitution reaction. A few remarks are in place. First of all, one can consider in the type of simulations performed only reactions taking place in the same local environment of the active site. The locality refers to the definitions given at the start of section 4. Second, the different reactions considered in an enhanced-sampling MD run are mostly determined by chemical intuition and are critically dependent on the CVs defined by the user. For more complex reaction networks, such as the initial reactions taking place in the methanol to hydrocarbons process, where a lot of competitive reactions can take place simultaneously, or the CO_2 to hydrocarbons process, which has an equally large number of reactions that are possible, the approach sketched above will potentially fail, as only a limited number of CVs would not be able to capture the full complexity of the reaction network. In these cases, it might be beneficial to rely on methods where we can automatically discover potential reactions and where we could more sample them on the fly without the a priori definition of CVs.[28,253] On the positive side, with first-principles MD, one can simulate in one run various competitive pathways simultaneously, in contrast to static approaches, where information on competitive pathways is gathered from separated simulations not necessarily starting from similar points in configuration space.

4.4. Regular and Enhanced-Sampling Molecular Dynamics Simulations to Study Diffusion at Operating Conditions. Diffusion of reactive species and products is an essential part of the catalytic cycle and may contribute substantially to product selectivity. If diffusion of some species becomes hindered, then this may be the onset for catalyst deactivation. As an example, it was recently found through operando Kerr-gated Raman spectroscopy studies in combination with advanced simulation tools that polyenes are crucial

https://doi.org/10.1021/acscatal.3c01945
ACS Catal. 2023, 13, 11455−11493

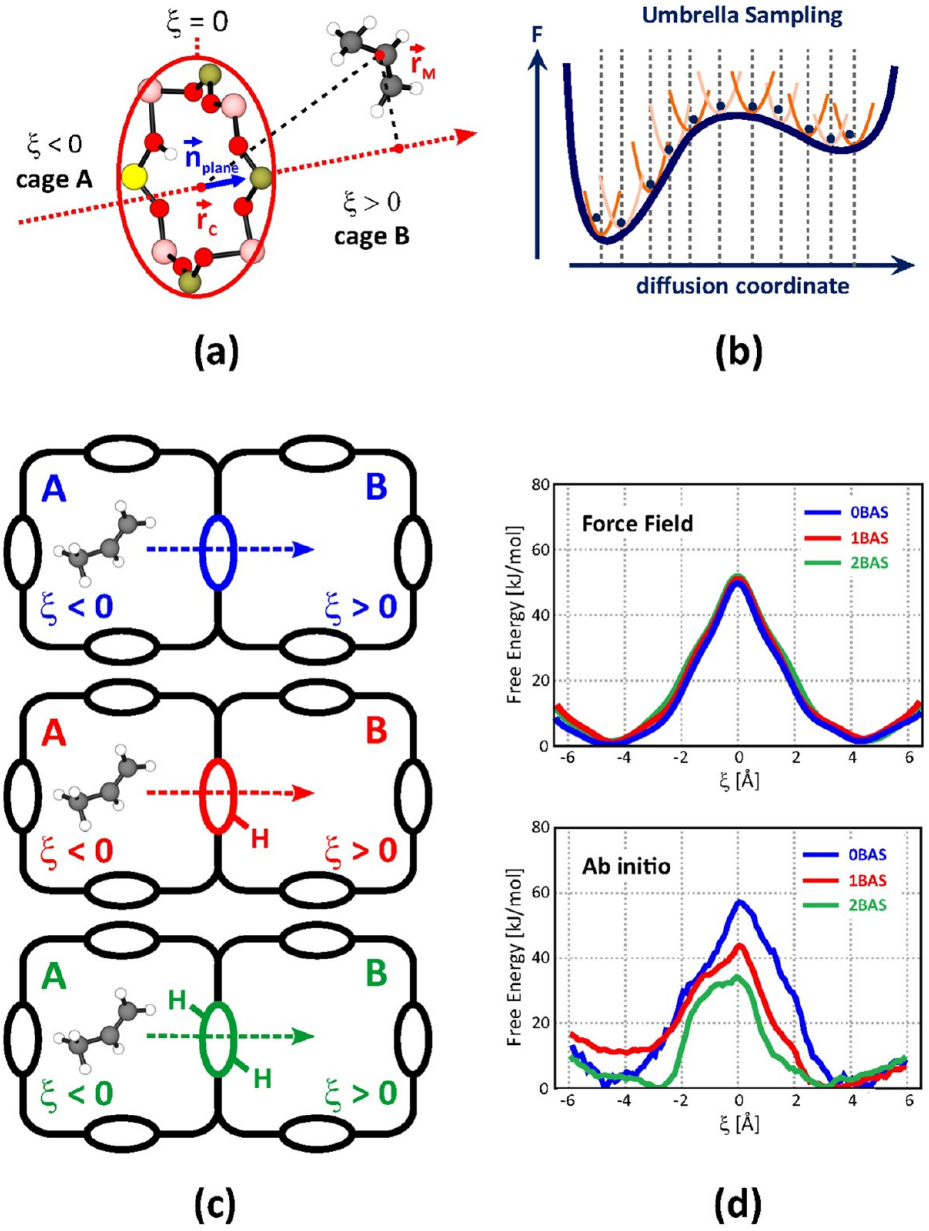

Figure 15. Illustration of enhanced-sampling molecular dynamics methods to study hindered diffusion in zeolites. (a) Definition of the collective variable for propene diffusion through the 8-ring of H-SAPO-34. (b) Schematic illustration of the umbrella sampling method to construct the free energy profile along the collective variable. (c) Three molecular models for H-SAPO-34 with a varying number of Brønsted acid sites on the 8-ring window. (d) Free energy profiles at 600 K constructed with force-field- and DFT-based methods. Adapted from ref 30 (CC BY 4.0), ref 40 (CC BY-NC-ND 4.0), and ref 41 (copyright 2020 American Chemical Society).

intermediates in the onset of coke formation in the methanol-to-olefin conversion.[254] In zeolite topologies with spacious cages but small windows, such as chabazite, the formation of branched, longer polyenes completely blocks the pores and was found to be the start of the deactivation phase. In zeolite ZSM-5, composed of both straight and sinusoidal channels, polyenes were also detected by Raman spectroscopy, but their formation did not immediately lead to deactivation as transport was still possible or the polyenes did not immediately react further to form species that completely blocked the channel system. These examples show how transport and diffusion of intermediates are inherent key components of the overall catalytic process and that in-depth knowledge on transport is necessary to obtain insight into the factors governing the selectivity and lifetime of the catalyst.

Diffusion typically takes place over longer length and time scales and is therefore typically described using force-field-based techniques.[74,255] To reliably estimate diffusion coefficients from regular MD simulations, one needs simulation times on the order of hundreds of nanoseconds, which is certainly not feasible at the DFT level.[256,257] From such regular MD simulations, one can extract a self-diffusion coefficient by determining the mean square displacement (MSD) of an adsorbate molecule during a time interval τ (which is also called the lag time). The MSD is a measure of the distance traveled by the molecule during this time interval:

$$\mathrm{MSD}(\tau) = \frac{1}{N_{\mathrm{ads}}} \sum_{i=1}^{N_{\mathrm{ads}}} \frac{1}{N_\tau} \sum_{t_0}^{N_\tau} |\mathbf{R}_i(t_0 + \tau) - \mathbf{R}_i(t_0)|^2 \quad (12)$$

https://doi.org/10.1021/acscatal.3c01945
ACS Catal. 2023, 13, 11455−11493

Herein, the squared length of the displacement vector is averaged over many N_τ intervals, where t_0 can freely vary along the trajectory as long as the total simulation time covers $t_0 + \tau$. Furthermore, we average over the number of adsorbate molecules to improve the statistics from a single trajectory. In principle one can also calculate the MSD from a series of independent shorter trajectories. The self-diffusion constant D^s is then defined as the slope of the MSD versus time, according to the so-called Einstein relation:

$$\mathrm{MSD}(\tau) = 6D^s\tau + b \tag{13}$$

where b is the offset at time zero.

To illustrate the concept more clearly, the MSDs of ethene and propene are shown for a series of 8-ring small-pore aluminophosphates with spacious cages (Figure 14).[256] The results are taken from the work of Ghysels et al.[256] A series of zeotype materials with AEI, CHA and AFX topology were studied as they received quite some interest within the MTO process. These topologies can host the necessary bulky aromatics part of the hydrocarbon pool and produce quite selectively light olefins, such as ethene and propene. The selectivity for these smaller olefins is partly attributed to the fact that larger olefins or branched species cannot diffuse through the 8-ring windows, in contrast to another often used catalysts within MTO namely H-ZSM-5, having the MFI topology.[98,258]

The computational details on the specific results can be found in the original work of Ghysels et al.[256] It is important to note that the simulations in that work were performed with a tailored force field to describe the range of considered materials with and without Brønsted acid sites. It is immediately clear that ethene can diffuse quite freely through all of the considered materials, as a straight line is found for the MSD versus time plots. However, the ethene diffusivity is also observed to increase with temperature, suggesting that ethene diffusion through the 8-rings is still a (mildly) activated process, as will be confirmed later in this section from more advanced molecular simulations. For propene, the situation is different, as no straight line is obtained for the MSD versus time plot, indicating that the diffusive regime is not yet reached in this time span. This could be explained by the fact that diffusion of a propene molecule from one cage to another is hindered. As such, propene has to overcome a free energy barrier when squeezing through the narrow window, making it an activated process and hence a rare event on the time scale of the simulation. The results shown here were obtained from MD runs extending to 3 ns, which may be considered on the short side—certainly with current computational capacities much longer simulations would be feasible—but still the transport of propene should be rather considered as a hopping process between adjacent cages. From the simulations, diffusion coefficients were also reported and carefully compared with other literature data—both experimental and theoretical—available at that time. The absolute values for the diffusion coefficients are quite sensitive to the force field used, and thus, it would be very beneficial to also determine diffusivities from first-principles MD simulations. The latter might become possible with the use of cheaper methods to describe the PES, such as MLPs (vide infra). To the best of our knowledge, diffusion coefficients based on an underlying quantum-mechanical description of the PES in combination with regular MD simulations have not yet been determined. Using DFT in combination with some model to describe the long-range interactions would be on the verge of what is possible today with the available computer sources.[259] In general, it should be noted that a quantitative comparison between theoretical and experimental diffusion coefficients is extremely difficult due to the various scales on which the diffusivities are determined. We refer to excellent seminal works by Kärger and co-workers for more detailed explanations on the subject.[260−262] Furthermore, we also refer the interested reader to the review by Smit and Maesen, which contains a section on how various diffusion coefficients are theoretically defined both from macroscopic and thermodynamic points of view and their relation with microscopic simulations.[74]

The previous discussion clearly reveals that diffusion itself can be hindered, as was the case for propene in small-pore zeolites. The sketched approach based on regular MD simulations is thus valid provided that the diffusion barriers are not too high to allow efficient generation of statistically relevant trajectories during the simulation. Furthermore, previous results relied on a force field to generate the MD trajectories, which assumes that the employed force field is capable of describing all interactions present in the complex catalytic environment. The latter may be rather problematic if specific interactions with active sites occur or if one wants to account for the true loading of the catalyst under operating conditions. To illustrate this more clearly, we revert to the diffusion of ethene and propene through H-SAPO-34, which was mentioned above. As the diffusion is hindered, an enhanced sampling methodology based on underlying MD simulations was devised, which allowed the free energy profiles to be constructed for discrete jumps between various sites or cages. Furthermore, we explicitly investigated the role of Brønsted acid sites on the transport of small olefins and paraffins through the 8-rings of the zeotype material. The concept and setup of the simulations is illustrated in Figure 15. Jumps of adsorbate molecules between two neighboring cages—denoted as cages A and B—through 8-rings containing zero, one, or two acid sites were simulated. A collective variable ξ was defined as the projection of the center of mass of the adsorbate molecule onto the ring-plane normal, as illustrated in Figure 15a. A series of umbrella sampling simulations was performed along the diffusion coordinate ξ. In this case, the diffusion coordinate was divided into a set of 25 equidistant windows, and for each window a restrained MD simulation of 50 ps was performed to ensure that all points along the diffusion path were sampled equally well. This led to a total simulation time of 1250 ps. All US simulations were carried out with the CP2K software package interfaced with the advanced simulations library PLUMED.[263,264] The free energy profile was reconstructed by combining the sampling probability distributions of each window using the weighted histogram analysis method (WHAM) as implemented in ThermoLIB.[129]

The enhanced sampling protocol can be performed with any methodology to describe the energies and forces of the atoms. The capability of the force field to describe the specific interactions with the BAS was explicitly tested by performing both force-field-based simulations—with the force field derived in ref 256—and DFT-based simulations at the revPBE-D3 level of theory. As can be seen in Figure 15d, where the obtained free energy profiles of propene diffusion for various acid site densities are plotted, the force field fails to describe the specific interaction of propene with the acid sites. The ab initio results clearly reveal a promotional effect of acid sites on the diffusivity, which was ascribed to favorable π−H interactions with the olefins. For ethane and propane, having no double bonds, such promotional effects were not observed. The π−H interaction between the acidic proton of the zeolite and the double bond keeps the

https://doi.org/10.1021/acscatal.3c01945
ACS Catal. 2023, 13, 11455−11493

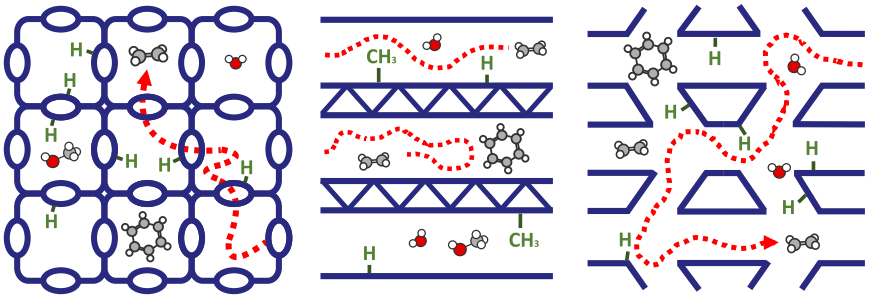

Figure 16. Schematic representation of various zeolites having different topologies, characterized either by spacious cages with windows, channels in one direction, or various channel systems. For each of the zeolites a realistic representation is shown at working conditions, where various active sites with different loadings are included. The red lines and arrows show schematically various transport paths for ethene as a diffusing molecule.

alkene in the proximity of the 8-ring and helps in steering the molecules to the next cage. Overall, the results showed that C_3 species are more hindered than C_2 species, which is to be expected given their larger size.

In other related studies, we observed that the diffusion ability was strongly dependent on the loading of the zeolite. For example, at high propene loading, the diffusion was enhanced, whereas when the cages were occupied by large hydrocarbon pool species, the diffusion toward these filled cages became completely blocked.[41] These observations clearly led to the concept of spatiotemporal evolution of the catalyst, where the catalyst evolves with the time on stream, which may lead to changing product distributions. Previous discussion reveals that the current classical force field does not correctly describe the specific interactions of a working catalyst, and thus, one ideally needs to resort to first-principles simulations where the interatomic interactions are determined at the quantum-mechanical level. For hindered diffusion, the enhanced sampling techniques in combination with, for example, underlying DFT-based MD simulations provide a solution to obtain free energy barriers at operating conditions. However, it is important to emphasize that the simulations are computationally extremely costly. For example, the case illustrated above necessitated more than 1 ns of simulation time at the DFT level. Clearly, when the aim is to use this methodology in a mainstream way, more efficient methods are necessary to evaluate the underlying forces. The MLPs have a lot of potential, but careful testing is necessary to determine accurate underlying training data and also to capture all interatomic interactions, including long-range interactions between adsorbate molecules and the host zeolite framework.

Finally it is interesting to note that one can, in principle, also deduce diffusion coefficients from the obtained free energy barriers. To this end, the self-diffusion coefficient for the intracrystalline diffusion in the bulk zeolite is estimated according to the random-walk model described by Beerdsen et al.[265,266] Herein, diffusion is modeled as an analogue of a chemical reaction with a reactant state representing the molecule in the initial cage, a transition state representing the molecule in the intermediate window, and a product state representing the molecule in the neighboring cage. By applying transition state theory, one can derive the hopping rate from the reactant cage to the product cage from eq 5 in which the diffusion coordinate ξ takes on the role of the collective variable:

$$k = \sqrt{\frac{1}{2\pi\beta}} \langle |\nabla_x \xi| \rangle_{\xi=\xi^*} \frac{e^{-\beta F(\xi^*)}}{\int_{-\infty}^{\xi^*} e^{-\beta F(\xi)}\, d\xi} \tag{14}$$

where ξ^* represents the diffusion coordinate for the window and the denominator of the ratio is proportional to the probability for the molecule to be in the initial cage (the reactant state). Finally, this rate constant can be translated toward a diffusion constant through application of a hopping model. Assuming symmetric forward and backward hopping rates in all d dimensions, we arrive at

$$D = \frac{1}{2d} f k \lambda^2 \tag{15}$$

where k is the jump frequency, λ is the lattice hop distance, d is the dimensionality of the system, and f is a correlation factor containing memory effects arising from ordering and inter-particle interactions (which is usually assumed to be 1). For the case of SAPO-34 having the CHA topology and where the molecules can escape in three dimensions, we find $d = 3$. We also assumed the correlation factor $f = 1$, meaning the individual hopping events are uncorrelated. In reality, certainly at realistic acid site densities and loadings, there will be some preferential directions and correlations between hopping events. The diffusion coefficients obtained with this methodology are approximations of the effective hopping rates. Without having the ambition to make a detailed quantitative comparison of all possible experimental and theoretical values reported, it may be interesting to compare a few diffusion constants, at least to have an idea of the order of magnitude. Self-diffusion constants determined at 295 K from ^{1}H PFG NMR measurements on large crystals (20−30 μm) of H-SAPO-34 samples with a different amount of acid sites were on the order of 10^{-11} m^2/s. The diffusion constants determined from the free energy profiles were in reasonably good agreement. However, given the simplicity of eq 15, where no directionality in terms of acid sites is taken into account, one should not aim to pursue exact quantitative agreement.

Lastly, it is interesting to reflect on the possible extension of the sketched enhanced sampling methodology to more complicated zeolites with nonsymmetrical escape channels. In this case, more complex CVs would have to be defined. A schematic representation of various zeolites having different topologies and different diffusion channels is shown in Figure 16. For example, in the case of the H-ZSM-5 having the MFI topology with straight and sinusoidal channels, diffusion coordinates along both channels need to be defined, which may eventually be coupled. It would be very interesting to determine from first-principles MD simulations the competition of diffusion along various zeolite channels. So far, simulations performed by Hibbitts et al. studied the competition for diffusion of benzene and substituted methylbenzene species

https://doi.org/10.1021/acscatal.3c01945
ACS Catal. 2023, 13, 11455−11493

between the various channels in ZSM-5, albeit using nudged elastic band calculations.[267] It was found that diffusion along the straight channels was lower activated compared to the sinusoidal channels; however, it might be interesting to also study this using MD simulations which fully account for the entropic effects. In general, the methods sketched above, albeit in combination with more efficient methods to evaluate the forces with quantum accuracy, have a huge potential to investigate how transport is affected by different topologies, loadings, and presence of active sites. In other words, it would be very interesting to investigate how transport is affected for realistic zeolites at true working conditions. A schematic representation of such realistic configurations of various zeolites with various loadings and active sites is shown in Figure 16.

Finally, it needs to be mentioned that comparison of experimental and theoretical diffusion coefficients needs to be done with extreme care, as was pointed out nicely by Kärger et al.[260,261] Experimental diffusion coefficients are typically determined using pulsed field gradient (PFG) NMR experiments on large crystals to ensure that intracrystalline diffusivities are measured, whereas our theoretical protocol samples single cage hopping events on systems having a much smaller size. Complementary techniques may be used to link theoretical observations with experiments. A promising technique is the pulse-response temporal analysis of products (TAP) methodology, which measures residence times of probe molecules.[268,269] In this case, various effects contribute to the measured TAP results, such as surface barriers, intracrystalline diffusion, adsorption at the active site, and finally kinetics.[270−272] From an experimental point of view, it is very difficult to disentangle all these contributions. Very interesting work has recently been performed by the group of Olsbye to develop adsorption−diffusion models for hydrocarbon transport in zeolites that account for surface barriers, intraporous diffusion, and diffusivity.[273] It should be mentioned that these models are top-down mathematical models to rightfully interpret the measured TAP data. Ideally, it would be possible to also build bottom-up models starting from the atomic scale to study the various components contributing to the TAP data; however, this would necessitate methodologies to estimate the various contributions such as surface barriers, intracrystalline diffusion, and specific interactions with active sites in a consistent way based on first principles. Further elaborations are given in the next section with the outlook.

Summarizing this section, it has become clear that first-principles molecular dynamics simulations may also be very important to obtain more insight into the transport of reactants, intermediates, and products in the zeolite. The applicability of first-principles MD, thus based on an underlying quantum-mechanical evaluation of the PES, is a bottleneck for the study of diffusion, as typically longer length and time scales are necessary to reliably study transport phenomena. However, using enhanced sampling procedures in combination with DFT, it becomes possible to also derive free energy profiles along well-defined CVs in the zeolite. The extension toward complex zeolite topologies and the derivation of accurate diffusion constants remain major challenges for future method development.

5. OUTLOOK AND FUTURE DIRECTIONS

Within this Perspective, we have aimed to critically reflect on the role of first-principles molecular dynamics simulations—which are also sometimes called ab initio molecular dynamics simulations—in the field of zeolite catalysis. More specifically, we have reflected on the question of how far such simulations may help in understanding or even predicting the catalytic function under operating conditions.

When trying to answer this question, it is very important to realize that catalysis is an inherently multiple length/time scale process. Relevant length scales vary from the subnanometer level to the level of a reactor having macroscopic dimensions, and time scales vary from the (sub)picosecond scale, typical for molecular vibrations, to seconds or hours for macroscopic observations. Additionally, the dynamic evolution of the catalyst is coupled to spatial gradients in the catalyst particle and beyond. This coupling between time and space phenomena led to the terminology of spatiotemporal evolution of a material or catalyst.[6] A critical aspect to evaluate the catalytic function is the importance of operating conditions. Depending on small variations in the temperature window, composition of the feedstock, presence of water, or other reacting agents, the catalytic function will change. It is very important to account for these complexities in any modeling endeavor to mimic the catalyst as closely as possible to its true working conditions.

Being aware of all these levels of complexity encountered in a realistic catalytic process, one can rightfully ask the question of how far molecular simulations starting from the molecular scale can provide insight into this complex puzzle. Various models have been devised to tackle the multiple length/time scale problem, such as microkinetic modeling, kinetic Monte Carlo models, and heat and mass transport models to account for the inhomogeneities in temperatures and reactant concentrations in the reactor. This complementary set of techniques aims to bridge from the atomistic scale to the reactor scale.[29,274] Excellent recent reviews have appeared on the broad variety of multiple length/time scale models.[29,53,274−276] First-principles microkinetic models and kinetic Monte Carlo methods within the field of heterogeneous catalysis have been developed which rely on atomic-scale input for reaction rates of elementary reactions and thermodynamics on adsorption.[53] The latter are computed using quantum-mechanics-based simulations or even simpler methods based on group contribution methods. As many reactions and a broad diversity of active sites are involved in complex catalytic systems, the necessary atomistic information is typically obtained from static approaches, which rely on the optimization to a few discrete points on the potential energy surface. Around these local (meta)stable states, one evaluates energetic properties by performing geometry optimizations and uses the principles of statistical thermodynamics to obtain thermodynamic and kinetic properties at finite temperatures. Using microkinetic models, where one ideally includes all possible elementary reactions, one can deduce the preferred reaction mechanism at a given set of reaction conditions, surface coverages, and concentration profiles for the various intermediates and products as a function of time.[276] Setting up detailed microkinetic models for large reaction networks is particularly challenging, and construction of microkinetic models within the field of zeolite catalysis at operating conditions starting from ab initio kinetic data is far from trivial. With kMC models, one includes spatial distribution of active sites and gets insight into the time evolution of surface transformations. This is done by generating a series of stochastic trajectories that propagate the system from one state to the other, after which the correct dynamics is retrieved by ensemble averaging over all of these trajectories.[277] kMC models have been used with great success in the field of heterogeneous

https://doi.org/10.1021/acscatal.3c01945
ACS Catal. 2023, 13, 11455−11493

catalysis taking place at metallic surfaces, but their use within the field of zeolite catalysis and certainly considering realistic materials having defects and spatial heterogeneities remains a huge challenge.[278] In all of the previously mentioned first-principles microkinetic or kMC models, the necessary ab initio input is retrieved from static simulation methods. Despite the great advantages of such multiple length/time scale models with input from static quantum-mechanics-based simulations, clear evidence has been given in the past few years that the simple static approach is not able to capture the complexity of the catalyst at working conditions. It is within this area that first-principles molecular dynamics simulations can play an instrumental role to unravel the catalyst complexity at the molecular scale.

To showcase this, we have presented in this Perspective some illustrative examples which clearly demonstrate the importance of dynamic phenomena at operating conditions to unravel the catalytic function at the molecular scale. For example, for catalytic cracking at very high temperatures, it was shown that the reactive intermediates are not correctly predicted from static simulations due to improper account of entropic contributions. One should thus be very careful in using a standard textbook representation of a chemical reaction with a well-defined reactant state, transition state, and product, as each of these states might be very dependent on the operating conditions. Another prototype example concerns the impact of water on the reaction mechanism or the nature of active sites. The Brønsted acidic site cannot simply be represented by a local proton attached to the lattice, but depending on the conditions, the proton may become mobile and may interact with other guest species, thereby completely altering the nature of the active sites. The impact of water on the reaction mechanisms and rates was also clearly emphasized for the electrophilic aromatic substitution reaction in the synthesis of ethylbenzene from benzene and ethene. For future technological advances, more processes will be explored where new feedstocks like biomass or CO_2 need to be converted in the presence of water or other agents, and in this sense it will be very important to have access to modeling techniques that can correctly incorporate these intricacies. Lastly, although first-principles molecular dynamics simulations have so far for the majority been used for studying chemical reactions, it has been showcased in this Perspective that enhanced-sampling molecular dynamics techniques may also be used for the description of hindered diffusion in zeolites under operating conditions. The examples presented in this Perspective are only a few cases to highlight the importance of dynamic changes under the operating conditions. We certainly did not have the intention to be comprehensive or complete in the presented examples; many groups have shown similar features highlighting the intricacies of zeolites at working conditions. In this sense, first-principles molecular dynamics techniques have now matured to a level where they have become instrumental to discover reaction mechanisms under operating conditions and determine rates and thermodynamic quantities beyond the so-called harmonic oscillator approximation. Using such techniques, one can account in a more correct way for entropic contributions which depend on the configurational freedom of the involved species.[157]

Despite the great advantages of first-principles molecular dynamics techniques in the field of zeolite catalysis, we certainly have not reached the point where output from first-principles molecular dynamics simulations can be used as input for multiple length/time scale models that aim to bridge from the molecular scale to the reactor scale. In what follows, we elaborate on a few hurdles that prevent first-principles MD simulations from being easily integrated in a multiple length/time scale catalysis workflow. Today we have even not reached the phase where first-principles MD methods themselves can be regarded as a set of black-box methods that can be smoothly integrated into a standard computational workflow. One of the main hurdles relates to the computational expense of the first-principles molecular dynamics simulations, as the forces and energies are currently calculated at the DFT level, leading typically to simulations of hundreds of picoseconds and attainable length scales of the order of a few nanometers. These dimensions are much shorter than those of realistic catalytic particles, which typically have sizes on the order of 50 nm to even micrometers. Furthermore, realistic crystal particles have defects, various spatial gradients, and external surfaces, which affect the chemistry of the catalytic process. Within this respect, a major challenge to model catalytic processes in a more realistic way is the development of algorithms that enable the building of representative molecular structures of the catalytic particle in the mesoscale range. We did not elaborate on these aspects in this Perspective, but some interesting reflections can be found in other recent literature works.[9,30]

Regarding computer infrastructures, we are now entering the era of exascale computing, which will open new possibilities for computationally very demanding disciplines, such as computational materials science. Together with dedicated software optimization, hardware architectures, help of massive parallelization, and extensive usage of graphical processing units (GPUs), this will certainly lead to further optimizations of accessible length and time scales within computational catalysis.[259] However, even with the strongest computers available, it will not be possible to close the length/time scale gap between molecular simulations and experimental observations. For this also fundamental new methods will have to be developed.[30,259] Hereafter some hurdles and future avenues are mentioned to enable a better integration of first-principles molecular dynamics simulations into a standard computational workflow and to enable their output to be used in multiple length/time scale models.

Computational Cost of Force Evaluations at the QM Level. A first hurdle relates to the computational cost of force evaluations at the quantum-mechanical level. To further progress in this field and to enable the use of first-principles MD simulations in a more standard way, it would be necessary to have access to methods which allow construction of the PES with chemical accuracy albeit at a much lower computational cost than currently available methods. The terminology "chemical accuracy" or "quantum-chemical accuracy" refers to methods that aim to obtain energies with an accuracy of 4 kJ/mol compared to exact benchmark values.[188] It should be mentioned that even when using DFT-based methods, currently chemical accuracy is often not achieved; for this more expensive composite methods or wavefunction-based methods are required, as was explained in section 2 and highlighted from a more application point of view in section 4.1.[160,161,166] Current first-principles MD-based simulations rely mostly on underlying forces calculated at the DFT level. An interesting direction to extend accessible length and time scales is the development of machine learning potentials (MLPs), where a numerical potential is derived based on underlying quantum-mechanics-based training data using some (non)linear regression method. When trained correctly, the final MLP should be able to

https://doi.org/10.1021/acscatal.3c01945
ACS Catal. 2023, 13, 11455−11493

calculate the energies and forces with similar accuracy as the underlying quantum-mechanical data. The field of MLPs is certainly not new: the first-generation MLPs were already introduced about 25 years ago first on rather small molecular systems, but later, with the seminal work of Behler and Parrinello on high-dimensional neural network potentials, their range of applications was extended to much more complex systems.[279] Since then, many mathematical MLP frameworks have been developed, which can be broadly categorized into kernel regression methods and neural network potentials.[85,280] Many dedicated reviews have appeared recently on the status of MLPs and their usage within the field of materials science, and we refer the interested reader to these reference works.[85,86,281,282] The application of MLPs within the field of complex nanostructured materials and in particular zeolite catalysis remains rather limited. Some notable examples where MLPs were derived within the field of zeolite chemistry include the work of Erlebach, where a neural-network-based MLP was derived on a diverse set of zeolite structures to predict thermodynamic stabilities, vibrational properties, and reactive and nonreactive phase transformations,[92] and our own work, where an MLP was derived to study the proton hopping kinetics within zeolites.[4] Thanks to the dramatic speedup of the MLP force evaluations, MLP-based MD simulations could be performed on time scales on the order of submicroseconds, which is clearly beyond the capabilities of current DFT simulations. Thanks to these more efficient force evaluations, it was possible to calculate reaction rates beyond transition state theory, include nuclear quantum effects, and obtain a much better sampling of phase space. This recent work is a proof of concept within the field of zeolite chemistry, showing which new avenues could be explored when having access to methods that allow evaluation of the PES with the accuracy of quantum-mechanics-based methods yet at a much lower computational cost.

While the development of MLPs is very promising, the usage and implementation of MLPs to make them straightforward accessible for systems having the complexity sketched in this Perspective is far from trivial. Extensive testing will be necessary to investigate how far accurate MLPs can be trained for complex reactive events having a semilocal character or complex reaction coordinates. In this respect it will be very important to have access to innovative algorithms to generate the underlying quantum-mechanical training data in an efficient way. It was recently shown that a data-generation scheme relying on underlying DFT-based MD techniques is not very efficient.[283] During a regular MD run, subsequent structures are very much correlated, and thus, a strategy where training data are derived from underlying DFT-based MD simulations is not very efficient. In this case a lot of quantum-mechanical evaluations are performed which do not give substantial new information to train the MLP. To circumvent this caveat, we proposed an active learning scheme in which an iterative procedure is used to train the MLP.[283] A first-generation MLP is trained based on a small set of underlying training data and then used in enhanced-sampling MD simulations. When new portions of phase space are encountered which have not yet been seen, new DFT evaluations are performed to train the next iteration of the MLP. This procedure is continued until all relevant parts of phase space for the transformation of interest have been completely sampled. Such active learning schemes show great potential but have so far not yet been explored within the field of catalysis.

Related to efficient generation of MLPs, it needs to be investigated how transferable MLPs can be generated. Transferability may refer to changing thermodynamic conditions, e.g., how far is an MLP derived at a given set of conditions applicable to other conditions? Transferability may also refer to changing the applicability of the MLP to another zeolite compared to the one on which it was trained. Is it necessary to always train an MLP for each reactive event of interest, or can we train more universal MLPs based on a well-defined training set, which allow them to be used to a broader set of materials or reactions?

While MLPs are in essence designed to describe short-range interactions, further studies are necessary to investigate how far MLPs need to be complemented with physical models to describe long-range interactions. Treatment of long-range interactions is in full development within the MLP community, and various schemes have been proposed to complement the MLP with physical models for long-range interactions.[85,91,284−286] Particularly for zeolite catalysis, such interactions might be important when studying diffusion pathways through large-pore zeolites or in general confinement of molecules in large-cage zeolites or zeotype systems having mesopores.

Finally, the successful development of MLPs does not imply that fundamental work at the DFT level or more generally quantum-mechanical methods to describe the electronic structure problem are unnecessary. A correctly trained MLP will at best be as accurate as the underlying quantum-mechanical data on which it was generated. Particularly within the field of zeolite catalysis, where long-range interactions are important for adsorption and diffusion, the quality of the underlying quantum-mechanical data remains an important point of attention, and further advancements are necessary to describe with chemical accuracy the interatomic interactions within zeolite catalysis. The advantage of MLPs relies on the fact that when having access to very accurate training data generated with highly accurate quantum-mechanical methods, highly accurate MLPs could be trained having an accuracy comparable to the underlying highly accurate training data. As such, MLP-based molecular dynamics simulations could be performed on potential energy surfaces evaluated with chemical accuracy. Thanks to the dynamic sampling, also entropies would be obtained from such simulations. Such methodologies would be particularly interesting to determine the stability of carbenium ions, as explained in section 4.1, or to determine kinetic information—both intrinsic and apparent rate constants—fully from first-principles MD simulation. As explained in section 3, it is currently very challenging to directly compare theoretical and experimental kinetic data with chemical accuracy for reactions taking place at operating conditions. This target would necessitate dynamic sampling methods to properly account for entropic contributions in combination with chemically accurate sampling of the PES. Current DFT methods do not often provide chemically accurate energies. However, with the rise of machine learning methods, innovative algorithms have been proposed to meet this target. An interesting example is the recent study by Bučko et al. on methanol carbonylation over acid mordenite, where finite-temperature free energies of activation were computed by means of ab initio molecular dynamics calculations with various more expensive electronic structure methods.[153] To achieve this goal, the methodology introduced in section 4.1 relying on the coupling between machine learning and a free energy perturbation method was applied. Similar concepts might be used to calculate adsorption free energies from MD simulations. With DFT excessively long simulation

https://doi.org/10.1021/acscatal.3c01945
ACS Catal. 2023, 13, 11455−11493

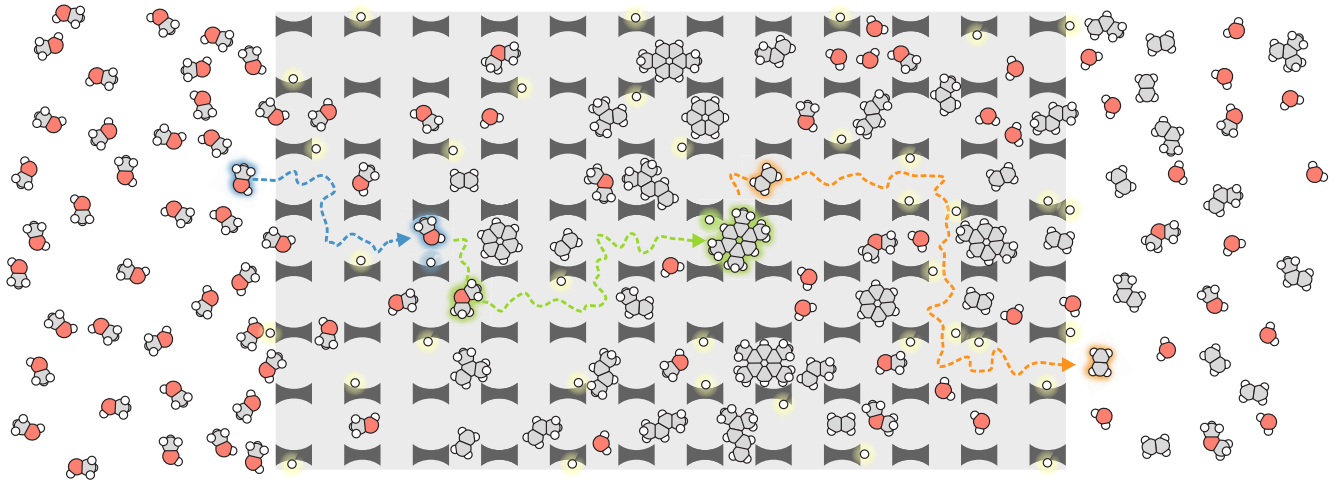

Figure 17. Schematic representation of a catalytic particle at operating conditions, where various active sites are present and species are captured within the catalytic pores. The picture is inspired by the methanol to olefin process, where a methanol feed is sent over a zeolitic catalyst. The methanol molecules first need to enter the crystal, diffuse in the crystal, and perform some pre-equilibration steps. Then a reaction occurs in a supramolecular cage having both a Brønsted acidic proton and a hydrocarbon pool species to form ethene. Finally, ethene needs to diffuse through the crystal to be detected as a product species. Obviously, the catalytic particle with its components will change with time on stream, giving another level of complexity to the overall catalytic process.

times would be necessary, and innovative approaches relying on machine learning methods might open new directions.

Methods for Enhanced Sampling and CV Selection. A second hurdle to integrate first-principles molecular dynamics simulations into the standard computational workflow relates to the methods used to perform enhanced sampling of the PES, the discovery of important collective variables which are indicative of the phenomena of interest, and the subsequent derivation of the kinetics. Throughout this Perspective, it has become clear that enhanced sampling techniques are instrumental for studying activated processes. Any catalytic reaction is an activated process, but as was explained in section 4.4, also transport may become hindered. Most of the simulations performed in zeolite catalysis still hinge on the definition of some collective variables that are representative of the transformation of interest. In most cases such collective variables are defined based on chemical insight. This might not always be possible or be a good practice, especially when complex transformations take place or when many reactions can take place simultaneously, where phenomena in many dimensions need to be studied. In this sense, there is a need to explore more systematic methods for discovery of collective variables also within the field of zeolite catalysis. In section 3, some references were given to recent reviews on data-driven methods to discover in an automated way proper CVs, but so far their implementation and development within the field of catalysis are nearly nonexistent.[139] Alternatively, it would be interesting to explore in a more in depth way transition path sampling methods and related methods such as transition interface sampling or replica-exchange transition interface sampling for complex catalytic phenomena. Such methods do not rely on a prior definition of collective variables, but instead, an ensemble of reactive paths connecting reactants and products is generated with random moves in a Monte Carlo fashion, from which the reaction rates can be obtained. So far TPS methods have mainly been used to obtain qualitative insights in the field of zeolite catalysis, as the number of paths necessary to generate reliable kinetics becomes very high. When the forces and energies are evaluated at the quantum-mechanical (i.e., DFT) level, generation of such high numbers of paths has thus far not been feasible. When having access to computationally cheaper methods to evaluate the PES (see previous point), such methods might become possible. The use of such methods might first of all be beneficial to generate relevant training data for training of MLPs for the reaction under study, and second, once a reliable MLP is available, such methods may yield kinetic data without defining collective variables. Related to determination of kinetics, there is still a need to benchmark methods in a systematic way to derive the kinetics from enhanced sampling simulations including the adsorption step, as elaborated in the previous paragraph and in section 3. As was shown in section 3, reaction rates are currently derived from transition state theory or a straightforward extension of it. In principle it would be desirable to go beyond a standard transition state methodology and use methods like the Bennett−Chandler approach, where also reaction barrier recrossings are systematically accounted for, or to directly use methods in the family of transition interface sampling.

Outlook. Finally, to conclude this Perspective, we give an outlook on how to model in a more realistic way dynamical processes taking place in an active catalyst, as schematically shown in Figure 17. The picture is inspired by the methanol to olefin process, where a methanol feed is sent over a zeolitic catalyst. The catalyst feed—here simplistically represented as a flow of methanol molecules—first needs to diffuse into the pores of the crystal, thereby potentially overcoming a surface barrier, after which the molecules undergo intracrystalline diffusion to reach the active site. At the active site they react, and when the reaction has taken place, the formed products need to desorb and diffuse out of the crystal. Each of the mentioned steps—crystal entrance, diffusion, adsorption, reaction—is characterized by vastly different time and length scales. In current modeling strategies, each of these steps is modeled using different strategies, leading to thermodynamic and/or kinetic information which is not comparable. First-principles molecular dynamics is for the majority used to study the reactive events or local events, and the other mentioned phenomena, such as diffusion into and within the crystal, are mostly performed with

https://doi.org/10.1021/acscatal.3c01945
ACS Catal. 2023, 13, 11455−11493

force fields given the vastly different time and length scales involved. This inconsistency leads to the lack of integrative models for the overall kinetics of the catalytic process at the catalyst particle level. It would in the future be very interesting to describe consistently all steps—crystal entrance, diffusion, adsorption, reaction—when a feed of guest molecules is brought in contact with a catalyst particle, thus using a quantum-mechanics-based evaluation of the PES, and deduce kinetic constants and thermodynamics accounting for the full dynamics at operating conditions. First-principles molecular dynamics models certainly will be an important ingredient to reach this goal, but a leap forward is necessary in accessible length and time scales, as explained above.

We believe that with the advances in MLPs and other data-driven methods, the possibilities of molecular dynamics simulations in combination with computationally more feasible methods to evaluate the forces will be greatly extended. Probably in the future, fewer DFT-based MD simulations will be performed and more MLP-based MD simulations will be conducted. This will hopefully lead to consistently derived kinetic constants for the various steps in a catalytic cycle, which are characterized by disparate time scales. When having access to such consistently derived kinetic constants for the various events taking place when a feed of molecules is brought into contact with a catalyst particle, it still remains a puzzle on how to reconcile the kinetic information on phenomena taking place on vastly different time scales in an overall integrative kinetic model which would allow the overall dynamics taking place at the catalyst particle to be followed. Within this respect, it is important to emphasize that such an ambitious goal will need optimal use of a broad plethora of methods, where each method is used for the appropriate target. For example, the current methodology to study phenomena with vastly different times scales is the usage of kinetic Monte Carlo methods, where a series of stochastic trajectories is generated that propagate the system from one state to the other, and afterward the correct dynamics is retrieved by ensemble averaging over all of these trajectories.[277] There are only a few examples of kMC approaches within the field of nanoporous frameworks, and the combination of diffusional, reaction, and adsorption sites has thus far not been performed.[277,287−291] As mentioned earlier in this section, kMC methods and also first-principles microkinetic models currently rely on kinetic and thermodynamics information from static-based simulations. However, it may be envisaged that in the future kMC models could be constructed for complex zeolitic systems, where input from first-principles MD simulations is used. The kMC models mentioned and their integration with first-principles MD methods are only one example of a potential avenue on how to study the overall dynamics of a flow of particles over an active catalyst. The overall dynamics of all events taking place at the crystal particle level at operating conditions is obviously very complex, and it is foreseen that also new integrative methods will have to be developed which allow the study of the dynamics of adsorption, reaction, and diffusion in a consistent way. First-principles MD methods will certainly play an important role in the whole ecosystem of methods necessary to study the dynamics of processes taking place at the catalyst particle level, but they will have to be combined in an innovative way with many other methods to for example automatically discover reaction paths and networks which will allow the complexity at operating conditions to be tackled.[9,53,278]

AUTHOR INFORMATION

Corresponding Author

Veronique Van Speybroeck − *Center for Molecular Modeling, Ghent University, 9052 Zwijnaarde, Belgium;* orcid.org/0000-0003-2206-178X; Email: veronique.vanspeybroeck@ugent.be

Authors

Massimo Bocus − *Center for Molecular Modeling, Ghent University, 9052 Zwijnaarde, Belgium;* orcid.org/0000-0001-9474-6644

Pieter Cnudde − *Center for Molecular Modeling, Ghent University, 9052 Zwijnaarde, Belgium;* orcid.org/0000-0002-6735-0078

Louis Vanduyfhuys − *Center for Molecular Modeling, Ghent University, 9052 Zwijnaarde, Belgium;* orcid.org/0000-0001-6747-3388

Complete contact information is available at: https://pubs.acs.org/10.1021/acscatal.3c01945

Notes

The authors declare no competing financial interest.

ACKNOWLEDGMENTS

M.B. acknowledges financial support from the Fund for Scientific Research (Grants G024019N and G0D0518N) and Excellence of Science (EOS) Project BioFact (EOS ID 30902231). P.C. gratefully acknowledges financial support from the Fund for Scientific Research Flanders (FWO) (Grant 1246922N). V.V.S. and L.V. are grateful for financial support from the Research Fund of Ghent University (BOF). V.V.S. acknowledges funding from the European Research Council under the European Union's Horizon 2020 Research and Innovation Programme (Consolidator ERC Grant Agreement 647755 − DYNPOR (2015-2020)).

REFERENCES

(1) Markland, T. E.; Ceriotti, M. Nuclear quantum effects enter the mainstream. *Nat. Rev. Chem.* **2018**, *2* (3), 0109.

(2) Kapil, V.; Rossi, M.; Marsalek, O.; Petraglia, R.; Litman, Y.; Spura, T.; Cheng, B. Q.; Cuzzocrea, A.; Meissner, R. H.; Wilkins, D. M.; Helfrecht, B. A.; Juda, P.; Bienvenue, S. P.; Fang, W.; Kessler, J.; Poltavsky, I.; Vandenbrande, S.; Wieme, J.; Corminboeuf, C.; Kuhne, T. D.; Manolopoulos, D. E.; Markland, T. E.; Richardson, J. O.; Tkatchenko, A.; Tribello, G. A.; Van Speybroeck, V.; Ceriotti, M. i-PI 2.0: A universal force engine for advanced molecular simulations. *Comput. Phys. Commun.* **2019**, *236*, 214−223.

(3) Marx, D.; Parrinello, M. Ab initio path integral molecular dynamics: Basic ideas. *J. Chem. Phys.* **1996**, *104* (11), 4077−4082.

(4) Bocus, M.; Goeminne, R.; Lamaire, A.; Cools-Ceuppens, M.; Verstraelen, T.; Van Speybroeck, V. Nuclear quantum effects on zeolite proton hopping kinetics explored with machine learning potentials and path integral molecular dynamics. *Nat. Commun.* **2023**, *14* (1), 1008.

(5) Urakawa, A.; Baiker, A. Space-Resolved Profiling Relevant in Heterogeneous Catalysis. *Top. Catal.* **2009**, *52* (10), 1312−1322.

(6) Buurmans, I. L. C.; Weckhuysen, B. M. Heterogeneities of individual catalyst particles in space and time as monitored by spectroscopy. *Nat. Chem.* **2012**, *4* (11), 873−886.

(7) Ye, G. H.; Sun, Y. Y.; Guo, Z. Y.; Zhu, K. K.; Liu, H. L.; Zhou, X. G.; Coppens, M. O. Effects of zeolite particle size and internal grain boundaries on Pt/Beta catalyzed isomerization of n-pentane. *J. Catal.* **2018**, *360*, 152−159.

(8) Yarulina, I.; De Wispelaere, K.; Bailleul, S.; Goetze, J.; Radersma, M.; Abou-Hamad, E.; Vollmer, I.; Goesten, M.; Mezari, B.; Hensen, E. J. M.; Martinez-Espin, J. S.; Morten, M.; Mitchell, S.; Perez-Ramirez, J.;

Olsbye, U.; Weckhuysen, B. M.; Van Speybroeck, V.; Kapteijn, F.; Gascon, J. Structure-performance descriptors and the role of Lewis acidity in the methanol-to-propylene process. *Nat. Chem.* **2018**, *10* (8), 804−812.
(9) Chizallet, C. Toward the Atomic Scale Simulation of Intricate Acidic Aluminosilicate Catalysts. *ACS Catal.* **2020**, *10* (10), 5579−5601.
(10) Weckhuysen, B. M. Studying birth, life and death of catalytic solids with operando spectroscopy. *Natl. Sci. Rev.* **2015**, *2* (2), 147−149.
(11) Ertl, G. Reactions at surfaces: From atoms to complexity (Nobel lecture). *Angew. Chem., Int. Ed.* **2008**, *47* (19), 3524−3535.
(12) Van Speybroeck, V.; Vandenhaute, S.; Hoffman, A. E. J.; Rogge, S. M. J. Towards modeling spatiotemporal processes in metal-organic frameworks. *Trends Chem.* **2021**, *3* (8), 605−619.
(13) Gao, M.; Li, H.; Liu, W.; Xu, Z.; Peng, S.; Yang, M.; Ye, M.; Liu, Z. Imaging spatiotemporal evolution of molecules and active sites in zeolite catalyst during methanol-to-olefins reaction. *Nat. Commun.* **2020**, *11* (1), 3641.
(14) Goetze, J.; Weckhuysen, B. M. Spatiotemporal coke formation over zeolite ZSM-5 during the methanol-to-olefins process as studied with operando UV-vis spectroscopy: a comparison between H-ZSM-5 and Mg-ZSM-5. *Catal. Sci. Technol.* **2018**, *8* (6), 1632−1644.
(15) Banares, M. A. Operando methodology: combination of in situ spectroscopy and simultaneous activity measurements under catalytic reaction conditions. *Catal. Today* **2005**, *100* (1−2), 71−77.
(16) Bañares, M. A.; Guerrero-Pérez, M. O.; Urakawa, A. Preface of SI: Operando. *Catal. Today* **2019**, *336*, 1.
(17) Weckhuysen, B. M. Snapshots of a working catalyst: possibilities and limitations of in situ spectroscopy in the field of heterogeneous catalysis. *Chem. Commun.* **2002**, *2*, 97−110.
(18) Weckhuysen, B. M. Determining the active site in a catalytic process: Operando spectroscopy is more than a buzzword. *Phys. Chem. Chem. Phys.* **2003**, *5* (20), 4351−4360.
(19) Chakrabarti, A.; Ford, M. E.; Gregory, D.; Hu, R. R.; Keturakis, C. J.; Lwin, S.; Tang, Y. D.; Yang, Z.; Zhu, M. H.; Bañares, M. A.; Wachs, I. E. A decade plus of operando spectroscopy studies. *Catal. Today* **2017**, *283*, 27−53.
(20) Portela, R.; Perez-Ferreras, S.; Serrano-Lotina, A.; Bañares, M. A. Engineering operando methodology: Understanding catalysis in time and space. *Front. Chem. Sci. Eng.* **2018**, *12* (3), 509−536.
(21) Jones, C. W.; Tao, F.; Garland, M. V. Introduction to Special Issue on Operando and In Situ Studies of Catalysis. *ACS Catal.* **2012**, *2* (11), 2444−2445.
(22) Meirer, F.; Weckhuysen, B. M. Spatial and temporal exploration of heterogeneous catalysts with synchrotron radiation. *Nat. Rev. Mater.* **2018**, *3* (9), 324−340.
(23) Whiting, G. T.; Nikolopoulos, N.; Nikolopoulos, I.; Chowdhury, A. D.; Weckhuysen, B. M. Visualizing pore architecture and molecular transport boundaries in catalyst bodies with fluorescent nanoprobes. *Nat. Chem.* **2019**, *11* (1), 23−31.
(24) Fraux, G.; Chibani, S.; Coudert, F. X. Modelling of framework materials at multiple scales: current practices and open questions. *Philos. Trans. R. Soc. A* **2019**, *377* (2149), 20180220.
(25) Wang, S.; He, Y.; Jiao, W. Y.; Wang, J. G.; Fan, W. B. Recent experimental and theoretical studies on Al siting/acid site distribution in zeolite framework. *Curr. Opin. Chem. Eng.* **2019**, *23*, 146−154.
(26) Li, G. N.; Pidko, E. A. The Nature and Catalytic Function of Cation Sites in Zeolites: a Computational Perspective. *ChemCatChem* **2019**, *11* (1), 134−156.
(27) Grajciar, L.; Heard, C. J.; Bondarenko, A. A.; Polynski, M. V.; Meeprasert, J.; Pidko, E. A.; Nachtigall, P. Towards operando computational modeling in heterogeneous catalysis. *Chem. Soc. Rev.* **2018**, *47* (22), 8307−8348.
(28) Margraf, J. T.; Jung, H.; Scheurer, C.; Reuter, K. Exploring catalytic reaction networks with machine learning. *Nat. Catal.* **2023**, *6* (2), 112−121.
(29) Bruix, A.; Margraf, J. T.; Andersen, M.; Reuter, K. First-principles-based multiscale modelling of heterogeneous catalysis. *Nat. Catal.* **2019**, *2* (8), 659−670.
(30) Van Speybroeck, V. Challenges in modelling dynamic processes in realistic nanostructured materials at operating conditions. *Philos. Trans. R. Soc. A.* **2023**, *381* (2250), 20220239.
(31) Pidko, E. A. Toward the Balance between the Reductionist and Systems Approaches in Computational Catalysis: Model versus Method Accuracy for the Description of Catalytic Systems. *ACS Catal.* **2017**, *7* (7), 4230−4234.
(32) Van Speybroeck, V.; Hemelsoet, K.; Joos, L.; Waroquier, M.; Bell, R. G.; Catlow, C. R. A. Advances in theory and their application within the field of zeolite chemistry. *Chem. Soc. Rev.* **2015**, *44* (20), 7044−7111.
(33) Ma, H.; Chen, Y.; Wei, Z.; Wang, S.; Qin, Z.; Dong, M.; Li, J.; Wang, J.; Fan, W. Reaction Mechanism for Direct Cyclization of Linear C5, C6, and C7 Alkenes over H-ITQ-13 Zeolite Investigated Using Density Functional Theory. *ChemPhysChem* **2018**, *19* (4), 496−503.
(34) Yi, X.; Xiao, Y.; Li, G.; Liu, Z.; Chen, W.; Liu, S.-B.; Zheng, A. From One to Two: Acidic Proton Spatial Networks in Porous Zeolite Materials. *Chem. Mater.* **2020**, *32* (3), 1332−1342.
(35) Rey, J.; Raybaud, P.; Chizallet, C. Ab Initio Simulation of the Acid Sites at the External Surface of Zeolite Beta. *ChemCatChem* **2017**, *9* (12), 2176−2185.
(36) Treps, L.; Gomez, A.; de Bruin, T.; Chizallet, C. Environment, Stability and Acidity of External Surface Sites of Silicalite-1 and ZSM-5 Micro and Nano Slabs, Sheets, and Crystals. *ACS Catal.* **2020**, *10* (5), 3297−331.
(37) Treps, L.; Demaret, C.; Wisser, D.; Harbuzaru, B.; Methivier, A.; Guillon, E.; Benedis, D. V.; Gomez, A.; de Bruin, T.; Rivallan, M.; Catita, L.; Lesage, A.; Chizallet, C. Spectroscopic Expression of the External Surface Sites of H-ZSM-5. *J. Phys. Chem. C* **2021**, *125* (3), 2163−2181.
(38) Witman, M.; Ling, S. L.; Boyd, P.; Barthel, S.; Haranczyk, M.; Slater, B.; Smit, B. Cutting Materials in Half: A Graph Theory Approach for Generating Crystal Surfaces and Its Prediction of 2D Zeolites. *ACS Cent. Sci.* **2018**, *4* (2), 235−245.
(39) Bučko, T.; Hafner, J.; Benco, L. Active sites for the vapor phase Beckmann rearrangement over mordenite: An ab initio study. *J. Phys. Chem. A* **2004**, *108* (51), 11388−11397.
(40) Cnudde, P.; Redekop, E. A.; Dai, W. L.; Porcaro, N. G.; Waroquier, M.; Bordiga, S.; Hunger, M.; Li, L. D.; Olsbye, U.; Van Speybroeck, V. Experimental and Theoretical Evidence for the Promotional Effect of Acid Sites on the Diffusion of Alkenes through Small-Pore Zeolites. *Angew. Chem., Int. Ed.* **2021**, *60* (18), 10016−10022.
(41) Cnudde, P.; Demuynck, R.; Vandenbrande, S.; Waroquier, M.; Sastre, G.; Van Speybroeck, V. Light Olefin Diffusion during the MTO Process on H-SAPO-34: A Complex Interplay of Molecular Factors. *J. Am. Chem. Soc.* **2020**, *142* (13), 6007−6017.
(42) Hajek, J.; Van der Mynsbrugge, J.; De Wispelaere, K.; Cnudde, P.; Vanduyfhuys, L.; Waroquier, M.; Van Speybroeck, V. On the stability and nature of adsorbed pentene in Brønsted acid zeolite H-ZSM-5 at 323 K. *J. Catal.* **2016**, *340*, 227−235.
(43) Tuma, C.; Kerber, T.; Sauer, J. The tert-Butyl Cation in H-Zeolites: Deprotonation to Isobutene and Conversion into Surface Alkoxides. *Angew. Chem., Int. Ed.* **2010**, *49* (27), 4678−4680.
(44) Goncalves, T. J.; Plessow, P. N.; Studt, F. On the Accuracy of Density Functional Theory in Zeolite Catalysis. *ChemCatChem* **2019**, *11* (17), 4368−4376.
(45) Chehaibou, B.; Badawi, M.; Bučko, T.; Bazhirov, T.; Rocca, D. Computing RPA Adsorption Enthalpies by Machine Learning Thermodynamic Perturbation Theory. *J. Chem. Theory Comput.* **2019**, *15* (11), 6333−6342.
(46) Sauer, J. Ab Initio Calculations for Molecule-Surface Interactions with Chemical Accuracy. *Acc. Chem. Res.* **2019**, *52* (12), 3502−3510.
(47) Grimme, S.; Antony, J.; Ehrlich, S.; Krieg, H. A consistent and accurate ab initio parametrization of density functional dispersion

https://doi.org/10.1021/acscatal.3c01945
ACS Catal. 2023, 13, 11455−11493

correction (DFT-D) for the 94 elements H-Pu. *J. Chem. Phys.* **2010**, *132* (15), 154104.
(48) Maurer, R. J.; Freysoldt, C.; Reilly, A. M.; Brandenburg, J. G.; Hofmann, O. T.; Björkman, T.; Lebègue, S.; Tkatchenko, A. Advances in Density-Functional Calculations for Materials Modeling. *Annu. Rev. Mater. Res.* **2019**, *49* (1), 1−30.
(49) Stöhr, M.; Van Voorhis, T.; Tkatchenko, A. Theory and practice of modeling van der Waals interactions in electronic-structure calculations. *Chem. Soc. Rev.* **2019**, *48* (15), 4118−4154.
(50) Hermann, J.; DiStasio, R. A.; Tkatchenko, A. First-Principles Models for van der Waals Interactions in Molecules and Materials: Concepts, Theory, and Applications. *Chem. Rev.* **2017**, *117* (6), 4714−4758.
(51) Grimme, S.; Hansen, A.; Brandenburg, J. G.; Bannwarth, C. Dispersion-Corrected Mean-Field Electronic Structure Methods. *Chem. Rev.* **2016**, *116* (9), 5105−5154.
(52) Perdew, J. P.; Schmidt, K. Jacob's ladder of density functional approximations for the exchange-correlation energy. *AIP Conf. Proc.* **2001**, *577*, 1−20.
(53) Chen, B. W. J.; Xu, L.; Mavrikakis, M. Computational Methods in Heterogeneous Catalysis. *Chem. Rev.* **2021**, *121* (2), 1007−1048.
(54) Perdew, J. P.; Burke, K.; Ernzerhof, M. Generalized gradient approximation made simple. *Phys. Rev. Lett.* **1996**, *77* (18), 3865−3868.
(55) Perdew, J. P.; Burke, K.; Ernzerhof, M. Generalized gradient approximation made simple. *Phys. Rev. Lett.* **1997**, *78* (7), 1396−1396.
(56) Grimme, S. Accurate description of van der Waals complexes by density functional theory including empirical corrections. *J. Comput. Chem.* **2004**, *25* (12), 1463−1473.
(57) Grimme, S. Semiempirical GGA-type density functional constructed with a long-range dispersion correction. *J. Comput. Chem.* **2006**, *27* (15), 1787−1799.
(58) Grimme, S.; Antony, J.; Schwabe, T.; Muck-Lichtenfeld, C. Density functional theory with dispersion corrections for supramolecular structures, aggregates, and complexes of (bio)organic molecules. *Org. Biomol. Chem.* **2007**, *5* (5), 741−758.
(59) Stanciakova, K.; Louwen, J. N.; Weckhuysen, B. M.; Bulo, R. E.; Göltl, F. Understanding Water-Zeolite Interactions: On the Accuracy of Density Functionals. *J. Phys. Chem. C* **2021**, *125* (37), 20261−20274.
(60) Hargreaves, J. S. J.; Munnoch, A. L. A survey of the influence of binders in zeolite catalysis. *Catal. Sci. Technol.* **2013**, *3* (5), 1165−1171.
(61) Li, X.; Rezaei, F.; Rownaghi, A. A. Methanol-to-olefin conversion on 3D-printed ZSM-5 monolith catalysts: Effects of metal doping, mesoporosity and acid strength. *Microporous Mesoporous Mater.* **2019**, *276*, 1−12.
(62) Frenkel, D.; Smit, B. *Understanding Molecular Simulation*, 2nd ed.; Academic Press, 2002.
(63) Sutto, L.; Marsili, S.; Gervasio, F. L. New advances in metadynamics. *Wiley Interdiscip. Rev.: Comput. Mol. Sci.* **2012**, *2* (5), 771−779.
(64) Laio, A.; Parrinello, M. Escaping free-energy minima. *Proc. Natl. Acad. Sci. U.S.A.* **2002**, *99* (20), 12562−12566.
(65) Valsson, O.; Tiwary, P.; Parrinello, M. Enhancing Important Fluctuations: Rare Events and Metadynamics from a Conceptual Viewpoint. *Annu. Rev. Phys. Chem.* **2016**, *67*, 159−84.
(66) The PLUMED Consortium. Promoting transparency and reproducibility in enhanced molecular simulations. *Nat. Methods* **2019**, *16* (8), 670−673.
(67) Hénin, J.; Lelièvre, T.; Shirts, M. R.; Valsson, O.; Delemotte, L. Enhanced Sampling Methods for Molecular Dynamics Simulations [Article v1.0]. *Living J. Comput. Mol. Sci.* **2022**, *4* (1), 1583.
(68) Piccini, G. M.; Lee, M. S.; Yuk, S. F.; Zhang, D. F.; Collinge, G.; Kollias, L.; Nguyen, M. T.; Glezakou, V. A.; Rousseau, R. Ab initio molecular dynamics with enhanced sampling in heterogeneous catalysis. *Catal. Sci. Technol.* **2022**, *12* (1), 12−37.
(69) Vanduyfhuys, L.; Vandenbrande, S.; Verstraelen, T.; Schmid, R.; Waroquier, M.; Van Speybroeck, V. QuickFF: A Program for a Quick and Easy Derivation of Force Fields for Metal-Organic Frameworks from Ab Initio Input. *J. Comput. Chem.* **2015**, *36* (13), 1015−1027.
(70) Vanduyfhuys, L.; Vandenbrande, S.; Wieme, J.; Waroquier, M.; Verstraelen, T.; Van Speybroeck, V. Extension of the QuickFF force field protocol for an improved accuracy of structural, vibrational, mechanical and thermal properties of metal-organic frameworks. *J. Comput. Chem.* **2018**, *39* (16), 999−1011.
(71) Combariza, A. F.; Gomez, D. A.; Sastre, G. Simulating the properties of small pore silica zeolites using interatomic potentials. *Chem. Soc. Rev.* **2013**, *42* (1), 114−127.
(72) Fang, H.; Demir, H.; Kamakoti, P.; Sholl, D. S. Recent developments in first-principles force fields for molecules in nanoporous materials. *J. Mater. Chem. A* **2014**, *2* (2), 274−291.
(73) Dubbeldam, D.; Walton, K. S.; Vlugt, T. J. H.; Calero, S. Design, Parameterization, and Implementation of Atomic Force Fields for Adsorption in Nanoporous Materials. *Adv. Theory Simul.* **2019**, *2* (11), 1900135.
(74) Smit, B.; Maesen, T. L. M. Molecular simulations of zeolites: Adsorption, diffusion, and shape selectivity. *Chem. Rev.* **2008**, *108* (10), 4125−4184.
(75) Dubbeldam, D.; Torres-Knoop, A.; Walton, K. S. On the inner workings of Monte Carlo codes. *Mol. Simul.* **2013**, *39* (14−15), 1253−1292.
(76) Dubbeldam, D.; Calero, S.; Ellis, D. E.; Snurr, R. Q. RASPA: molecular simulation software for adsorption and diffusion in flexible nanoporous materials. *Mol. Simul.* **2016**, *42* (2), 81−101.
(77) Bai, P.; Tsapatsis, M.; Siepmann, J. I. TraPPE-zeo: Transferable Potentials for Phase Equilibria Force Field for All-Silica Zeolites. *J. Phys. Chem. C* **2013**, *117* (46), 24375−24387.
(78) Bai, C.; Liu, L.; Sun, H. Molecular Dynamics Simulations of Methanol to Olefin Reactions in HZSM-5 Zeolite Using a ReaxFF Force Field. *J. Phys. Chem. C* **2012**, *116* (12), 7029−7039.
(79) Joshi, K. L.; van Duin, A. C. T. Molecular Dynamics Study on the Influence of Additives on the High-Temperature Structural and Acidic Properties of ZSM-5 Zeolite. *Energy Fuels* **2013**, *27* (8), 4481−4488.
(80) Joshi, K. L.; Psofogiannakis, G.; van Duin, A. C. T.; Raman, S. Reactive molecular simulations of protonation of water clusters and depletion of acidity in H-ZSM-5 zeolite. *Phys. Chem. Chem. Phys.* **2014**, *16* (34), 18433−18441.
(81) Pitman, M. C.; van Duin, A. C. T. Dynamics of Confined Reactive Water in Smectite Clay-Zeolite Composites. *J. Am. Chem. Soc.* **2012**, *134* (6), 3042−3053.
(82) Noé, F.; Tkatchenko, A.; Müller, K.-R.; Clementi, C. Machine Learning for Molecular Simulation. *Annu. Rev. Phys. Chem.* **2020**, *71*, 361−390.
(83) Behler, J. Perspective: Machine learning potentials for atomistic simulations. *J. Chem. Phys.* **2016**, *145* (17), 170901.
(84) Bartók, A. P.; De, S.; Poelking, C.; Bernstein, N.; Kermode, J. R.; Csányi, G.; Ceriotti, M. Machine learning unifies the modeling of materials and molecules. *Sci. Adv.* **2017**, *3* (12), e1701816.
(85) Behler, J. Four Generations of High-Dimensional Neural Network Potentials. *Chem. Rev.* **2021**, *121* (16), 10037−10072.
(86) Friederich, P.; Hase, F.; Proppe, J.; Aspuru-Guzik, A. Machine-learned potentials for next-generation matter simulations. *Nat. Mater.* **2021**, *20* (6), 750−761.
(87) Zhang, L.; Han, J.; Wang, H.; Car, R.; E, W. Deep Potential Molecular Dynamics: A Scalable Model with the Accuracy of Quantum Mechanics. *Phys. Rev. Lett.* **2018**, *120* (14), 143001.
(88) Jinnouchi, R.; Miwa, K.; Karsai, F.; Kresse, G.; Asahi, R. On-the-Fly Active Learning of Interatomic Potentials for Large-Scale Atomistic Simulations. *J. Phys. Chem. Lett.* **2020**, *11* (17), 6946−6955.
(89) Ramakrishnan, R.; Dral, P. O.; Rupp, M.; von Lilienfeld, O. A. Big Data Meets Quantum Chemistry Approximations: The Delta-Machine Learning Approach. *J. Chem. Theory Comput.* **2015**, *11* (5), 2087−2096.
(90) Unke, O. T.; Chmiela, S.; Sauceda, H. E.; Gastegger, M.; Poltavsky, I.; Schutt, K. T.; Tkatchenko, A.; Muller, K. R. Machine Learning Force Fields. *Chem. Rev.* **2021**, *121* (16), 10142−10186.
(91) Ko, T. W.; Finkler, J. A.; Goedecker, S.; Behler, J. General-Purpose Machine Learning Potentials Capturing Nonlocal Charge Transfer. *Acc. Chem. Res.* **2021**, *54* (4), 808−817.

https://doi.org/10.1021/acscatal.3c01945
ACS Catal. 2023, 13, 11455−11493

(92) Erlebach, A.; Nachtigall, P.; Grajciar, L. Accurate large-scale simulations of siliceous zeolites by neural network potentials. *npj Comput. Mater.* **2022**, *8* (1), 174.
(93) Ma, S.; Liu, Z.-P. Machine learning potential era of zeolite simulation. *Chem. Sci.* **2022**, *13* (18), 5055−5068.
(94) Sours, T. G.; Kulkarni, A. R. Predicting Structural Properties of Pure Silica Zeolites Using Deep Neural Network Potentials. *J. Phys. Chem. C* **2023**, *127* (3), 1455−1463.
(95) Marx, D.; Hutter, J. *Ab Initio Molecular Dynamics: Basic Theory and Advanced Methods*; Cambridge University Press, 2009.
(96) Van Speybroeck, V.; Meier, R. J. A recent development in computational chemistry: chemical reactions from first principles molecular dynamics simulations. *Chem. Soc. Rev.* **2003**, *32* (3), 151−157.
(97) Tuckerman, M. E. *Statistical Mechanics: Theory and Molecular Simulation*; Oxford University Press, 2001.
(98) Van Speybroeck, V.; De Wispelaere, K.; Van der Mynsbrugge, J.; Vandichel, M.; Hemelsoet, K.; Waroquier, M. First principle chemical kinetics in zeolites: the methanol-to-olefin process as a case study. *Chem. Soc. Rev.* **2014**, *43* (21), 7326−7357.
(99) Hänggi, P.; Talkner, P.; Borkovec, M. Reaction-rate theory: fifty years after Kramers. *Rev. Mod. Phys.* **1990**, *62* (2), 251−341.
(100) Truhlar, D. G.; Garrett, B. C.; Klippenstein, S. J. Current status of transition-state theory. *J. Phys. Chem.* **1996**, *100* (31), 12771−12800.
(101) Torrie, G. M.; Valleau, J. P. Nonphysical sampling distributions in Monte Carlo free-energy estimation: Umbrella sampling. *J. Comput. Phys.* **1977**, *23* (2), 187−199.
(102) Bolhuis, P. G.; Swenson, D. W. H. Transition Path Sampling as Markov Chain Monte Carlo of Trajectories: Recent Algorithms, Software, Applications, and Future Outlook. *Adv. Theory Simul.* **2021**, *4* (4), 2000237.
(103) Dellago, C.; Bolhuis, P. G.; Geissler, P. L. Transition Path Sampling. *Adv. Chem. Phys.* **2003**, *123*, 1−78.
(104) Peters, B., Chapter 19 - Transition path sampling. In *Reaction Rate Theory and Rare Events Simulations*; Peters, B., Ed.; Elsevier: Amsterdam, 2017; pp 507−537.
(105) van Erp, T. S.; Bolhuis, P. G. Elaborating transition interface sampling methods. *J. Comput. Phys.* **2005**, *205* (1), 157−181.
(106) Peters, B., Chapter 13 - Reactive flux. In *Reaction Rate Theory and Rare Events Simulations*; Peters, B., Ed.; Elsevier: Amsterdam, 2017; pp 335−362.
(107) van Erp, T. S.; Moroni, D.; Bolhuis, P. G. A novel path sampling method for the calculation of rate constants. *J. Chem. Phys.* **2003**, *118* (17), 7762−7774.
(108) Moroni, D.; Bolhuis, P. G.; van Erp, T. S. Rate constants for diffusive processes by partial path sampling. *J. Chem. Phys.* **2004**, *120* (9), 4055−4065.
(109) Cabriolu, R.; Skjelbred Refsnes, K. M.; Bolhuis, P. G.; van Erp, T. S. Foundations and latest advances in replica exchange transition interface sampling. *J. Chem. Phys.* **2017**, *147* (15), 152722.
(110) Bučko, T.; Benco, L.; Dubay, O.; Dellago, C.; Hafner, J. Mechanism of alkane dehydrogenation catalyzed by acidic zeolites: Ab initio transition path sampling. *J. Chem. Phys.* **2009**, *131* (21), 214508.
(111) Bucko, T.; Hafner, J. Entropy effects in hydrocarbon conversion reactions: free-energy integrations and transition-path sampling. *J. Phys.: Condens. Matter* **2010**, *22* (38), 384201.
(112) Bučko, T.; Benco, L.; Hafner, J.; Ángyán, J. G. Monomolecular cracking of propane over acidic chabazite: An ab initio molecular dynamics and transition path sampling study. *J. Catal.* **2011**, *279* (1), 220−228.
(113) Bučko, T.; Hafner, J. The role of spatial constraints and entropy in the adsorption and transformation of hydrocarbons catalyzed by zeolites. *J. Catal.* **2015**, *329*, 32−48.
(114) Rey, J.; Bignaud, C.; Raybaud, P.; Bučko, T.; Chizallet, C. Dynamic Features of Transition States for β-Scission Reactions of Alkenes over Acid Zeolites Revealed by AIMD Simulations. *Angew. Chem., Int. Ed.* **2020**, *59* (43), 18938−18942.
(115) van Erp, T. S. How far can we stretch the timescale with RETIS? *Europhys. Lett.* **2023**, *143*, 30001.
(116) Lo, C. S.; Radhakrishnan, R.; Trout, B. L. Application of transition path sampling methods in catalysis: A new mechanism for CC bond formation in the methanol coupling reaction in chabazite. *Catal. Today* **2005**, *105* (1), 93−105.
(117) Peters, B. Reaction Coordinates and Mechanistic Hypothesis Tests. *Annu. Rev. Phys. Chem.* **2016**, *67*, 669−690.
(118) Pérez de Alba Ortíz, A.; Tiwari, A.; Puthenkalathil, R. C.; Ensing, B. Advances in enhanced sampling along adaptive paths of collective variables. *J. Chem. Phys.* **2018**, *149* (7), 072320.
(119) Maragliano, L.; Fischer, A.; Vanden-Eijnden, E.; Ciccotti, G. String method in collective variables: Minimum free energy paths and isocommittor surfaces. *J. Chem. Phys.* **2006**, *125* (2), 024106.
(120) Bailleul, S.; Dedecker, K.; Cnudde, P.; Vanduyfhuys, L.; Waroquier, M.; Van Speybroeck, V. Ab initio enhanced sampling kinetic study on MTO ethene methylation reaction. *J. Catal.* **2020**, *388*, 38−51.
(121) Svelle, S.; Ronning, P. A.; Kolboe, S. Kinetic studies of zeolite-catalyzed methylation reactions 1. Coreaction of [^{12}C]ethene and [^{13}C]methanol. *J. Catal.* **2004**, *224* (1), 115−123.
(122) Svelle, S.; Ronning, P. O.; Olsbye, U.; Kolboe, S. Kinetic studies of zeolite-catalyzed methylation reactions. Part 2. Co-reaction of [^{12}C]propene or [^{12}C]*n*-butene and [^{13}C]methanol. *J. Catal.* **2005**, *234* (2), 385−400.
(123) Bučko, T.; Chibani, S.; Paul, J. F.; Cantrel, L.; Badawi, M. Dissociative iodomethane adsorption on Ag-MOR and the formation of AgI clusters: an *ab initio* molecular dynamics study. *Phys. Chem. Chem. Phys.* **2017**, *19* (40), 27530−27543.
(124) Ciccotti, G.; Ferrario, M. Blue Moon Approach to Rare Events. *Mol. Simul.* **2004**, *30* (11−12), 787−793.
(125) Carter, E. A.; Ciccotti, G.; Hynes, J. T.; Kapral, R. Constrained reaction coordinate dynamics for the simulation of rare events. *Chem. Phys. Lett.* **1989**, *156* (5), 472−477.
(126) Sprik, M.; Ciccotti, G. Free energy from constrained molecular dynamics. *J. Chem. Phys.* **1998**, *109* (18), 7737−7744.
(127) Bal, K. M.; Fukuhara, S.; Shibuta, Y.; Neyts, E. C. Free energy barriers from biased molecular dynamics simulations. *J. Chem. Phys.* **2020**, *153* (11), 114118.
(128) Dietschreit, J. C. B.; Diestler, D. J.; Hulm, A.; Ochsenfeld, C.; Gómez-Bombarelli, R. From free-energy profiles to activation free energies. *J. Chem. Phys.* **2022**, *157* (8), 084113.
(129) Vanduyfhuys, L. *THERMOLIB - Software package to construct and manipulate free energy surfaces (FES) as a function of a (set of) priori chosen collective variable(s) from output of molecular simulations*. https://molmod.ugent.be/software/ThermoLIB.
(130) Chen, W.; Sidky, H.; Ferguson, A. L. Nonlinear discovery of slow molecular modes using state-free reversible VAMPnets. *J. Chem. Phys.* **2019**, *150* (21), 214114.
(131) Sidky, H.; Chen, W.; Ferguson, A. L. Machine learning for collective variable discovery and enhanced sampling in biomolecular simulation. *Mol. Phys.* **2020**, *118* (5), e1737742.
(132) Wang, Y.; Lamim Ribeiro, J. M.; Tiwary, P. Machine learning approaches for analyzing and enhancing molecular dynamics simulations. *Curr. Opin. Struct. Biol.* **2020**, *61*, 139−145.
(133) Noé, F.; Clementi, C. Collective variables for the study of long-time kinetics from molecular trajectories: theory and methods. *Curr. Opin. Struct. Biol.* **2017**, *43*, 141−147.
(134) Bonati, L.; Piccini, G.; Parrinello, M. Deep learning the slow modes for rare events sampling. *Proc. Natl. Acad. Sci. U. S. A.* **2021**, *118* (44), No. e2113533118.
(135) Bhakat, S. Collective variable discovery in the age of machine learning: reality, hype and everything in between. *RSC Adv.* **2022**, *12* (38), 25010−25024.
(136) Chen, W.; Ferguson, A. L. Molecular Enhanced Sampling with Autoencoders: On-The-Fly Collective Variable Discovery and Accelerated Free Energy Landscape Exploration. *J. Comput. Chem.* **2018**, *39* (25), 2079−2102.
(137) Chen, W.; Tan, A. R.; Ferguson, A. L. Collective variable discovery and enhanced sampling using autoencoders: Innovations in

https://doi.org/10.1021/acscatal.3c01945
ACS Catal. 2023, 13, 11455−11493

network architecture and error function design. *J. Chem. Phys.* **2018**, *149* (7), 072312.
(138) Demuynck, R.; Wieme, J.; Rogge, S. M. J.; Dedecker, K. D.; Vanduyfhuys, L.; Waroquier, M.; Van Speybroeck, V. Protocol for Identifying Accurate Collective Variables in Enhanced Molecular Dynamics Simulations for the Description of Structural Transformations in Flexible Metal-Organic Frameworks. *J. Chem. Theory Comput.* **2018**, *14* (11), 5511−5526.
(139) Šípka, M.; Erlebach, A.; Grajciar, L. Constructing Collective Variables Using Invariant Learned Representations. *J. Chem. Theory Comput.* **2023**, *19* (3), 887−901.
(140) Van Speybroeck, V.; Van der Mynsbrugge, J.; Vandichel, M.; Hemelsoet, K.; Lesthaeghe, D.; Ghysels, A.; Marin, G. B.; Waroquier, M. First Principle Kinetic Studies of Zeolite-Catalyzed Methylation Reactions. *J. Am. Chem. Soc.* **2011**, *133* (4), 888−899.
(141) Bond, G. C.; Keane, M. A.; Kral, H.; Lercher, J. A. Compensation phenomena in heterogeneous catalysis: General principles and a possible explanation. *Catal. Rev.: Sci. Eng.* **2000**, *42* (3), 323−383.
(142) Svelle, S.; Tuma, C.; Rozanska, X.; Kerber, T.; Sauer, J. Quantum Chemical Modeling of Zeolite-Catalyzed Methylation Reactions: Toward Chemical Accuracy for Barriers. *J. Am. Chem. Soc.* **2009**, *131* (2), 816−825.
(143) Piccini, G.; Alessio, M.; Sauer, J. Ab Initio Calculation of Rate Constants for Molecule-Surface Reactions with Chemical Accuracy. *Angew. Chem., Int. Ed.* **2016**, *55* (17), 5235−5237.
(144) Piccini, G.; Sauer, J. Effect of Anharmonicity on Adsorption Thermodynamics. *J. Chem. Theory Comput.* **2014**, *10* (6), 2479−2487.
(145) Piccini, G.; Sauer, J. Quantum Chemical Free Energies: Structure Optimization and Vibrational Frequencies in Normal Modes. *J. Chem. Theory Comput.* **2013**, *9* (11), 5038−5045.
(146) Malviya, S.; Bai, P. Computational Investigation of Site-Dependent Activation Barriers of Zeolite-Catalyzed Protolytic Cracking Reactions. *ACS Catal.* **2023**, *13* (1), 179−190.
(147) De Wispelaere, K.; Ensing, B.; Ghysels, A.; Meijer, E. J.; Van Speybroeck, V. Complex Reaction Environments and Competing Reaction Mechanisms in Zeolite Catalysis: Insights from Advanced Molecular Dynamics. *Chem. - Eur. J.* **2015**, *21* (26), 9385−9396.
(148) Cnudde, P.; De Wispelaere, K.; Vanduyfhuys, L.; Demuynck, R.; Van der Mynsbrugge, J.; Waroquier, M.; Van Speybroeck, V. How Chain Length and Branching Influence the Alkene Cracking Reactivity on H-ZSM-5. *ACS Catal.* **2018**, *8* (10), 9579−9595.
(149) Thommes, M.; Kaneko, K.; Neimark, A. V.; Olivier, J. P.; Rodriguez-Reinoso, F.; Rouquerol, J.; Sing, K. S. W. Physisorption of gases, with special reference to the evaluation of surface area and pore size distribution (IUPAC Technical Report). *Pure Appl. Chem.* **2015**, *87* (9−10), 1051−1069.
(150) Schallmoser, S.; Haller, G. L.; Sanchez-Sanchez, M.; Lercher, J. A. Role of Spatial Constraints of Brønsted Acid Sites for Adsorption and Surface Reactions of Linear Pentenes. *J. Am. Chem. Soc.* **2017**, *139* (25), 8646−8652.
(151) Zhao, R.; Haller, G. L.; Lercher, J. A. Alkene adsorption and cracking on acidic zeolites - A gradual process of understanding. *Microporous Mesoporous Mater.* **2023**, *358*, 112390.
(152) Dai, W.; Wang, C.; Yi, X.; Zheng, A.; Li, L.; Wu, G.; Guan, N.; Xie, Z.; Dyballa, M.; Hunger, M. Identification of tert-Butyl Cations in Zeolite H-ZSM-5: Evidence from NMR Spectroscopy and DFT Calculations. *Angew. Chem., Int. Ed.* **2015**, *54* (30), 8783−8786.
(153) Gešvandtnerová, M.; Rocca, D.; Bučko, T. Methanol carbonylation over acid mordenite: Insights from ab initio molecular dynamics and machine learning thermodynamic perturbation theory. *J. Catal.* **2021**, *396*, 166−178.
(154) Chen, W.; Li, G.; Yi, X.; Day, S. J.; Tarach, K. A.; Liu, Z.; Liu, S.-B.; Edman Tsang, S. C.; Góra-Marek, K.; Zheng, A. Molecular Understanding of the Catalytic Consequence of Ketene Intermediates under Confinement. *J. Am. Chem. Soc.* **2021**, *143* (37), 15440−15452.
(155) Ramirez, A.; Dutta Chowdhury, A.; Dokania, A.; Cnudde, P.; Caglayan, M.; Yarulina, I.; Abou-Hamad, E.; Gevers, L.; Ould-Chikh, S.; De Wispelaere, K.; Van Speybroeck, V.; Gascon, J. Effect of Zeolite Topology and Reactor Configuration on the Direct Conversion of CO_2 to Light Olefins and Aromatics. *ACS Catal.* **2019**, *9* (7), 6320−6334.
(156) Chen, W.; Tarach, K. A.; Yi, X.; Liu, Z.; Tang, X.; Góra-Marek, K.; Zheng, A. Charge-separation driven mechanism via acylium ion intermediate migration during catalytic carbonylation in mordenite zeolite. *Nat. Commun.* **2022**, *13* (1), 7106.
(157) Collinge, G.; Yuk, S. F.; Nguyen, M.-T.; Lee, M.-S.; Glezakou, V.-A.; Rousseau, R. Effect of Collective Dynamics and Anharmonicity on Entropy in Heterogenous Catalysis: Building the Case for Advanced Molecular Simulations. *ACS Catal.* **2020**, *10* (16), 9236−9260.
(158) Cnudde, P.; De Wispelaere, K.; Van der Mynsbrugge, J.; Waroquier, M.; Van Speybroeck, V. Effect of temperature and branching on the nature and stability of alkene cracking intermediates in H-ZSM-5. *J. Catal.* **2017**, *345*, 53−69.
(159) Okamoto, Y. Generalized-ensemble algorithms: enhanced sampling techniques for Monte Carlo and molecular dynamics simulations. *J. Mol. Graphics Modell.* **2004**, *22* (5), 425−439.
(160) Galimberti, D. R.; Sauer, J. Chemically Accurate Vibrational Free Energies of Adsorption from Density Functional Theory Molecular Dynamics: Alkanes in Zeolites. *J. Chem. Theory Comput.* **2021**, *17* (9), 5849−5862.
(161) Berger, F.; Rybicki, M.; Sauer, J. Molecular Dynamics with Chemical Accuracy—Alkane Adsorption in Acidic Zeolites. *ACS Catal.* **2023**, *13* (3), 2011−2024.
(162) Rigby, A. M.; Kramer, G. J.; vanSanten, R. A. Mechanisms of hydrocarbon conversion in zeolites: A quantum mechanical study. *J. Catal.* **1997**, *170* (1), 1−10.
(163) Boronat, M.; Viruela, P.; Corma, A. Theoretical study of the mechanism of zeolite-catalyzed isomerization reactions of linear butenes. *J. Phys. Chem. A* **1998**, *102* (6), 982−989.
(164) Bhan, A.; Joshi, Y. V.; Delgass, W. N.; Thomson, K. T. DFT investigation of alkoxide formation from olefins in H-ZSM-5. *J. Phys. Chem. B* **2003**, *107* (38), 10476−10487.
(165) De Wispelaere, K.; Plessow, P. N.; Studt, F. Toward Computing Accurate Free Energies in Heterogeneous Catalysis: a Case Study for Adsorbed Isobutene in H-ZSM-5. *ACS Phys. Chem. Au* **2022**, *2* (5), 399−406.
(166) Plessow, P. N.; Studt, F. How Accurately Do Approximate Density Functionals Predict Trends in Acidic Zeolite Catalysis? *J. Phys. Chem. Lett.* **2020**, *11* (11), 4305−4310.
(167) Ren, Q.; Rybicki, M.; Sauer, J. Interaction of C_3−C_5 Alkenes with Zeolitic Brønsted Sites: π-Complexes, Alkoxides, and Carbenium Ions in H-FER. *J. Phys. Chem. C* **2020**, *124* (18), 10067−10078.
(168) Göltl, F.; Grüneis, A.; Bučko, T.; Hafner, J. Van der Waals interactions between hydrocarbon molecules and zeolites: Periodic calculations at different levels of theory, from density functional theory to the random phase approximation and Møller-Plesset perturbation theory. *J. Chem. Phys.* **2012**, *137* (11), 114111.
(169) Tuma, C.; Sauer, J. A hybrid MP2/planewave-DFT scheme for large chemical systems: proton jumps in zeolites. *Chem. Phys. Lett.* **2004**, *387* (4−6), 388−394.
(170) Tuma, C.; Sauer, J. Treating dispersion effects in extended systems by hybrid MP2: DFT calculations - protonation of isobutene in zeolite ferrierite. *Phys. Chem. Chem. Phys.* **2006**, *8* (34), 3955−3965.
(171) Berger, F.; Rybicki, M.; Sauer, J. Adsorption and cracking of propane by zeolites of different pore size. *J. Catal.* **2021**, *395*, 117−128.
(172) Herzog, B.; Chagas da Silva, M.; Casier, B.; Badawi, M.; Pascale, F.; Bučko, T.; Lebègue, S.; Rocca, D. Assessing the Accuracy of Machine Learning Thermodynamic Perturbation Theory: Density Functional Theory and Beyond. *J. Chem. Theory Comput.* **2022**, *18* (3), 1382−1394.
(173) Bučko, T.; Gešvandtnerová, M.; Rocca, D. Ab Initio Calculations of Free Energy of Activation at Multiple Electronic Structure Levels Made Affordable: An Effective Combination of Perturbation Theory and Machine Learning. *J. Chem. Theory Comput.* **2020**, *16* (10), 6049−6060.
(174) Del Ben, M.; Schütt, O.; Wentz, T.; Messmer, P.; Hutter, J.; VandeVondele, J. Enabling simulation at the fifth rung of DFT: Large

scale RPA calculations with excellent time to solution. *Comput. Phys. Commun.* **2015**, *187*, 120−129.
(175) Del Ben, M.; Hutter, J.; VandeVondele, J. Second-Order Møller-Plesset Perturbation Theory in the Condensed Phase: An Efficient and Massively Parallel Gaussian and Plane Waves Approach. *J. Chem. Theory Comput.* **2012**, *8* (11), 4177−4188.
(176) Kuhne, T. D.; Iannuzzi, M.; Del Ben, M.; Rybkin, V. V.; Seewald, P.; Stein, F.; Laino, T.; Khaliullin, R. Z.; Schutt, O.; Schiffmann, F.; Golze, D.; Wilhelm, J.; Chulkov, S.; Bani-Hashemian, M. H.; Weber, V.; Borstnik, U.; Taillefumier, M.; Jakobovits, A. S.; Lazzaro, A.; Pabst, H.; Muller, T.; Schade, R.; Guidon, M.; Andermatt, S.; Holmberg, N.; Schenter, G. K.; Hehn, A.; Bussy, A.; Belleflamme, F.; Tabacchi, G.; Gloss, A.; Lass, M.; Bethune, I.; Mundy, C. J.; Plessl, C.; Watkins, M.; VandeVondele, J.; Krack, M.; Hutter, J. CP2K: An electronic structure and molecular dynamics software package - Quickstep: Efficient and accurate electronic structure calculations. *J. Chem. Phys.* **2020**, *152* (19), 194103.
(177) Stein, F.; Hutter, J.; Rybkin, V. V. Double-Hybrid DFT Functionals for the Condensed Phase: Gaussian and Plane Waves Implementation and Evaluation. *Molecules* **2020**, *25* (21), 5174.
(178) Gounder, R.; Iglesia, E. The catalytic diversity of zeolites: confinement and solvation effects within voids of molecular dimensions. *Chem. Commun.* **2013**, *49* (34), 3491−3509.
(179) Sarazen, M. L.; Iglesia, E. Stability of bound species during alkene reactions on solid acids. *Proc. Natl. Acad. Sci. U. S. A.* **2017**, *114* (20), E3900−E3908.
(180) Sarazen, M. L.; Iglesia, E. Effects of Charge, Size, and Shape of Transition States, Bound Intermediates, and Confining Voids in Reactions of Alkenes on Solid Acids. *ChemCatChem* **2018**, *10* (18), 4028−4037.
(181) Nguyen, C. M.; De Moor, B. A.; Reyniers, M.-F.; Marin, G. B. Isobutene Protonation in H-FAU, H-MOR, H-ZSM-5, and H-ZSM-22. *J. Phys. Chem. C* **2012**, *116* (34), 18236−18249.
(182) Ensing, B.; Laio, A.; Parrinello, M.; Klein, M. L. A recipe for the computation of the free energy barrier and the lowest free energy path of concerted reactions. *J. Phys. Chem. B* **2005**, *109* (14), 6676−6687.
(183) Chen, W.; Huang, M.; Yi, X.; Hui, Y.; Gao, P.; Hou, G.; Stepanov, A. G.; Qin, Y.; Song, L.; Liu, S.-B.; Chen, Z.; Zheng, A. Protonated methylcyclopropane is an intermediate providing complete ^{13}C-label scrambling at C4 olefin isomerization in zeolite. *Chem. Catal.* **2023**, *3* (2), 100503.
(184) Tang, X.; Chen, W.; Yi, X.; Liu, Z.; Xiao, Y.; Chen, Z.; Zheng, A. In Situ Observation of Non-Classical 2-Norbornyl Cation in Confined Zeolites at Ambient Temperature. *Angew. Chem., Int. Ed.* **2021**, *60* (9), 4581−4587.
(185) Fang, H.; Zheng, A.; Xu, J.; Li, S.; Chu, Y.; Chen, L.; Deng, F. Theoretical Investigation of the Effects of the Zeolite Framework on the Stability of Carbenium Ions. *J. Phys. Chem. C* **2011**, *115* (15), 7429−7439.
(186) Janda, A.; Vlaisavljevich, B.; Smit, B.; Lin, L.-C.; Bell, A. T. Effects of Pore and Cage Topology on the Thermodynamics of n-Alkane Adsorption at Brønsted Protons in Zeolites at High Temperature. *J. Phys. Chem. C* **2017**, *121* (3), 1618−1638.
(187) Bocus, M.; Vanduyfhuys, L.; De Proft, F.; Weckhuysen, B. M.; Van Speybroeck, V. Mechanistic Characterization of Zeolite-Catalyzed Aromatic Electrophilic Substitution at Realistic Operating Conditions. *JACS Au* **2022**, *2* (2), 502−514.
(188) Pople, J. A. Nobel Lecture: Quantum chemical models. *Rev. Mod. Phys.* **1999**, *71* (5), 1267−1274.
(189) Amsler, J.; Plessow, P. N.; Studt, F.; Bučko, T. Anharmonic Correction to Free Energy Barriers from DFT-Based Molecular Dynamics Using Constrained Thermodynamic Integration. *J. Chem. Theory Comput* **2023**, *19* (9), 2455−2468.
(190) Paolucci, C.; Khurana, I.; Parekh, A. A.; Li, S. C.; Shih, A. J.; Li, H.; Di Iorio, J. R.; Albarracin-Caballero, J. D.; Yezerets, A.; Miller, J. T.; Delgass, W. N.; Ribeiro, F. H.; Schneider, W. F.; Gounder, R. Dynamic multinuclear sites formed by mobilized copper ions in NOx selective catalytic reduction. *Science* **2017**, *357* (6354), 898−903.
(191) Moors, S. L. C.; De Wispelaere, K.; Van der Mynsbrugge, J.; Waroquier, M.; Van Speybroeck, V. Molecular Dynamics Kinetic Study on the Zeolite-Catalyzed Benzene Methylation in ZSM-5. *ACS Catal.* **2013**, *3* (11), 2556−2567.
(192) Serna, P.; Gates, B. C. Zeolite-Supported Rhodium Complexes and Clusters: Switching Catalytic Selectivity by Controlling Structures of Essentially Molecular Species. *J. Am. Chem. Soc.* **2011**, *133* (13), 4714−4717.
(193) Brogaard, R. Y.; Komurcu, M.; Dyballa, M. M.; Botan, A.; Van Speybroeck, V.; Olsbye, U.; De Wispelaere, K. Ethene Dimerization on Zeolite-Hosted Ni Ions: Reversible Mobilization of the Active Site. *ACS Catal.* **2019**, *9* (6), 5645−5650.
(194) Shamzhy, M.; Opanasenko, M.; Concepcion, P.; Martinez, A. New trends in tailoring active sites in zeolite-based catalysts. *Chem. Soc. Rev.* **2019**, *48* (4), 1095−1149.
(195) Bocus, M.; Neale, S. E.; Cnudde, P.; Van Speybroeck, V. Dynamic evolution of catalytic active sites within zeolite catalysis. In *Reference Module in Chemistry, Molecular Sciences and Chemical Engineering*; Elsevier, 2021.
(196) Millan, R.; Cnudde, P.; Van Speybroeck, V.; Boronat, M. Mobility and Reactivity of Cu+ Species in Cu-CHA Catalysts under NH3-SCR-NOx Reaction Conditions: Insights from AIMD Simulations. *JACS Au* **2021**, *1* (10), 1778−1787.
(197) Ennaert, T.; Van Aelst, J.; Dijkmans, J.; De Clercq, R.; Schutyser, W.; Dusselier, M.; Verboekend, D.; Sels, B. F. Potential and challenges of zeolite chemistry in the catalytic conversion of biomass. *Chem. Soc. Rev.* **2016**, *45* (3), 584−611.
(198) Stanciakova, K.; Weckhuysen, B. M. Water-active site interactions in zeolites and their relevance in catalysis. *Trends Chem.* **2021**, *3* (6), 456−468.
(199) Heard, C. J.; Grajciar, L.; Uhlík, F.; Shamzhy, M.; Opanasenko, M.; Čejka, J.; Nachtigall, P. Zeolite (In)Stability under Aqueous or Steaming Conditions. *Adv. Mater.* **2020**, *32* (44), 2003264.
(200) Hu, Z.-P.; Han, J.; Wei, Y.; Liu, Z. Dynamic Evolution of Zeolite Framework and Metal-Zeolite Interface. *ACS Catal.* **2022**, *12* (9), 5060−5076.
(201) Resasco, D. E.; Crossley, S. P.; Wang, B.; White, J. L. Interaction of water with zeolites: a review. *Catal. Rev.* **2021**, *63* (2), 302−362.
(202) Nusterer, E.; Blöchl, P. E.; Schwarz, K. Interaction of water and methanol with a zeolite at high coverages. *Chem. Phys. Lett.* **1996**, *253* (5), 448−455.
(203) Termath, V.; Haase, F.; Sauer, J.; Hutter, J.; Parrinello, M. Understanding the Nature of Water Bound to Solid Acid Surfaces. Ab Initio Simulation on HSAPO-34. *J. Am. Chem. Soc.* **1998**, *120* (33), 8512−8516.
(204) Stich, I.; Gale, J. D.; Terakura, K.; Payne, M. C. Dynamical observation of the catalytic activation of methanol in zeolites. *Chem. Phys. Lett.* **1998**, *283* (5), 402−408.
(205) Schwarz, K.; Nusterer, E.; Blöchl, P. E. First-principles molecular dynamics study of small molecules in zeolites. *Catal. Today* **1999**, *50* (3), 501−509.
(206) Gale, J. D.; Shah, R.; Payne, M. C.; Stich, I.; Terakura, K. Methanol in microporous materials from first principles. *Catal. Today* **1999**, *50* (3), 525−532.
(207) Vener, M. V.; Rozanska, X.; Sauer, J. Protonation of water clusters in the cavities of acidic zeolites: $(H_2O)_n$·H-chabazite, n = 1−4. *Phys. Chem. Chem. Phys.* **2009**, *11* (11), 1702−1712.
(208) Shah, R.; Payne, M. C.; Lee, M.-H.; Gale, J. D. Understanding the Catalytic Behavior of Zeolites: A First-Principles Study of the Adsorption of Methanol. *Science* **1996**, *271* (5254), 1395−1397.
(209) Liu, P.; Mei, D. Identifying Free Energy Landscapes of Proton-Transfer Processes between Brønsted Acid Sites and Water Clusters Inside the Zeolite Pores. *J. Phys. Chem. C* **2020**, *124* (41), 22568−22576.
(210) Grifoni, E.; Piccini, G.; Lercher, J. A.; Glezakou, V.-A.; Rousseau, R.; Parrinello, M. Confinement effects and acid strength in zeolites. *Nat. Commun.* **2021**, *12* (1), 2630.
(211) Liu, Y.; Vjunov, A.; Shi, H.; Eckstein, S.; Camaioni, D. M.; Mei, D.; Baráth, E.; Lercher, J. A. Enhancing the catalytic activity of

https://doi.org/10.1021/acscatal.3c01945
ACS Catal. 2023, 13, 11455−11493

hydronium ions through constrained environments. *Nat. Commun.* **2017**, *8* (1), 14113.
(212) Shi, H.; Eckstein, S.; Vjunov, A.; Camaioni, D. M.; Lercher, J. A. Tailoring nanoscopic confines to maximize catalytic activity of hydronium ions. *Nat. Commun.* **2017**, *8* (1), 15442.
(213) Pfriem, N.; Hintermeier, P. H.; Eckstein, S.; Kim, S.; Liu, Q.; Shi, H.; Milakovic, L.; Liu, Y. S.; Haller, G. L.; Barath, E.; Liu, Y.; Lercher, J. A. Role of the ionic environment in enhancing the activity of reacting molecules in zeolite pores. *Science* **2021**, *372* (6545), 952−957.
(214) De Wispelaere, K.; Wondergem, C. S.; Ensing, B.; Hemelsoet, K.; Meijer, E. J.; Weckhuysen, B. M.; Van Speybroeck, V.; Ruiz-Martinez, J. Insight into the Effect of Water on the Methanol-to-Olefins Conversion in H-SAPO-34 from Molecular Simulations and in Situ Microspectroscopy. *ACS Catal.* **2016**, *6* (3), 1991−2002.
(215) Bailleul, S.; Rogge, S. M. J.; Vanduyfhuys, L.; Van Speybroeck, V. Insight into the Role of Water on the Methylation of Hexamethylbenzene in H-SAPO-34 from First Principle Molecular Dynamics Simulations. *ChemCatChem* **2019**, *11* (16), 3993−4010.
(216) Liu, P.; Yan, Z.; Mei, D. Insights into protonation for cyclohexanol/water mixtures at the zeolitic Brønsted acid site. *Phys. Chem. Chem. Phys.* **2021**, *23* (17), 10395−10401.
(217) Liu, P.; Hao, W.; Mei, D. Understanding the Effects of Water Molecules on Cyclohexanol Dehydration over Zeolitic Acid Sites. *J. Phys. Chem. C* **2021**, *125* (28), 15283−15291.
(218) Chen, F.; Shetty, M.; Wang, M.; Shi, H.; Liu, Y.; Camaioni, D. M.; Gutiérrez, O. Y.; Lercher, J. A. Differences in Mechanism and Rate of Zeolite-Catalyzed Cyclohexanol Dehydration in Apolar and Aqueous Phase. *ACS Catal.* **2021**, *11* (5), 2879−2888.
(219) Bates, J. S.; Bukowski, B. C.; Greeley, J.; Gounder, R. Structure and solvation of confined water and water-ethanol clusters within microporous Brønsted acids and their effects on ethanol dehydration catalysis. *Chem. Sci.* **2020**, *11* (27), 7102−7122.
(220) Heard, C. J.; Grajciar, L.; Rice, C. M.; Pugh, S. M.; Nachtigall, P.; Ashbrook, S. E.; Morris, R. E. Fast room temperature lability of aluminosilicate zeolites. *Nat. Commun.* **2019**, *10*, 4690.
(221) Sun, T.; Xu, S.; Xiao, D.; Liu, Z.; Li, G.; Zheng, A.; Liu, W.; Xu, Z.; Cao, Y.; Guo, Q.; Wang, N.; Wei, Y.; Liu, Z. Water-Induced Structural Dynamic Process in Molecular Sieves under Mild Hydrothermal Conditions: Ship-in-a-Bottle Strategy for Acidity Identification and Catalyst Modification. *Angew. Chem., Int. Ed.* **2020**, *59* (46), 20672−20681.
(222) Ravi, M.; Sushkevich, V. L.; van Bokhoven, J. A. Towards a better understanding of Lewis acidic aluminium in zeolites. *Nat. Mater.* **2020**, *19* (10), 1047−1056.
(223) Nielsen, M.; Hafreager, A.; Brogaard, R. Y.; De Wispelaere, K.; Falsig, H.; Beato, P.; Van Speybroeck, V.; Svelle, S. Collective action of water molecules in zeolite dealumination. *Catal. Sci. Technol.* **2019**, *9* (14), 3721−3725.
(224) Stanciakova, K.; Ensing, B.; Goltl, F.; Bulo, R. E.; Weckhuysen, B. M. Cooperative Role of Water Molecules during the Initial Stage of Water-Induced Zeolite Dealumination. *ACS Catal.* **2019**, *9* (6), 5119−5135.
(225) Liu, P.; Liu, Q.; Mei, D. Dealumination of the H-BEA Zeolite via the S_N2 Mechanism: A Theoretical Investigation. *J. Phys. Chem. C* **2021**, *125* (44), 24613−24621.
(226) Zhang, H.; Snurr, R. Q. Computational Study of Water Adsorption in the Hydrophobic Metal-Organic Framework ZIF-8: Adsorption Mechanism and Acceleration of the Simulations. *J. Phys. Chem. C* **2017**, *121* (43), 24000−24010.
(227) Vandenbrande, S.; Waroquier, M.; Van Speybroeck, V.; Verstraelen, T. Ab Initio Evaluation of Henry Coefficients Using Importance Sampling. *J. Chem. Theory Comput.* **2018**, *14* (12), 6359−6369.
(228) Bai, P.; Neurock, M.; Siepmann, J. I. First-Principles Grand-Canonical Simulations of Water Adsorption in Proton-Exchanged Zeolites. *J. Phys. Chem. C* **2021**, *125* (11), 6090−6098.
(229) Bukowski, B. C.; Bates, J. S.; Gounder, R.; Greeley, J. Defect-Mediated Ordering of Condensed Water Structures in Microporous Zeolites. *Angew. Chem., Int. Ed.* **2019**, *58* (46), 16422−16426.
(230) Malviya, S.; Tapia, J. C.; Bai, P. Calculating adsorption isotherms using the two-phase thermodynamic method and molecular dynamics simulations. *J. Appl. Phys.* **2022**, *132* (3), 034701.
(231) Lin, S.-T.; Maiti, P. K.; Goddard, W. A., III. Two-Phase Thermodynamic Model for Efficient and Accurate Absolute Entropy of Water from Molecular Dynamics Simulations. *J. Phys. Chem. B* **2010**, *114* (24), 8191−8198.
(232) Lin, S.-T.; Blanco, M.; Goddard, W. A., III. The two-phase model for calculating thermodynamic properties of liquids from molecular dynamics: Validation for the phase diagram of Lennard-Jones fluids. *J. Chem. Phys.* **2003**, *119* (22), 11792−11805.
(233) Pascal, T. A.; Lin, S.-T.; Goddard, W. A., III. Thermodynamics of liquids: standard molar entropies and heat capacities of common solvents from 2PT molecular dynamics. *Phys. Chem. Chem. Phys.* **2011**, *13* (1), 169−181.
(234) Liu, C.; Li, G.; Hensen, E. J. M.; Pidko, E. A. Nature and Catalytic Role of Extraframework Aluminum in Faujasite Zeolite: A Theoretical Perspective. *ACS Catal.* **2015**, *5* (11), 7024−7033.
(235) Pham, T. N.; Nguyen, V.; Wang, B.; White, J. L.; Crossley, S. Quantifying the Influence of Water on the Mobility of Aluminum Species and Their Effects on Alkane Cracking in Zeolites. *ACS Catal.* **2021**, *11* (12), 6982−6994.
(236) Chen, K.; Gan, Z.; Horstmeier, S.; White, J. L. Distribution of Aluminum Species in Zeolite Catalysts: 27Al NMR of Framework, Partially-Coordinated Framework, and Non-Framework Moieties. *J. Am. Chem. Soc.* **2021**, *143* (17), 6669−6680.
(237) Fan, B.; Zhu, D.; Wang, L.; Xu, S.; Wei, Y.; Liu, Z. Dynamic evolution of Al species in the hydrothermal dealumination process of CHA zeolites. *Inorg. Chem. Front.* **2022**, *9* (14), 3609−3618.
(238) Rey, J.; Gomez, A.; Raybaud, P.; Chizallet, C.; Bučko, T. On the origin of the difference between type A and type B skeletal isomerization of alkenes catalyzed by zeolites: The crucial input of ab initio molecular dynamics. *J. Catal.* **2019**, *373*, 361−373.
(239) De Wispelaere, K.; Bailleul, S.; Van Speybroeck, V. Towards molecular control of elementary reactions in zeolite catalysis by advanced molecular simulations mimicking operating conditions. *Catal. Sci. Technol.* **2016**, *6* (8), 2686−2705.
(240) Fečík, M.; Plessow, P. N.; Studt, F. A Systematic Study of Methylation from Benzene to Hexamethylbenzene in H-SSZ-13 Using Density Functional Theory and Ab Initio Calculations. *ACS Catal.* **2020**, *10* (15), 8916−8925.
(241) Svelle, S.; Kolboe, S.; Swang, O.; Olsbye, U. Methylation of alkenes and methylbenzenes by dimethyl ether or methanol on acidic zeolites. *J. Phys. Chem. B* **2005**, *109* (26), 12874−12878.
(242) Hill, I.; Malek, A.; Bhan, A. Kinetics and Mechanism of Benzene, Toluene, and Xylene Methylation over H-MFI. *ACS Catal.* **2013**, *3* (9), 1992−2001.
(243) Van der Mynsbrugge, J.; Moors, S. L. C.; De Wispelaere, K.; Van Speybroeck, V. Insight into the Formation and Reactivity of Framework-Bound Methoxide Species in H-ZSM-5 from Static and Dynamic Molecular Simulations. *ChemCatChem* **2014**, *6* (7), 1906−1918.
(244) Jones, A. J.; Iglesia, E. Kinetic, Spectroscopic, and Theoretical Assessment of Associative and Dissociative Methanol Dehydration Routes in Zeolites. *Angew. Chem., Int. Ed.* **2014**, *53* (45), 12177−12181.
(245) DeLuca, M.; Kravchenko, P.; Hoffman, A.; Hibbitts, D. Mechanism and Kinetics of Methylating C6-C12 Methylbenzenes with Methanol and Dimethyl Ether in H-MFI Zeolites. *ACS Catal.* **2019**, *9* (7), 6444−6460.
(246) Wen, Z.; Zhu, H.; Zhu, X. Density Functional Theory Study of the Zeolite-Catalyzed Methylation of Benzene with Methanol. *Catal. Lett.* **2020**, *150* (1), 21−30.
(247) Westgård Erichsen, M.; De Wispelaere, K.; Hemelsoet, K.; Moors, S. L. C.; Deconinck, T.; Waroquier, M.; Svelle, S.; Van Speybroeck, V.; Olsbye, U. How zeolitic acid strength and composition alter the reactivity of alkenes and aromatics towards methanol. *J. Catal.* **2015**, *328*, 186−196.
(248) Martinez-Espin, J. S.; De Wispelaere, K.; Westgård Erichsen, M.; Svelle, S.; Janssens, T. V. W.; Van Speybroeck, V.; Beato, P.; Olsbye,

https://doi.org/10.1021/acscatal.3c01945
ACS Catal. 2023, 13, 11455−11493

U. Benzene co-reaction with methanol and dimethyl ether over zeolite and zeotype catalysts: Evidence of parallel reaction paths to toluene and diphenylmethane. *J. Catal.* **2017**, *349*, 136−148.
(249) Brogaard, R. Y.; Henry, R.; Schuurman, Y.; Medford, A. J.; Moses, P. G.; Beato, P.; Svelle, S.; Norskov, J. K.; Olsbye, U. Methanol-to-hydrocarbons conversion: The alkene methylation pathway. *J. Catal.* **2014**, *314*, 159−169.
(250) Zalazar, M. F.; Paredes, E. N.; Romero Ojeda, G. D.; Cabral, N. D.; Peruchena, N. M. Study of Confinement and Catalysis Effects of the Reaction of Methylation of Benzene by Methanol in H-Beta and H-ZSM-5 Zeolites by Topological Analysis of Electron Density. *J. Phys. Chem. C* **2018**, *122* (6), 3350−3362.
(251) De Wispelaere, K.; Martínez-Espín, J. S.; Hoffmann, M. J.; Svelle, S.; Olsbye, U.; Bligaard, T. Understanding zeolite-catalyzed benzene methylation reactions by methanol and dimethyl ether at operating conditions from first principle microkinetic modeling and experiments. *Catal. Today* **2018**, *312*, 35−43.
(252) Chowdhury, A. D.; Houben, K.; Whiting, G. T.; Chung, S.-H.; Baldus, M.; Weckhuysen, B. M. Electrophilic aromatic substitution over zeolites generates Wheland-type reaction intermediates. *Nat. Catal.* **2018**, *1* (1), 23−31.
(253) Mou, T.; Pillai, H. S.; Wang, S.; Wan, M.; Han, X.; Schweitzer, N. M.; Che, F.; Xin, H. Bridging the complexity gap in computational heterogeneous catalysis with machine learning. *Nat. Catal.* **2023**, *6* (2), 122−136.
(254) Lezcano-Gonzalez, I.; Campbell, E.; Hoffman, A. E. J.; Bocus, M.; Sazanovich, I. V.; Towrie, M.; Agote-Aran, M.; Gibson, E. K.; Greenaway, A.; De Wispelaere, K.; Van Speybroeck, V.; Beale, A. M. Insight into the effects of confined hydrocarbon species on the lifetime of methanol conversion catalysts. *Nat. Mater.* **2020**, *19* (10), 1081−1087.
(255) Yang, G.; Wang, C.-M.; Li, Y.; Du, Y.-J.; Wang, Y.-D.; Xie, Z.-K. Simple structure descriptors quantifying the diffusion of ethene in small-pore zeolites: insights from molecular dynamic simulations. *Inorg. Chem. Front.* **2022**, *9* (8), 1590−1602.
(256) Ghysels, A.; Moors, S. L. C.; Hemelsoet, K.; De Wispelaere, K.; Waroquier, M.; Sastre, G.; Van Speybroeck, V. Shape-Selective Diffusion of Olefins in 8-Ring Solid Acid Microporous Zeolites. *J. Phys. Chem. C* **2015**, *119* (41), 23721−23734.
(257) Ramsahye, N. A.; Maurin, G. Chapter 3 - Modeling of Diffusion in MOFs. In *Modelling and Simulation in the Science of Micro- and Meso-Porous Materials*; Catlow, C. R. A., Van Speybroeck, V., van Santen, R. A., Eds.; Elsevier, 2018; pp 63−97.
(258) Hemelsoet, K.; Van der Mynsbrugge, J.; De Wispelaere, K.; Waroquier, M.; Van Speybroeck, V. Unraveling the Reaction Mechanisms Governing Methanol-to-Olefins Catalysis by Theory and Experiment. *ChemPhysChem* **2013**, *14* (8), 1526−1545.
(259) Chang, C.; Deringer, V. L.; Katti, K. S.; Van Speybroeck, V.; Wolverton, C. M. Simulations in the era of exascale computing. *Nat. Rev. Mater.* **2023**, *8*, 309−313.
(260) Titze, T.; Lauerer, A.; Heinke, L.; Chmelik, C.; Zimmermann, N. E. R.; Keil, F. J.; Ruthven, D. M.; Kärger, J. Transport in Nanoporous Materials Including MOFs: The Applicability of Fick's Laws. *Angew. Chem., Int. Ed.* **2015**, *54* (48), 14580−14583.
(261) Hwang, S.; Kärger, J. Diffusion in nanopores: correlating experimental findings with "first-principles" predictions. *Adsorption* **2020**, *26* (7), 1001−1013.
(262) Chmelik, C.; Kärger, J. In situ study on molecular diffusion phenomena in nanoporous catalytic solids. *Chem. Soc. Rev.* **2010**, *39* (12), 4864−4884.
(263) Bonomi, M.; Branduardi, D.; Bussi, G.; Camilloni, C.; Provasi, D.; Raiteri, P.; Donadio, D.; Marinelli, F.; Pietrucci, F.; Broglia, R. A.; Parrinello, M. PLUMED: A portable plugin for free-energy calculations with molecular dynamics. *Comput. Phys. Commun.* **2009**, *180* (10), 1961−1972.
(264) Tribello, G. A.; Bonomi, M.; Branduardi, D.; Camilloni, C.; Bussi, G. PLUMED 2: New feathers for an old bird. *Comput. Phys. Commun.* **2014**, *185* (2), 604−613.
(265) Beerdsen, E.; Smit, B.; Dubbeldam, D. Molecular Simulation of Loading Dependent Slow Diffusion in Confined Systems. *Phys. Rev. Lett.* **2004**, *93* (24), 248301.
(266) Dubbeldam, D.; Beerdsen, E.; Vlugt, T. J. H.; Smit, B. Molecular simulation of loading-dependent diffusion in nanoporous materials using extended dynamically corrected transition state theory. *J. Chem. Phys.* **2005**, *122* (22), 224712.
(267) DeLuca, M.; Hibbitts, D. Predicting diffusion barriers and diffusivities of C6-C12 methylbenzenes in MFI zeolites. *Microporous Mesoporous Mater.* **2022**, *333*, 111705.
(268) Mortén, M.; Mentel, Ł.; Lazzarini, A.; Pankin, I. A.; Lamberti, C.; Bordiga, S.; Crocellà, V.; Svelle, S.; Lillerud, K. P.; Olsbye, U. A Systematic Study of Isomorphically Substituted H-MAlPO-5 Materials for the Methanol-to-Hydrocarbons Reaction. *ChemPhysChem* **2018**, *19* (4), 484−495.
(269) Redekop, E. A.; Lazzarini, A.; Bordiga, S.; Olsbye, U. A temporal analysis of products (TAP) study of C2-C4 alkene reactions with a well-defined pool of methylating species on ZSM-22 zeolite. *J. Catal.* **2020**, *385*, 300−312.
(270) Yoda, E.; Kondo, J. N.; Domen, K. Detailed process of adsorption of alkanes and alkenes on zeolites. *J. Phys. Chem. B* **2005**, *109* (4), 1464−1472.
(271) Gao, S. S.; Liu, Z. Q.; Xu, S. T.; Zheng, A. M.; Wu, P. F.; Li, B.; Yuan, X. S.; Wei, Y. X.; Liu, Z. M. Cavity-controlled diffusion in 8-membered ring molecular sieve catalysts for shape selective strategy. *J. Catal.* **2019**, *377*, 51−62.
(272) Han, J.; Liu, Z.; Li, H.; Zhong, J.; Zhang, W.; Huang, J.; Zheng, A.; Wei, Y.; Liu, Z. Simultaneous Evaluation of Reaction and Diffusion over Molecular Sieves for Shape-Selective Catalysis. *ACS Catal.* **2020**, *10* (15), 8727−8735.
(273) Shostak, V.; Redekop, E.; Olsbye, U. Parametric sensitivity analysis of the transient adsorption-diffusion models for hydrocarbon transport in microporous materials. *Catal. Today* **2023**, *417*, 113785.
(274) Marin, G. B.; Galvita, V. V.; Yablonsky, G. S. Kinetics of chemical processes: From molecular to industrial scale. *J. Catal.* **2021**, *404*, 745−759.
(275) Stamatakis, M.; Vlachos, D. G. Unraveling the Complexity of Catalytic Reactions via Kinetic Monte Carlo Simulation: Current Status and Frontiers. *ACS Catal.* **2012**, *2* (12), 2648−2663.
(276) Motagamwala, A. H.; Dumesic, J. A. Microkinetic Modeling: A Tool for Rational Catalyst Design. *Chem. Rev.* **2021**, *121* (2), 1049−1076.
(277) Andersen, M.; Panosetti, C.; Reuter, K. A Practical Guide to Surface Kinetic Monte Carlo Simulations. *Front. Chem.* **2019**, *7*, 202.
(278) Chizallet, C. Achievements and Expectations in the Field of Computational Heterogeneous Catalysis in an Innovation Context. *Top. Catal.* **2022**, *65* (1−4), 69−81.
(279) Behler, J.; Parrinello, M. Generalized neural-network representation of high-dimensional potential-energy surfaces. *Phys. Rev. Lett.* **2007**, *98* (14), 146401.
(280) Christensen, A. S.; Bratholm, L. A.; Faber, F. A.; von Lilienfeld, O. A. FCHL revisited: Faster and more accurate quantum machine learning. *J. Chem. Phys.* **2020**, *152* (4), 044107.
(281) Behler, J.; Csányi, G. Machine learning potentials for extended systems: a perspective. *Eur. Phys. J. B* **2021**, *94* (7), 142.
(282) Kulik, H. J.; Hammerschmidt, T.; Schmidt, J.; Botti, S.; Marques, M. A. L.; Boley, M.; Scheffler, M.; Todorović, M.; Rinke, P.; Oses, C.; Smolyanyuk, A.; Curtarolo, S.; Tkatchenko, A.; Bartók, A. P.; Manzhos, S.; Ihara, M.; Carrington, T.; Behler, J.; Isayev, O.; Veit, M.; Grisafi, A.; Nigam, J.; Ceriotti, M.; Schütt, K. T.; Westermayr, J.; Gastegger, M.; Maurer, R. J.; Kalita, B.; Burke, K.; Nagai, R.; Akashi, R.; Sugino, O.; Hermann, J.; Noé, F.; Pilati, S.; Draxl, C.; Kuban, M.; Rigamonti, S.; Scheidgen, M.; Esters, M.; Hicks, D.; Toher, C.; Balachandran, P. V.; Tamblyn, I.; Whitelam, S.; Bellinger, C.; Ghiringhelli, L. M. Roadmap on Machine learning in electronic structure. *Electron. Struct.* **2022**, *4* (2), 023004.
(283) Vandenhaute, S.; Cools-Ceuppens, M.; DeKeyser, S.; Verstraelen, T.; Van Speybroeck, V. Machine learning potentials for

https://doi.org/10.1021/acscatal.3c01945
ACS Catal. 2023, 13, 11455−11493

metal-organic frameworks using an incremental learning approach. *npj Comput. Mater.* **2023**, *9* (1), 19.
(284) Unke, O. T.; Meuwly, M. PhysNet: A Neural Network for Predicting Energies, Forces, Dipole Moments, and Partial Charges. *J. Chem. Theory Comput.* **2019**, *15* (6), 3678−3693.
(285) Grisafi, A.; Ceriotti, M. Incorporating long-range physics in atomic-scale machine learning. *J. Chem. Phys.* **2019**, *151* (20), 204105.
(286) Boselt, L.; Thurlemann, M.; Riniker, S. Machine Learning in QM/MM Molecular Dynamics Simulations of Condensed-Phase Systems. *J. Chem. Theory Comput.* **2021**, *17* (5), 2641−2658.
(287) Laloue, N.; Laroche, C.; Jobic, H.; Methivier, A. Kinetic Monte Carlo Modelling to Study Diffusion in Zeolite Understanding the Impact of Dual Site Isotherm on the Loading Dependence of *n*-Hexane and *n*-Heptane Diffusivities in MFI Zeolite, as Revealed by QENS Experiments. *Oil Gas Sci. Technol.* **2009**, *64* (6), 773−793.
(288) DeLuca, M.; Hibbitts, D. D. Prediction of C_6−C_{12} Interconversion Rates Using DFT and Zeolite-Specific Kinetic Monte Carlo Simulation Methods. *ChemRxiv* **2019**, DOI: 10.26434/chemrxiv.8035565.v1.
(289) Krishna, R.; van Baten, J. M. Kinetic Monte Carlo Simulations of the loading dependence of diffusion in zeolites. *Chem. Eng. Technol.* **2005**, *28* (2), 160−167.
(290) Schneider, D.; Hwang, S.; Haase, J.; Miersemann, E.; Kärger, J. Quantitating Diffusion Enhancement in Pore Hierarchies. *Langmuir* **2022**, *38*, 11565−11572.
(291) Huang, W. L.; Li, J.; Liu, Z.; Zhou, J.; Ma, C.; Wen, L.-X. Mesoscale distribution of adsorbates in ZSM-5 zeolite. *Chem. Eng. Sci.* **2019**, *198*, 253−259.

NOTE ADDED AFTER ASAP PUBLICATION

This paper was originally published ASAP on August 15, 2023. Due to a production error, the first author's surname was indexed incorrectly. The revised version reposted on August 15, 2023.

https://doi.org/10.1021/acscatal.3c01945
ACS Catal. 2023, 13, 11455−11493